Universidad de Concepción
Dirección de Postgrado
Facultad de Ciencias Naturales y Oceanográficas
Programa de Doctorado en Oceanografía

# INTERACCIONES TRÓFICAS Y MIGRACIÓN VERTICAL COMO MECANISMOS DE TRANSFERENCIA DEL CARBONO ORGÁNICO HACIA EL OCÉANO PROFUNDO

Tesis presentada a la Facultad de Ciencias Naturales y Oceanográficas de la Universidad de Concepción para optar al grado académico de Doctora en Oceanografía

POR: Susana Cabrera Nuñez

Profesor Guía: Dr. Rubén Escribano

Profesor Co-guía: Igor Fernández-Urruzola

Concepción, Chile 2025

# AGRADECIMIENTOS

A la Agencia Nacional de Investigación y Desarrollo (ANID) por el apoyo otorgado a través de la beca N° 21211977 (2021-2024), así como al Instituto Milenio de Oceanografía (AIM23-0003) (2024-2025), FONDECYT 11221079, al proyecto núcleo milenio DEOXs (NCN2024_113) y al proyecto Anillo Eclipse (ACT210071), por el financiamiento para hacer posible la realización de esta investigación.

Además de a la Universidad de Concepción, Dirección de Postgrado, por el respaldo institucional y beca de estipendio, así como de pasantía internacional, y especialmente a Fabiola Gaete por su constante apoyo y gestión durante este proceso académico.

A lo Drs. Rubén Escribano e Igor Fernández-Urruzola, profesores guías de esta tesis, por sus valiosas revisiones, comentarios y orientación que enriquecieron tanto el proyecto como las publicaciones derivadas de este trabajo, así también a cada uno de los miembros del comité el Dr. Sergio Hernández, Dra. Pamela Hidalgo y al Dr. Marcelo Oliva. De manera especial, agradezco al Dr. Antonio Bode, con quien realicé una estancia de investigación y cuyo apoyo fue fundamental en el desarrollo de la tesis, en particular en los análisis de isótopos estables. Al Dr. Jaime Gómez por sus comentarios como evaluador externo.

A mi Mamá y mis hermanas, a uds les debo tanto, pese a la lejanía su apoyo y amor lo he sentido en cada momento, gracias por crecer conmigo y estar siempre presentes.

Leissing, sin duda formas parte medular de mi desarrollo no solo durante el posgrado sino también en poder establecerme en un lugar lejos de casa. A Daniel Toledo, por su apoyo dentro del desarrollo y obtención de muestras de este proyecto, así como su amistad y enseñanzas siempre motivadoras.

Generación 2020, sin duda mi eterno agradecimiento por esas horas frente al computador. Cristóbal y Paula, mi amistad sigue en deuda con ustedes, son grandes personas que admiro y respeto tanto, los considero un parte esencial de mi formación.

A Bárbara, Tamara y Sofia por proveerme de tanto cariño, por estar a mi lado y cuidarme. Club de lulu, por haber compartido y creado un lugarcito seguro lleno de mujeres maravillosas.

Darío, poder agradecerte es una manera de retribuir lo que me has otorgado, gracias por tu apoyo, mostrarme un mundo rodeado de calma y risas, además de recordarme constantemente lo lejos que se puede llegar.

Dejar a tras a tu familia y tu país sin duda es un reto dentro del desarrollo profesional, sin embargo, agradezco a cada persona que me hizo parte de su familia y me brindo su amistad haciendo mis días más cálidos en este país ahora ya no tan extraño.

***Curriculum Vitae***

Susana Cabrera Nuñez

Nacida el 14 de mayo, 1992, en Santo Domingo Tehuantepec Oaxaca, México

2010-2015: Título profesional de Biólogo Marino, Universidad del Mar, México
2016-2018: Maestría en Ciencias en Manejo de Recursos Marinos, CICIMAR-IPN, México.
2020-2024: Doctorado en Oceanografía, Universidad de Concepción, Chile.

**ÁREAS DE INVESTIGACIÓN**

Principal: Oceanografía biológica
Secundaria: Ecología trófica
Otras: Ecología marina; ecología del zooplancton; taxonomía de copépodos

**PUBLICACIONES**

**Cabrera-Núñez, S.,** Fernández-Urruzola, I., Bode, A., Hernández-Trujillo, S., Hidalgo, P., & Escribano, R. (2025). Assessing the food web structure of the mesozooplankton community in the highly variable coastal upwelling system of the southeast Pacific. Progress in Oceanography, 239, 103580. doi: 10.1016/j.pocean.2025.103580

**Cabrera-Núñez, S.**, R. De Silva-Dávila & S. Hernández-Trujillo. 2023. Copepod community structure and functional feeding groups off the Central Mexican Pacific (spring of 2015). doi: 10.3856/vol51-issue5-fulltext-2961.

Villegas-Zurita, F., F. Castillejos-Moguel, **S. Cabrera-Núñez** & R.F. Ramírez-Barragán. 2016. First records of *Balaenoptera edeni* (Cetartiodactyla: Balaenopteridae) in the coast of Oaxaca, Mexico. doi: 10.12933/therya-16-396.

**BECAS Y PREMIOS**

- Beca DEOSX para estudiante de doctorado (1er semestre 2025)
- Beca IMO para estudiante de doctorado (2024-2025)
- Beca ECOP- PICES asistencia al 7th simposio Hobart (marzo, 2024)
- Beca de Doctorado Nacional de la Agencia Nacional de Investigación y Desarrollo (2021-2024)
- Beca de pasantía doctoral ANID (2023)
- Beca de la Dirección de Posgrado, Universidad de Concepción para pasantía (2023)
- Beca UCO de la Universidad de Concepción (2020)
- Beca de manutención (CVU: 819483) del Consejo Nacional de Ciencia y Tecnología (2016-2018).

**EXPERIENCIA DOCENTE**

- 2020-2024: Ayudante de Cátedra en la asignatura electiva de pregrado/postgrado “Ecología del Océano profundo” a cargo del Dr. Rubén Escribano, Universidad de Concepción.
- 2024: Ponente en la semana de la Ciencia “STEM day” del colegio Thomas Jefferson School de la Comuna de Concepción, Chile.
- 2022: Profesora invitada dentro de la asignatura Métodos Oceanográficos de la Licenciatura en Biología Marina de la Universidad del Mar (México), para alumnos de pregrado de últimos semestres y estudiantes de magíster del programa "Ecología Marina" de la misma institución.
- 2022: Profesora invitada dentro de la asignatura Ecología de Comunidades de la Licenciatura en Biología Marina de la Universidad del Mar (México), para alumnos de pregrado de últimos semestres y estudiantes de magíster del programa "Ecología Marina" de la misma institución.
- 2019-2022: Profesora en el Instituto de Estudios Superiores América a cargo de las asignaturas de Desarrollo sustentables, Epistemología, Estadística II, Sistemas de Manejo Ambiental, Seminario de tesis y Desarrollo Profesional, Ecología I.

**TESIS**

- Miembro del comité de Proyecto de Tesis de Elida Mijangos Velázquez, alumna de la licenciatura en Biología Marina de la Universidad del Mar, México, con el proyecto titulado "Dinámica de nutrientes en Puerto Chiapas y Acapulco: efectos en la distribución espacial y estructura comunitaria del zooplancton"

**CRUCEROS OCEANOGRÁFICOS**

- 2024: Crucero oceanográfico IDOOS-II, Cabo de Hornos, Fosa de Atacama, Chile.
- 2023: Crucero oceanográfico MAPUCHE (SO296/2 LEG-1), RV SONNE, Concepción, Chile.
- 2017: Crucero oceanográfico MAREIA IX, B/O "EL PUMA", Pacífico Central Mexicano.

**ESTADÍAS DE INVESTIGACIÓN O ENTRENAMIENTO**

- 2024: Estadía de investigación en la Universidad de Antofagasta, Chile. Supervisor: Dr. Igor Fernández-Urruzola
- 2023: Estadía de investigación en el Instituto Español Oceanográfico A. Coruña CSIC, Supervisor: Dr. Antonio Bode
- -2014: Estadía de investigación en la Estación de Biología Mariana de la Universidad de Concepción, Supervisor: Dr. Rubén Escribano
- 2013: Estadía de investigación en el CICIMAR-IPN, Supervisor: Dr. Sergio Hernández Trujillo
- 2022: Curso “Plankton Ecology and Processes”, impartido por el Dr. Kam Tang, en la Universidad de Concepción.
- 2022: Curso “Scientific Presentation Workshop”, impartido por el Dr. Kam Tang, en la Universidad de Concepción.

- 2017: Curso “Basic Workshop on Mitochondrial DNA Sequence Analysis”, impartido por M. in C. Griselda Gallegos, Dr. Claudia A. Silva Segundo, Dr. Noé Díaz Viloria, en el CICIMAR-IPN.
- 2012: Curso “Methods of collection and identification of zooplankton”, impartido por M. in C. Antonio López Serrano, en la Universidad del Mar

**PRESENTACIONES EN CONGRESOS**

Presentaciones de resultados de la presente tesis:

- Mayo 2024: presentación oral en el XLIII Congreso de Ciencias del Mar.
- Marzo 2024: Presentación oral en 7th International Zooplankton Production Symposium.

# Tabla de Contenidos

# Índice de Figuras

## RESUMEN

El transporte de carbono orgánico hacia el océano profundo es un componente clave de la bomba biológica, a través del cual la materia orgánica producida en la zona fótica es transferida a capas más profundas, promoviendo así el secuestro de carbono. En los sistemas de surgencia costera, como el del Pacífico suroriental, este proceso se ve fuertemente influido por la alta productividad biológica, la variabilidad oceanográfica y las complejas interacciones entre los procesos físicos y biológicos. Dentro de este marco, el zooplancton y el micronecton desempeñan un papel esencial en el flujo vertical de carbono, no solo contribuyendo al hundimiento pasivo de partículas de sus fecas y mudas (transporte pasivo), sino también a través de su comportamiento migratorio vertical (transporte activo). En este último proceso, se ha postulado que las migraciones verticales escalonadas (escalera de migración propuesta por Vinogradov 1962) combinadas con las interacciones presa-depredador pueden exacerbar el flujo vertical de C orgánico. Esta hipótesis sugiere que el suministro más importante de alimento en el océano profundo es el transporte activo de materia orgánica mediante migraciones asincrónicas de organismos pelágicos y sus interacciones tróficas desde la zona superior a grandes profundidades en la columna de agua. A este proceso combinado lo llamaremos “escalera trófica”.

Una escalera trófica favoreciendo el transporte vertical de carbono en el sistema de surgencia del centro-sur de Chile, sugiere que las interacciones presa-depredador y las migraciones verticales de los organismos pelágicos dan lugar a un flujo vertical escalonado de C que puede acelerar su transporte

desde la capa fótica hacia las capas meso y batipelágicas, integrando así procesos ecológicos y biogeoquímicos dentro del funcionamiento de la bomba biológica del carbono. En este marco conceptual, se ha desarrollado la presente tesis, planteando como objetivo central la puesta a prueba de la hipótesis nula de la existencia de dicha escalera trófica en el sistema de surgencia del Pacífico sur oriental frente a la costa de Chile considera las zonas de Iquique y Concepción como áreas de estudio.

El capítulo 1 se centró en la caracterización de estructura y dinámica trófica de un componente clave del ecosistema pelágico, el mesozooplancton. Para tales fines, se analizaron muestras de zooplancton obtenidas durante el crucero LowPhox-II del verano austral del 2018 frente a la zona norte de Chile (Iquique). Las muestras obtenidas en 5 estratos verticales entre los 900 y 0 m de la columna de agua en condiciones diurnas y nocturnas se analizaron mediante métodos automatizados para cuantificar e identificar los grupos taxonómicos de la comunidad del mesozooplancton. El análisis incluyó adicionalmente la determinación de isótopos estables de C y N en cuatro clases de tamaño de la comunidad. Durante el crucero se obtuvieron también variables ambientales hidrográficas. Se estimó la migración vertical diurna-nocturna del zooplancton (DVM) y sus interacciones tróficas basadas en la composición isotópica de los diferentes grupos taxonómicos y fracciones de tamaño. El estudio propuso un Índice de Comportamiento Trófico (Trophic Behavior Index, TBI). Este índice integra tres atributos biológicos claves del zooplancton: el tamaño del individuo, la amplitud de la migración vertical diaria (DVM), y la posición trófica estimada mediante el uso de isótopos estables de nitrógeno que compone la biomasa del zooplancton. Su aplicación

permitió clasificar la comunidad en cuatro grupos funcionales: consumidores primarios, predadores moderados, predadores fuertes y predadores tope; y evidenció que la estructura trófica de la comunidad está determinada principalmente por características biológicas más que por la variabilidad ambiental. Los depredadores fuertes y tope dominaron las zonas oceánicas, mientras que los consumidores primarios prevalecieron en la costa, demostrando que el TBI constituye una herramienta para evaluar la organización funcional del zooplancton en sistemas de surgencia altamente variables y otorga un criterio para definir las relaciones presa-depredador.

El Capítulo 2 se enfocó en cuantificar el transporte lateral (costa-océano) y transporte activo de carbono mediado por el zooplancton y el micronecton durante el verano de 2023 frente a la zona de surgencia de Chile centro-sur (36 °S). Los análisis se realizaron utilizando muestras de zooplancton y micronecton obtenidas durante el crucero MAPUCHE. Los muestreos fueron también en estratos verticales en la zona costera en los primero 200 m de la columna de agua y la zona oceánica para condiciones diurnas y nocturnas en los primeros 1000 m, acompañados con información ambiental hidrográfica. Se analizó la composición taxonómica de las comunidades del mesozooplancton y del micronecton, así como se determinó la composición isotópica de cuatro clases de tamaño del zooplancton y desde organismos seleccionados del micronecton. El estudio además integró análisis isotópicos de aminoácidos (CSIA-AA) en ambos componentes de la comunidad pelágica. Utilizando los datos de variables hidrográficas, complementados con data satelital, el estudio estimó el transporte lateral por advección (Transporte de Ekman) durante surgencia activa. Los análisis de

la composición isotópica en el aminoácido fenilalanina ($\delta^{15}$N-fenilalanina) mostraron una baja variabilidad entre estaciones costeras y oceánicas, lo que sugiere una fuente común de nitrógeno derivada de la producción costera que se redistribuye lateralmente hacia zonas más oceánicas. A lo largo del gradiente costa-océano, las posiciones tróficas aumentaron desde herbívoros (~2.0) hasta carnívoros de niveles superiores (>5.0). La estimación integrada del transporte activo de carbono mediado por zooplancton y micronecton hasta los 1000 m de profundidad alcanzó los 38.3 mg C $m^{-2}$ $d^{-1}$, lo que equivale al 2.7% de la producción primaria neta (PPN) en la zona oceánica y al 2.1% de la PPN en la zona de surgencia costera. El micronecton es uno de los principales vectores en el transporte activo de carbono desde la superficie hacia la Zona Mínima de Oxígeno, integrando el carbono previamente procesado por el zooplancton migrador y superficial-no migrante.

Los resultados proveen apoyo a la existencia de una "escalera trófica", en la cual el zooplancton migrador y el micronecton participan de manera complementaria en la transferencia activa de carbono hacia las profundidades. Este mecanismo se ve reforzado por la circulación costera y los procesos de advección lateral asociados al transporte de Ekman y otros procesos físicos que redistribuyen la biomasa generados en la zona de surgencia hacia el océano abierto. En conjunto, los hallazgos de esta tesis sugieren que la interacción entre procesos físicas acoplados a procesos biológicos del zooplancton y micronecton, tales como la migración vertical y las interacciones tróficas, conforman un mecanismo efectivo dentro de la bomba biológica del carbono, promoviendo la conexión entre la alta productividad costera y el secuestro de carbono en el océano profundo.

ABSTRACT

The transport of organic carbon to the deep ocean is a key component of the biological pump, through which organic matter produced in the photic zone is transferred to deeper layers, thus promoting carbon sequestration. In coastal upwelling systems, such as that of the southeastern Pacific, this process is strongly influenced by high biological productivity, oceanographic variability, and the complex interactions between physical and biological processes. Within this framework, zooplankton and micronekton play an essential role in the vertical flux of carbon, contributing not only to the passive sinking of particle flux from their fecal pellets and molts (passive transport), but also through their vertical migratory behavior (active transport). In this latter process, it has been proposed that stepped vertical migrations (the migration ladder proposed by Vinogradov 1962), combined with predator–prey interactions, may exacerbate the vertical flux of organic C. This hypothesis suggests that the most important supply of food to the deep ocean is the active transport of organic matter through asynchronous migrations of pelagic organisms and their trophic interactions from the upper zone to great depths in the water column. We refer to this combined process as a "trophic ladder."

A trophic ladder favoring the vertical transport of carbon in the upwelling system off central-southern Chile suggests that predator–prey interactions and the vertical migrations of pelagic organisms give rise to a stepped vertical flux of C that may accelerate its transport from the photic layer to the meso- and bathypelagic layers, thereby integrating ecological and biogeochemical processes within the functioning of the biological carbon

pump. Within this conceptual framework, the present thesis was developed, with the central objective of testing the null hypothesis of the existence of such a trophic ladder in the upwelling system of the southeastern Pacific off the coast of Chile, considering the areas of Iquique and Concepción as study sites.

Chapter 1 focused on characterizing the structure and trophic dynamics of a key component of the pelagic ecosystem, the mesozooplankton. To this end, zooplankton samples collected during the LowPhox-II cruise in the austral summer of 2018 off northern Chile (Iquique) were analyzed. Samples obtained from 5 vertical strata between 900 and 0 m of the water column under daytime and nighttime conditions were analyzed using automated methods to quantify and identify the taxonomic groups of the mesozooplankton community. The analysis additionally included the determination of stable isotopes of C and N in four size classes of the community. Hydrographic environmental variables were also obtained during the cruise. Diel vertical migration (DVM) of zooplankton was estimated, along with their trophic interactions based on the isotopic composition of the different taxonomic groups and size fractions. The study proposed a Trophic Behavior Index (TBI). This index integrates three key biological attributes of zooplankton: individual body size, the amplitude of daily vertical migration (DVM), and trophic position estimated using stable nitrogen isotopes that comprise zooplankton biomass. Its application allowed the classification of the community into four functional groups: primary consumers, moderate predators, strong predators, and top predators; and showed that the trophic structure of the community is determined mainly by

biological characteristics rather than environmental variability. Strong and top predators dominated oceanic zones, whereas primary consumers prevailed in coastal areas, demonstrating that the TBI constitutes a useful tool for assessing the functional organization of zooplankton in highly variable upwelling systems and provides a criterion for defining predator–prey relationships.

Chapter 2 focused on quantifying lateral (coast–ocean) and active carbon transport mediated by zooplankton and micronekton during the summer of 2023 off the upwelling zone of central–southern Chile (36°S). Analyses were conducted using zooplankton and micronekton samples collected during the MAPUCHE cruise. Sampling was also carried out in vertical strata: in the coastal zone within the first 200 m of the water column, and in the oceanic zone under daytime and nighttime conditions within the first 1000 m, accompanied by hydrographic environmental information. The taxonomic composition of the mesozooplankton and micronekton communities was analyzed, and the isotopic composition of four size classes of zooplankton and of selected micronekton organisms was determined. The study further integrated compound-specific stable isotope analyses of amino acids (CSIA-AA) in both components of the pelagic community. Using hydrographic variables complemented with satellite data, the study estimated lateral advective transport (Ekman transport) during active upwelling. Isotopic analyses of the amino acid phenylalanine ($\delta^{15}$N-phenylalanine) showed low variability between coastal and oceanic stations, suggesting a common nitrogen source derived from coastal production that is laterally redistributed toward more oceanic areas. Along the coast–ocean gradient,

trophic positions increased from herbivores (~2.0) to higher-level carnivores (>5.0). The integrated estimate of active carbon transport mediated by zooplankton and micronekton down to 1000 m depth reached 38.3 mg C $m^{-2}$ $d^{-1}$, equivalent to 2.7% of net primary production (NPP) in the oceanic zone and 2.1% of NPP in the coastal upwelling zone. Micronekton is one of the main vectors of active carbon transport from the surface to the Oxygen Minimum Zone, incorporating carbon previously processed by migrating and surface/non-migrating zooplankton.

The results provide support for the existence of a "trophic ladder," in which migrating zooplankton and micronekton participate complementarily in the active transfer of carbon to depth. This mechanism is reinforced by coastal circulation and lateral advection processes associated with Ekman transport and other physical processes that redistribute the biomass generated in the upwelling zone toward the open ocean. Taken together, the findings of this thesis suggest that the interaction between physical processes coupled with biological processes of zooplankton and micronekton such as vertical migration and trophic interactions constitutes an effective mechanism within the biological carbon pump, promoting the connection between high coastal productivity and carbon sequestration in the deep ocean.

# 1. INTRODUCCIÓN

## 1.1 El transporte activo en la bomba biológica

La bomba biológica es un proceso dinámico que representa la exportación neta de carbono orgánico hacia el océano profundo (a partir de los 200 m de profundidad) (Boyd et al., 2019), sobre la base de la relación entre los productores primarios y los niveles tróficos superiores (ej.: zooplancton y micronecton) (Buesseler & Boyd, 2009; Honjo et al., 2008), por ello es uno de los procesos claves del ciclo del carbono en el océano (Ariza et al., 2015; Bates, 2019; Le Moigne, 2019; Steinberg & Landry, 2017). El carbono orgánico es exportado a la forma de carbono orgánico disuelto (DOC) o particulado (POC). Aproximadamente el 80% del carbono exportado a nivel mundial se encuentra en forma de POC, el DOC puede representar entre el 30% y el 50% de las exportaciones de carbono en los 500 m superiores de la columna de agua en sitios oceánicos específicos (Turner, 2015; Bates, 2019).

Se estima que la bomba biológica anualmente remueve >10 billones de toneladas de carbono en la zona epipelágica, pero solo 10% de ese flujo llega a la zona mesopelágica, y esto sugiere que el gradiente vertical está controlado por procesos biológicos además de la solubilidad del $CO_2$ (Turner, 2015). Los componentes de la bomba biológica son responsables de la transformación del carbono inorgánico disuelto (DIC) en carbono orgánico. Así, el fitoplancton incorpora el $CO_2$ por medio de la fotosíntesis en la zona eufótica y luego es consumido por micro o mesozooplancton herbívoros (pastoreo o “grazing”), o sujeto a degradación por parte de la comunidad microbiana. Dentro de los primeros estratos de la columna de agua la mayoría del carbono es respirado, además que existe depredación (ej.: microzooplancton presa del mesozooplancton y éste por peces). El POC fitoplantónicos es respirado por el

zooplancton y procariotas, proceso mediante el cual se libera $CO_2$, y que se excreta como DOC, siendo utilizado también en el ciclo microbiano. El mesozooplancton como copépodos y otros depredadores como peces, producen además POC en forma de pellets fecales los cuales se agregan y se hunden, pero a su vez pueden ser remineralizado por la actividad microbiana y coprofagos (Fig. 1) (Longhurst & Harrison, 1989; Ducklow et al., 2001; Steinberg & Landry, 2017).

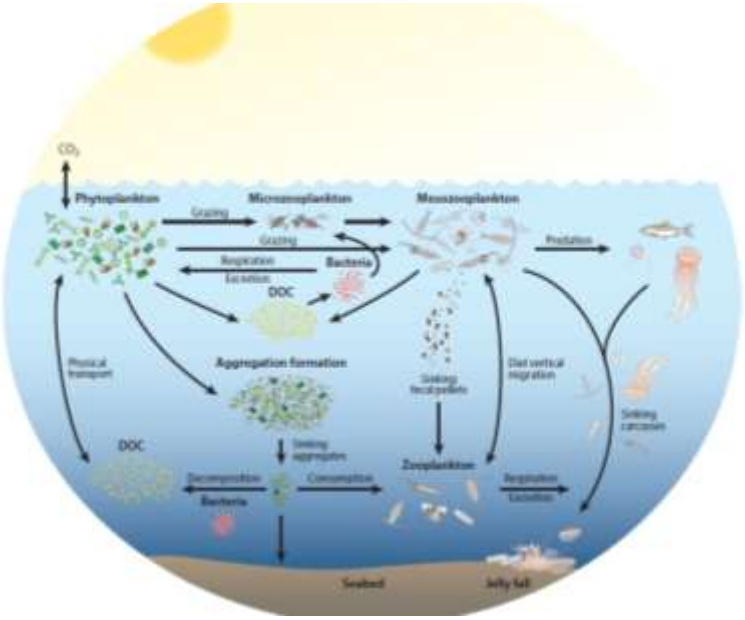


Figura 1. Esquema conceptual simplificado de la bomba biológica. Tomado de Steiberg & Landry, 2017.

Se considera que la exportación del carbono en el océano es efectiva una vez que atraviesa la zona eufótica (>200 m de profundidad), considerando que uno de los mecanismos la exportación por la bomba biológica, la cual lleva carbono a aguas más profundas o al fondo marino en sus forma disuelta o particulada.

El transporte de carbono al océano profundo puede ser pasivo o activo; el primero representa el hundimiento de materia orgánica a través de la columna

de agua, cuyo flujo puede ser estimado por trampas de sedimento, tales como los pellets fecales de zooplancton y peces, que es una forma de exportar POC o por las agregaciones de materia orgánica (nieve marina) (Turner, 2015; Hansen & Visser, 2016). Para evaluar la eficiencia de este transporte es necesario considerar la velocidad de hundimiento, lo cual dependerá del tamaño y forma del material o las agregaciones que pudiera formar, además de la densidad, porosidad, y procesos biológicos como la degradación bacteriana (de La Rocha & Passow, 2007). Este tipo de transporte constituye una fuente de alimento para organismos no migrantes del océano profundo (Steinberg et al., 2008). El segundo tipo de transporte de carbono es el activo, el cual está representado principalmente por la migración vertical de los organismos, la cual puede ser nictímera (día-noche), estacional y ontogénica. Este tipo de transporte depende de la ingesta de carbono, crecimiento, reproducción y su liberación en aguas profundas por la respiración, egestión, excreción, y mortalidad (Davison et al., 2013; Ariza et al., 2015; Turner, 2015; Steinberg & Landry, 2017). El zooplancton predomina el flujo activo, debido a que incluye diversos organismos que realizan migración vertical y que se alimentan en las aguas superficiales durante la noche y regresan a las aguas profundas durante el día, transportando activamente material disuelto y particulado a la profundidad, donde una parte se metaboliza (Bates, 2019; Kelly et al., 2019).

### 1.1.1 La migración vertical y las interacciones tróficas

La migración vertical diaria es una respuesta adaptativa de comunidades pelágicas, principalmente para la alimentación o para evadir la depredación y ahorro energético. En el zooplancton se han originado adaptaciones fisiológicas y de comportamiento asociadas a la migración vertical, también exhibiendo diferencias ontogénicas, las cuales se pueden observar en los estadios de

nauplios de copépodos que no tienen el mismo comportamiento que los adultos, larvas de peces presentan un cambio morfológico conforme a su desarrollo por lo que sus patrones de migración también cambian (Ringelberg, 2010).

La migración vertical en el océano es desarrollada por diferentes especies de diferentes tamaños, demostrando una alta diversidad y agregaciones, como zooplancton (meso y macrozooplancton) y micronecton (mayoría peces mesopelágicas y decápodos). El zooplancton migrante es de tamaño grande como ciertas especies de copépodos (*Calanus finmarchicus, C. pacificus, y Eucheta elongata*) y eufáusidos (*Euphausia mucronata, E. pacifica y E. eximia*), los cuales puede presentar una residencia variable en la columna de agua durante las horas de luz, y se asume que migran desde los 800 m a la superficie, aunque esto depende de las condiciones fisicoquímicas de la columna de agua (Bode & Hernández-León, 2018; Ringelberg, 2010; Riquelme-Bugueño et al., 2020).

La amplitud y patrones de migración varían con la estacionalidad, algunos peces planctívoros varían su distribución de acuerdo con la abundancia y cambios en la concertación de su alimento, por ejemplo, el incremento de la concentración de clorofila *a* entre los primeros 15 m fue correlacionada positivamente con la amplitud de migración, generando que la migración vertical diaria incremente la producción exportada hasta un 14% anual (Archibald et al., 2019b; Hernández-León et al., 2019, 2020).

Las migraciones verticales han sido estudiadas ampliamente en diversos sistemas, principalmente en la zona pelágica y mesopelágica, observando una diferencia en las agregaciones por tamaño y la migración diaria (Steinberg & Landry, 2017; Kelly et al., 2019). La magnitud del transporte activo dependerá entonces de la migración vertical, la cual varía espacio-temporalmente. El transporte activo esta correlacionado con la biomasa y la composición

taxonómica, entonces los flujos altos de respiración serán el resultado de un incremento en el transporte activo comparado con el pasivo, lo cual se ha observado en las migraciones diurnas/nocturnas al núcleo de la Zona Mínima de Oxígeno de *Pleuromamma abdominalis* y *Nematobrachion flexipes*, y de especies dominantes como *Euphausia gibboides*, *Sergia splendens* y *Lobianchia dofleini* en el océano Atlántico (Ariza et al., 2015; Wishner et al., 2018), donde las especies del micronecton contribuye a la exportación de carbono en aguas más profundas, lo que sugiere que los flujos de carbono impulsados por esta comunidad son importantes para los modelos futuros de la bomba de carbono biológica (Ariza et al., 2015; Hernández-León et al., 2019).

Otro proceso involucrado en la cantidad de carbono que es secuestrado al océano profundo es mediante la interacción trófica de organismos migrantes, este principio fue propuesto por Vinogradov, (1962), denominado como "escalera de migración". La hipótesis se basa en que el suministro más importante de alimento en el océano profundo es el transporte activo de materia orgánica mediante migraciones asincrónicas de organismos pelágicos y sus interacciones tróficas desde la zona superior a grandes profundidades en la columna de agua.

Las estimaciones de la exportación de carbono mediante trampas de sedimentación en su mayoría ignoran el transporte activo y se basan únicamente en mediciones directas del flujo pasivo (Davison et al., 2013; Steinberg & Landry, 2017), además no se ha considerado la interacción trófica en que participan los organismos migrantes, es decir a la fecha no se ha comprobado la forma en que la escalera de migración puede contribuir en la exportación de carbono mediante el transporte activo (Fig. 2).

La escalera de migración esquematiza que, en la zona epipelágica, está representada por la migración de especies de aguas superficiales, que a su vez

se relacionan con el siguiente escalón que migra en la zona mesopelágica, denominada como capa de transición, dada la posibilidad de alimentación de especies de superficie y de la zona batipelágica superior; el siguiente escalón se refiere a los migrantes en la porción batipelágica donde se encuentran pocos organismos de superficie y más especies de capas profundas, principalmente carnívoros, lo cual influirá en el transporte de carbono hacia el fondo marino. Se ha descrito que pocas especies interzonales descienden a la zona batipelágica superior, sin embargo, permanecen por encima de los 1,100 m, sin considerar así las relaciones tróficas que pudieran estar ocurriendo (Vinogradov, 1962; Weikert, 1982).

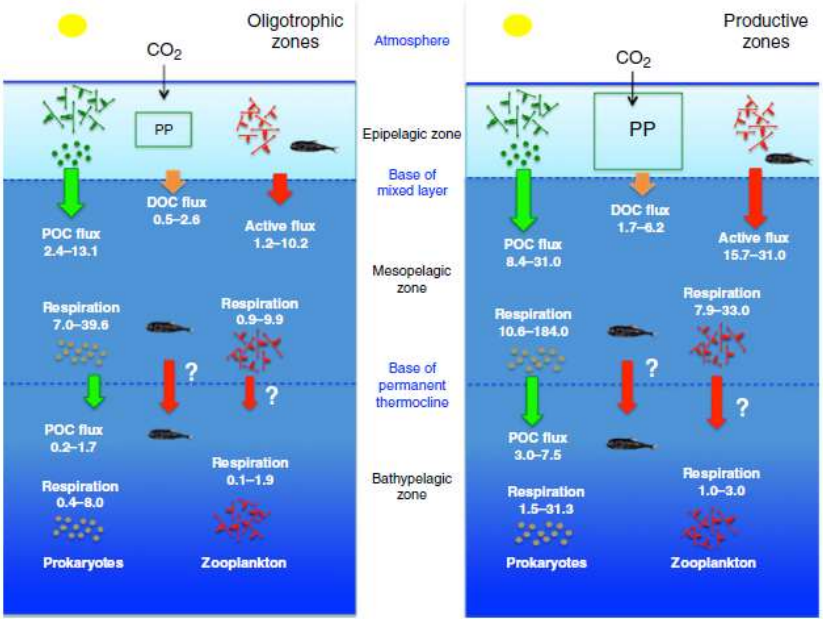


Figura 2. Exportación (desde la zona epipelágica hacia la zona mesopelágica) y secuestro de Carbono (desde la zona mesopelágica hacia la zona batipelágica). Representación del POC (flechas verdes), flujo activo debido al zooplancton migrante y micronecton (flechas rojas) y flujo estimado de carbono orgánico disuelto (DOC, flechas naranjas). Los valores se dan en g C $m^{-2}$ $y^{-1}$, signos de interrogación hacen referencia al flujo de secuestro activo desconocido. Esquema tomado de Hernández-León et al., (2020).

Las técnicas para el estudio de tramas tróficas y flujo de energía en los ecosistemas pueden dividirse en técnicas tradicionales (contenido estomacal, análisis de fecas, análisis parasitológico etc.) y más avanzadas como el análisis de isotopos estables (SIA por sus siglas en ingles) y modelos ecotróficos, hasta llegar a los análisis modernos como ácidos grasos, técnicas moleculares e isotopos estables en compuestos específicos (Hyslop, 1980; Iverson et al., 2004; Lorrain et al., 2009; Post, 2002, Ñacari et al. 2022).

El uso de proporciones de isótopos estables total se basa en el supuesto de que la composición isotópica de un consumidor refleja la media ponderada de la composición isotópica de sus fuentes de alimentos. Esta suposición generalmente se da para los isótopos estables de carbono y de nitrógeno (Mcclelland & Montoya, 2002). Una ventaja de las técnicas de isótopos estables es que proporcionan una medida continua de la posición trófica que integra la asimilación de energía o flujo de masa a través de todas las diferentes vías tróficas que conducen a un organismo (Post, 2002).

En el caso de los isótopos estables en compuestos específicos (ej.: aminoácidos) pueden proporcionar información sobre la dieta y la fisiología de los organismos, así como los orígenes de materia orgánica (Mcclelland & Montoya, 2002). El análisis de la estructura trófica ha entregado evidencia de que la migración activa causa diferencias en la diversidad y número de niveles tróficos, así como en el tamaño y superposición del nicho trófico, asociado a las estrategias de búsqueda de alimento en capas superficiales. Adicionalmente la biomasa de zooplancton de aguas profundas y el incremento en los niveles tróficos con la profundidad, impacta al transporte de carbono (Archibald, et al. 2019; Hernández-León et al., 2019). Por tal razón, los organismos migrantes y el proceso de remineralización por microrganismos se consideran potenciadores

del transporte de C a la profundidad (Bode & Hernández-León, 2018; Hernández-León et al., 2019, 2020)

Las interacciones tróficas en los peces mesopelágicos, como las estudiadas en el en el mar del Sur de China, son complejas y están fundamentalmente determinadas por sus hábitos migratorios y su papel en el transporte de energía a través de la columna de agua, en el caso peces planctívoros migradores actúan transfiriendo energía del zooplancton de la superficie hasta los peces piscívoros que habitan en la capa mesopelágica, observando que la migración de los depredadores está ligada a la de su presa, es decir los peces piscívoros migradores se sincroniza con la migración de los planctívoros (Wang et al., 2019). Este transporte activo de C por los peces mesopelágicos podría representar una proporción notable del flujo de carbono exportado, especialmente en las profundidades mesopelágicas y batipelágicas (Hernández-León et al., 2019; Kelly et al., 2019; Wang et al., 2019; Bode et al., 2021). Por ello es necesario conocer las interacciones tróficas y la forma que influyen junto a la migración vertical, en la transferencia de carbono vía redes tróficas presentes en la columna de agua y que llega al océano profundo.

# 2. HIPÓTESIS Y OBJETIVOS

## 2.2. Hipótesis

El efecto combinado de las interacciones presa-depredador y sus migraciones verticales originan una escalera trófica que promueve significativamente el transporte vertical de carbono orgánico desde la capa fótica hacia el océano profundo.

## 2.3. Objetivo general

Contribuir a la determinación de la existencia de una escalera trófica que promueve el flujo vertical de carbono orgánico hacia al océano profundo.

### 2.3.1. Objetivos específicos

1) Establecer la interacción entre las relaciones presa-depredador del zooplancton y sus migraciones verticales en un sistema de surgencia, utilizando como biomarcadores los isotopos estables de $\delta^{13}C$ y $\delta^{15}N$.
2) Caracterizar la estructura trófica y migraciones verticales diurna-nocturna del mesozooplancton en un sistema de surgencia altamente productivo en relación con las condiciones oceanográficas.
3) Evaluar si la escalera trófica constituye un mecanismo que contribuye significativamente al transporte vertical de carbono orgánico hacia el océano profundo en un sistema de surgencia altamente productivo.

# 3. MATERIAL Y MÉTODOS

## 3.1 Área de estudio

La zona de estudio está localizada en el Océano Pacífico Sur Oriental frente a Chile, donde se localiza el Sistema de la Corriente de Humboldt (SCH), la cual es una corriente fría que fluye aproximadamente desde los 42° S (Chiloé) con dirección al norte, extendiéndose así por toda la zona costera del sur de Chile hasta el Ecuador, con la presencia de distintas masas de agua: Agua Subtropical (AST), Agua intermedia del Pacifico Sur Este (AIPSE), Agua Ecuatorial Subsuperficial (AESS), Agua Intermedia Antártica (AIAA) y Agua Profunda del Pacifico (APP) (Strub et al., 1998; Schneider et al. 2004).

En la zona norte de Chile (18° S a 30°S), la surgencia es semipermanente debido a que los vientos sur y Sur Oeste prevalecen a través de todo el año (Escribano & Morales, 2004). En esta región de surgencia, y debido a la alta producción primaria, existe un alto consumo de oxígeno por la descomposición de ésta, sumado a la ventilación lenta, por lo cual se genera una zona mínima de oxígeno (ZMO) extensa (40 a 500 m), con una oxiclina intensa (>1 μM/m) y concentraciones mínimas de oxígeno que alcanzan valores <1 μM en el núcleo de la ZMO. Su límite superior se localiza entre 25 a 50 m de profundidad frente a las costas de Perú y norte de Chile, respectivamente (Ulloa & Pantoja, 2009).

Por otra parte, en la zona centro-sur de Chile (33-40 °S) la surgencia es estacional y se manifiesta con su mayor intensidad en la primavera-verano austral y muy disminuida en el otoño-invierno (Sobarzo et al., 2007), de tal manera que se puede definir un período de surgencia activa y un período de relajación de la surgencia (Escribano et al., 2004). La ZMO también se manifiesta, aunque con menor intensidad que en la zona norte y principalmente en el período de surgencia (Sobarzo et al., 2007).

Tanto en el norte del país. como en la zona centro-sur, existe una alta producción de zooplancton, dominada por copépodos y eufáusidos (Escribano & Mclaren, 1999; Escribano et al., 2007; Riquelme-Bugueño et al., 2013), así como una alta producción pesquera dominada por peces pequeños pelágicos y grandes pelágicos (Cahuin et al., 2013).

### 3.2 Diseño de muestreo y adquisición de datos

Ambas áreas fueron muestreadas durante el verano austral, a bordo del RV Cabo de Hornos (St. T3 y St. T5 frente a Iquique, crucero LowpHox II, de 04 a 05 de febrero del 2018) y del RV Sonne (frente a Concepción, crucero So296/2, 22 al 27 de enero 2023) (ver Fig. 3). En ambos cruceros, los datos

hidrográficos fueron obtenidos mediante el despliegue de un CTD Seabird SBE-911 plus (sensores de conductividad, temperatura y presión), equipado con un sensor de oxígeno SBE-43 y un fluorómetro SeaTech.

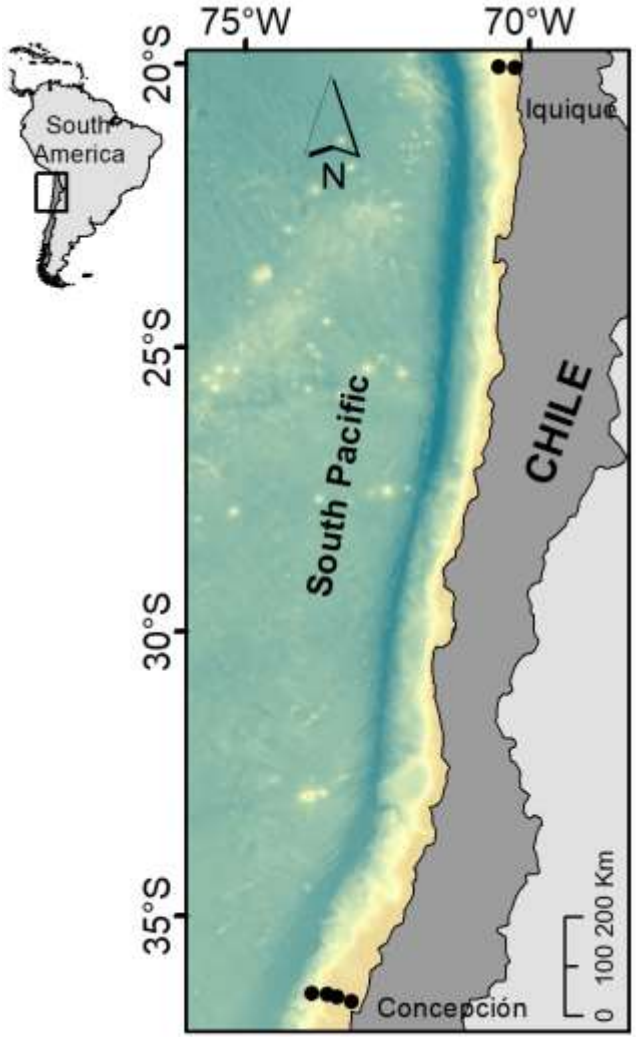


Figura 3. Área de estudio en la región de surgencia en la Pacifico sur oriental, con dos estaciones de muestreo al norte de Chile durante el crucero oceanográfico LowpHox II y una estación al centro-sur durante el crucero So296/2. Las estaciones están representadas por puntos negros.

Las muestras de zooplancton fueron recolectadas en cada estación durante el día (08:00 a 18:00, hora local) y durante la noche (21:00 a 04:00, hora local), en la región norte y sur respectivamente, mediante lances verticales

estratificados de un Multi Plankton Sampler Hydro-Bios (área de abertura de 0,25 m² y malla de 200 μm), que colectó zooplancton en cinco estratos de profundidad en los primeros 900 m (ver ANEXO). Estos estratos fueron definidos de acuerdo con el perfil de oxígeno, de modo que cada estrato representara condiciones distintas: desde la capa superficial altamente oxigenada, atravesando el núcleo de la ZMO, hasta por debajo de su límite inferior.

Las muestras fueron divididas en dos mitades mediante un divisor Motoda (T3 y T5) o recolectadas por duplicado en lances consecutivos con el Multinet (T39). En el caso de las muestras divididas, una mitad fue preservada en formalina al 5% tamponada con agua de mar para análisis taxonómico. La otra mitad fue fraccionada en cuatro clases de tamaño (200-500, 500-1000, 1000-2000 y 2000-5000 μm) a través de un tren de tamices de diferentes tamaños (200, 500, 1000 y 2000 μm) y congelada en nitrógeno líquido para análisis de isótopos estables. Las mediciones de isótopos de C y N se realizaron en muestras diurnas y nocturnas en las estaciones T3 y T5, mientras que en la estación T39 (región centro-sur) solo se analizaron muestras nocturnas. Cabe señalar que en T3 faltaron mediciones isotopos por falta de biomasa de zooplancton a 30, 90 y 150 m.

Específicamente en el área de estudio correspondiente al centro-sur, se muestreó la porción costera a lo largo de un transecto comprendido por las estaciones 18, 26 y 31 (ver ANEXO), localizadas sobre la plataforma continental, de las cuales se obtuvieron muestras de seston (0.7-100 μm) las cuales fueron recolectadas en la zona eufótica a lo largo del transecto mediante un muestreador de roseta equipado con botellas Niskin de 10 L. Posteriormente, las muestras fueron filtradas en filtros GF/F o en filtros de policarbonato de 0.8 μm de poro (47 mm de diámetro) para los análisis de CSIA-AA.

En el caso de los muestreos de zooplancton en las estaciones costera se definieron 2 a 3 estratos de profundidad entre la superficie y los 200 m (ver ANEXO). La red y procedimientos fueron iguales a los especificados anteriormente.

Adicionalmente, se utilizó una red MOCNESS (Multiple Opening-Closing Net and Environmental Sensing System) para la colecta de muestras de micronecton (2-20 cm), en la zona centro-sur (T39) tanto en el día como en la noche, hasta una profundidad de 1000 m. El marco de la red tuvo un área de abertura de 10 $m^2$ y estuvo equipado con 6 redes de malla de 3 mm cada una. El sistema MOCNESS operó en tiempo real a través de un cable conductor y una unidad de cubierta, lo que permitió monitorear el ángulo de arrastre y cerrar cada red a las profundidades seleccionadas. La red fue arrastrada a una velocidad de 2-3 nudos y recuperada a 0,5 m $s^{-1}$. Los individuos capturados en las redes fueron separados, medidos y congelados en nitrógeno líquido.

### 3.3 Procesamiento de muestras

Los análisis cuantitativos y cualitativos del zooplancton se realizaron mediante imágenes digitalizadas obtenidas con un sistema de escaneo digital ZooScan (Hydroptic) en ambas áreas de estudio. Submuestras fueron escaneadas y digitalizadas a una resolución de 2400 dpi y procesadas con el software ZooProcess (Gorsky et al., 2010). La biomasa de cada taxón fue estimada a partir del diámetro esférico equivalente (ESD, mm) de cada objeto escaneado (individuo), aplicando la ecuación empírica de Medellín-Mora et al. (2019) para calcular el peso seco (DW, mg):

$$DW = 34.3\ ESD^{2.38}$$

La biomasa de carbono de los individuos fue calculada asumiendo que el carbono corresponde al 40% del peso seco (Omori e Ikeda, 1984; Escribano et

al. 2007). Las abundancias de zooplancton (ind. $m^{-3}$) fueron obtenidas considerando el número de individuos por taxón y estandarizadas según el volumen de agua filtrado por el MultiNet ($m^3$).

Las muestras de micronecton fueron identificadas hasta el nivel de familia, pesadas (peso húmedo en gr) y medidas (cm), cabe resaltar que estas muestras corresponden únicamente al área de estudio representada para el sur enfrente de Concepción (T39). Aproximadamente 1 g de músculo fue obtenido, evitando huesos, piel y órganos internos o exoesqueleto, para los análisis isotópicos posteriores. Estas submuestras fueron liofilizadas y almacenadas en condiciones secas hasta su procesamiento.

La biomasa de carbono se estimó convirtiendo el peso húmedo (WM, por sus siglas en inglés) a peso seco (DW, por sus siglas en inglés), y posteriormente la DW a biomasa de carbono. Se asumió un contenido de agua del 75% para peces y crustáceos, de acuerdo con los valores reportados por Cotté et al. (2022). El porcentaje de carbono en la masa seca (%C en DW) se obtuvo a partir de nuestros resultados de isotopo del bulk realizados en taxones representativos de cada grupo. Estos valores fueron promediados por grupo y utilizados para convertir DW en biomasa de carbono para los análisis tróficos y de flujo de carbono.

La abundancia se estimó a partir del número de individuos de cada taxa identificados y recolectados en cada red; estos conteos fueron estandarizados a individuos por metro cúbico (ind. $m^{-3}$) usando el volumen de agua filtrada medido en cada lance. Esto permitió una comparación consistente de la abundancia de micronecton entre estratos de profundidad y estaciones.

### 3.4. Estimación de Migración vertical

Se calculó la profundidad Media Ponderada del Zooplancton (WMD,) para cada categoría taxonómica durante el día y la noche de acuerdo con Andersen et al. (2004), que incluye la variabilidad del espesor en cada estrato.

$$\mathrm{WMD} = \Sigma\,(n_i \times z_i \times d_i\,) / \Sigma\,(n_i \times z_i)$$

Donde $n_i$ es la abundancia o biomasa de la población $i$ (ind.1000 $m^{-3}$), $d_i$ la profundidad de la muestra $i$ (m), que se considera como el punto medio de cada estrato de profundidad y $z_i$ es el ancho del estrato (m).

Adicionalmente se calculó la amplitud de migración vertical (ΔMVD) mediante la diferencia entre la WMD durante el día y la noche para cada taxón, sin son valores positivos indican migración vertical normal (ascenso nocturno por los individuos residentes de profundad en el día) y valores negativos indica una migración vertical inversa (Tutasi & Escribano, 2020).

### 3.5 Análisis de isótopos estables

Los isótopos estables ($\delta^{13}C$ y $\delta^{15}N$) fueron determinados en aproximadamente 2 mg de muestras previamente homogenizadas y liofilizadas de cada fracción de tamaño. Los análisis fueron realizados en el Laboratorio de Ecología de Peces e Isótopos Estables de la Universidad de Antofagasta (Chile) y en el Servicio de Análisis Instrumental de la Universidad de A Coruña (España). Los resultados se expresaron en relación con Vienna Pee Dee Belemnite (VPDB) para $\delta^{13}C$ y con el aire atmosférico para $\delta^{15}N$. Para minimizar los posibles efectos del contenido lipídico, los valores de $\delta^{13}C$ fueron corregidos usando las relaciones C:N de masa, de acuerdo con la ecuación empírica: $\Delta\delta^{13}C = -3.32 + 0.99$ C: N donde $\Delta\delta^{13}C$ representa la depleción en $^{13}C$ causada por los lípidos (Post et al., 2007).

El análisis de isótopos compuestos específicos de $\delta^{15}N$ en aminoácidos individuales (CSIA-AA) se realizó en submuestras siguiendo las recomendaciones de Bode et al. (2021). Las muestras fueron derivatizadas para mejorar el comportamiento cromatográfico de los aminoácidos individuales. El procedimiento incluyó una hidrólisis con 2 mL de HCl 6N (20 h, 110 °C), seguida de filtración (filtros hidrofílicos de 0.2 μm) y evaporación bajo $N_2$ a 60 °C. Posteriormente, los extractos fueron esterificados con una mezcla de 2.5 mL de cloruro de acetilo:isopropanol (1:5) (60 min, 110 °C), y derivatizados con una mezcla de 0.9 mL de diclorometano:anhídrido trifluoroacético (DCM:TFAA, 3:1) (15 min, 110 °C).

Los derivados obtenidos fueron purificados mediante extracción en fase líquida usando 3 mL de cloroformo:buffer fosfato (1:2) ($Na_2HPO_4$ + $NaH_2PO_4$ en agua Milli-Q, pH=7.4), tras centrifugación (13,200 rpm, 10 min) y posterior evaporación a temperatura ambiente bajo $N_2$. Finalmente, los derivados acilo se re-disolvieron en 0.25 mL de DCM y se almacenaron en viales a −20 °C hasta su análisis.

El análisis de los aminoácidos derivatizados se llevó a cabo en un espectrómetro de masas de relaciones isotópicas DeltaV Advantage (Thermo Scientific), acoplado mediante una interfase de flujo continuo Conflo IV a un cromatógrafo de gases Trace1310GC (Thermo Scientific) y un módulo de combustión GC Isolink (Thermo Scientific). Los derivados TFA de los aminoácidos fueron separados en una columna TG-5MS (60 m, 0.32 mm × 1.0 μm); tras la separación, los compuestos fueron oxidados para generar $N_2$, el cual fue posteriormente analizado por ionización electrónica.

El método permitió el análisis de los siguientes aminoácidos individuales: alanina (Ala), glicina (Gly), treonina (Thr), serina (Ser), valina (Val), leucina (Leu), isoleucina (Ileu), prolina (Pro), metionina (Met), fenilalanina (Phe) y

lisina (Lys). Considerando que la hidrólisis ácida convierte la glutamina (Gln) en ácido glutámico (Glu) y la asparagina (Asn) en ácido aspártico (Asp), la abundancia isotópica de nitrógeno se determinó también para las combinaciones Gln+Glu (Glx) y Asn+Asp (Asx). Permitiendo así obtener los aminoácidos fuentes y tróficos. Los resultados de $\delta^{15}N$ se expresaron en ‰ relativos al aire atmosférico. Todos los análisis isotópicos se realizaron en el Servicio de Análisis Instrumental de la Universidad de A Coruña (España).

### 3.6 Ecología trófica

La posición trófica (PT) promedio se define sobre estimaciones discretas lineales basadas en el concepto tradicional de niveles tróficos. Para ello PT se estima sobre la base del contraste isotópico entre Glu y Phe, que se acepta como el mejor par de aminoácidos para estimaciones de niveles tróficos potenciales en el plancton para identificar autotrofia (PT de 1.0), herbívoro (PT de 2.0) y carnívoro de 1pt (PT de 3.0) y mixotrofia (1,0 < PT < 2.0) u omnívoro (2,0 < PT < 3,0) (Weber et al., 2021). La posición trófica (TP) de zooplancton y micronecton se calculó como:

$$TP_{Tr} = [(\delta^{15}N_{Tr} - \delta^{15}N_{PheC} - \beta)/(TDF)] + 1$$

donde Tr es el aminoácido trófico (Glx o Ala), β corresponde a la diferencia entre Tr y Phe en la base de la red trófica (3.4‰ y 3.2‰ para Glx y Ala, respectivamente para zooplancton), y el enriquecimiento isotópico en cada nivel trófico (TDF) se asumió como 7.6‰ y 4.5‰ para Glx y Ala, respectivamente (Fernández-Urruzola et al. 2023). En el micronecton, los valores fueron ligeramente distintos siguiendo a Bode et al. (2021), con β=3.6‰ y 3.2‰, y TDF=5.7‰ y 6.1‰ para Glx y Ala, respectivamente.

El efecto de la discriminación trófica en el aminoácido fuente Phe ($\delta^{15}$N_Phe) fue corregido ($\delta^{15}$N_PheC) (Xing et al., 2020) asumiendo un enriquecimiento de 0.4‰ por cada nivel trófico de acuerdo con Chikaraishi et al. (2009):

$$\delta^{15}N_{PheC} = \delta^{15}N_{Phe} - 0.4 \text{ x } (TP_{Glx} - 1)$$

La contribución fraccional del bucle microbiano a la red trófica metazooplanctónica se calculó a partir de la diferencia entre $TP_{Ala}$ y $TP_{Glx}$ (Fernández-Urruzola et al., 2023):

$$\%\ Microbial\ contribution = 100 \text{ x } \frac{TP_{Ala} - TP_{Glx}}{TP_{Ala}}$$

### 3.7 Cálculos de flujo activo

Para estimar el flujo activo de carbono (C flux), se cuantificó la biomasa de carbono del zooplancton y micronecton migratorio (mg C $m^{-2}$) a través de los estratos de profundidad muestreados durante el día y la noche. La biomasa migratoria se determinó como la diferencia en biomasa de carbono entre las muestras nocturnas y diurnas en cada estrato de profundidad. Posteriormente, estas diferencias de biomasa se usaron para calcular la biomasa integrada en por estratos en la columna de agua, con el fin de obtener el valor de biomasa migratoria (MB) utilizado en el cálculo del flujo de carbono, aplicando la siguiente fórmula:

$$C\ flux = MB\ \times \frac{R + E + M}{2}$$

donde R corresponde a las tasas de respiración, estimadas para el zooplancton (Ikeda, 2014) y para el micronecton (Belcher et al. 2020) para peces de la familia Myctophidae e Ikeda (2016) para micronecton en general. La tasa de excreción E, se obtuvo desde la literatura, asumiendo un 30% de la respiración.

Finalmente, M corresponde a la mortalidad, considerada como el 4% de la biomasa migratoria (Andersen, 2004; Tutasi & Escribano, 2020).

Las tasas vitales R, E y M son todas dependientes de la temperatura y del tamaño del organismo, por lo cual sus aplicaciones requieren incorporar estas variables. Las relaciones obtenidas de la literatura cubren amplias áreas geográficas del océano mundial (Ikeda 2014), por lo cual su aplicación en su sistema de surgencia es apropiada (Escribano et al. 2009, Tutasi & Escribano, 2020 ).

# 4. RESULTADOS

## 4.1. Capítulo 1: "Evaluación de la estructura trófica de la comunidad de mesozooplancton en el sistema de surgencia costera altamente variable del Pacífico suroriental"

Articulo científico publicado en la revista Progress in Oceanography 239 (2025),103580. doi

### Resumen

El zooplancton es un componente clave en la red trófica de los sistemas de surgencia costera altamente productivos, al vincular a los productores primarios con los niveles tróficos superiores. Sin embargo, la compleja taxonomía, el amplio espectro de tallas y la diversidad de comportamientos tróficos del zooplancton dificultan la caracterización de su estructura trófica. Este estudio propone un Índice de Comportamiento Trófico (TBI, por sus siglas en inglés) para evaluar la estructura trófica del zooplancton y poner a prueba la hipótesis de que atributos biológicos, clave como el tamaño corporal, el comportamiento de migración vertical diaria (DVM) y las interacciones tróficas, más que los factores ambientales, son los principales determinantes de la dinámica de la red trófica de las comunidades de mesozooplancton.

Para ello, analizamos muestras estratificadas en profundidad, colectadas de día y de noche, desde la superficie hasta los 900 m de profundidad en tres estaciones con condiciones oceanográficas contrastantes en el sistema de surgencia del Pacífico suroriental. Los gradientes verticales de temperatura, clorofila-a y oxígeno disuelto fueron examinados en relación con la abundancia

y composición del zooplancton, su comportamiento de DVM, los espectros de biomasa por tallas y la posición trófica.

El TBI propuesto fue construido a partir del tamaño corporal del zooplancton (estimado mediante análisis de imágenes automatizado), la amplitud de la DVM y la posición trófica de los grupos taxonómicos derivada de la composición isotópica de nitrógeno. Posteriormente, este índice se comparó entre diferentes condiciones ambientales, lo que permitió clasificar al mesozooplancton en cuatro grupos funcionales tróficos principales: depredadores bajos (consumidores primarios), depredadores moderados, depredadores fuertes y depredadore tope.

La variabilidad en las condiciones oceanográficas influyó en la composición comunitaria y en el espectro de tallas del zooplancton; sin embargo, nuestros resultados sugieren que el tamaño corporal, el comportamiento de DVM y la posición trófica son los determinantes principales de la estructura trófica. Esto se refleja en la abundancia relativa de los grupos funcionales, con los depredadores fuertes y tope predominando en zonas oceánicas, mientras que la zona costera estuvo dominada por consumidores primarios y depredadores moderados. En conjunto, nuestros hallazgos respaldan al TBI como un descriptor robusto de la estructura trófica del zooplancton en escenarios oceanográficos altamente variables.

Progress in Oceanography 239 (2025) 103580

Contents lists available at ScienceDirect

Progress in Oceanography

journal homepage: www.elsevier.com/locate/pocean

# Assessing the food web structure of the mesozooplankton community in the highly variable coastal upwelling system of the southeast Pacific

Cabrera-Núñez Susana [a,b], Fernández-Urruzola Igor [b,c,*], Bode Antonio [d], Hernández-Trujillo Sergio [e], Hidalgo Pamela [b,f], Escribano Ruben [b,f]

[a] Programa de Postgrado En Oceanografía, Departamento de Oceanografía, Facultad de Ciencias Naturales Y Oceanográficas, Universidad de Concepción, Casilla, Concepción 160-C, Chile
[b] Instituto Milenio de Oceanografía, Universidad de Concepción, Concepción, Chile
[c] Instituto de Ciencias Naturales Alexander von Humboldt, Facultad de Ciencias del Mar y Recursos Biológicos, Universidad de Antofagasta, Antofagasta, Chile
[d] Centro Oceanográfico de A Coruña, Instituto Español de Oceanografía, CSIC, A Coruña, Spain
[e] Instituto Politécnico Nacional, Centro Interdisciplinario de Ciencias Marinas, Departamento de Plancton y Ecología Marina, Av. I.P.N. S/n Col. Playa Palo de Sta. Rita, C.P. 23096, La Paz, B.C.S., Mexico
[f] Departamento de Oceanografía, Universidad de Concepción, Concepción, Chile

ARTICLE INFO

*Keywords:*
Zooplankton
Diel vertical migration
Size spectra
Trophic position
Upwelling zone
Oxygen minimum zone
Prey-predator interactions

ABSTRACT

Zooplankton are a key component in the food web of highly productive coastal upwelling systems linking primary producers to higher trophic levels. However, the complex taxonomy, wide size spectrum, and diverse trophic behaviors of zooplankton make it challenging to characterize their food web structure. This study proposes a Trophic Behavior Index (TBI) to assess the trophic structure of zooplankton and test the hypothesis that key biological attributes such as body size, diel vertical migration (DVM) behavior and trophic interactions, rather than environmental factors, primarily shape the food web dynamics of mesozooplankton communities. To this end, we analyzed depth-stratified daytime and nighttime samples of mesozooplankton collected from the upper 900 m at three oceanographically contrasting stations in the Southeast Pacific upwelling system. Vertical gradients in temperature, chlorophyll-a and dissolved oxygen were examined in relation to zooplankton abundance and composition, their DVM behavior, biomass size spectra and trophic position. The proposed TBI was constructed from zooplankton body size assessed by automated image analysis, DVM amplitude and trophic position of taxonomic groups derived from nitrogen stable isotope composition. This index was then compared across environmental conditions, allowing the classification of mesozooplankton into four major trophic functional groups: low predators (primary consumers), moderate predators, strong predators and top predators (very strong predators). Variability in oceanographic conditions influenced the zooplankton community composition and size spectrum; however, our findings suggest that zooplankton body size, DVM behavior and trophic position are the primary determinants of trophic structure. This is reflected in the relative abundance of functional groups, with strong and very strong predators prevailing in offshore areas, whereas the coastal zone was dominated by primary consumers and moderate predators. Overall, our findings support the TBI as a robust community descriptor of zooplankton trophic structure across highly variable oceanographic settings.

## 1. Introduction

Upwelling regions are key areas of marine productivity, acting as biodiversity hotspots and supporting important fishery resources. These ecosystems harbor numerous species at lower trophic levels, which play a crucial role in transferring energy to predatory fishes, seabirds and marine mammals of economic and ecological interests (Kämpf and Chapman, 2016). Zooplankton are pivotal intermediaries linking primary producers to higher trophic levels and, therefore, understanding their ecological role is essential for assessing the dynamics and productivity of marine food webs.

Characterizing the trophic structure of zooplankton communities,

* Corresponding author at: Instituto de Ciencias Naturales Alexander von Humboldt, Facultad de Ciencias del Mar y Recursos Biológicos, Universidad de Antofagasta, Antofagasta, Chile
*E-mail address:* igor.fernandez@uantof.cl (F.-U. Igor).

https://doi.org/10.1016/j.pocean.2025.103580
Received 13 May 2025; Received in revised form 16 September 2025; Accepted 25 September 2025
Available online 9 October 2025

however, is challenging due to their taxonomic complexity, wide size spectra and diverse feeding behaviors. The efficiency of trophic transfer, a key factor regulating the carbon flux, depends strongly on zooplankton biological traits: Body size affects the rate at which carbon is transferred from primary producers to higher consumers (Décima, 2022), species composition can influence feeding efficiency and growth rates (Zhou, 2006) and diel vertical migration (DVM) actively contributes to the downward transport of organic carbon (Steinberg and Landry, 2017; Tutasi and Escribano, 2020). Yet, most modeling approaches, such as Nutrients-Phytoplankton-Zooplankton (NPZ) models (Franks, 2002), fail to integrate these biological attributes, thus limiting predictions of food web dynamics in upwelling systems.

A proper characterization of the zooplankton community should be thus based on some of their fundamental traits. The structure of the pelagic food web, for example, may exhibit rich taxonomic diversity over a wide range of body sizes, which determines the energy flow across trophic levels and the overall transfer efficiency, with nutrients usually being transferred from the smallest organisms to the larger ones (Peters, 1983). Additionally, DVM plays a dual ecological role: It transports organic matter to depth and mediates predator–prey interactions through vertical linkages across depth strata, a mechanism known as the "trophic ladder" (Vinogradov, 1970). Tutasi and Escribano (2020) examined the DVM of mesozooplankton in the coastal upwelling zone of northern Chile and showed that these vertical movements contribute about 71.3 mg C $m^{-2}$ $d^{-1}$ to the downward flux of carbon, accounting for about 4 % of the net primary production, representing an efficient mechanism to deliver and incorporate freshly produced C to depth (Steinberg and Landry, 2017). Although DVM amplitudes have been described for various zooplankton groups in the Humboldt Current System (Escribano et al., 2009; Tutasi and Escribano, 2020), little is known about how these migratory behaviors interact with feeding strategies to shape the food web structure. Here, we apply a stable isotope approach to get insights about feeding modes of mesozooplankton taxa, allowing us to infer how diel vertical migration influences trophic interactions among functional groups, thereby regulating the carbon transfer through the "trophic ladder" mechanism. Stable isotopes of carbon and nitrogen are widely used to investigate trophic dynamics, with $\delta^{13}C$ providing information on primary food sources and $\delta^{15}N$ serving as an indicator of trophic position (Post, 2002). However, isotopic signatures can be affected by factors such as species composition, nutritional condition and food quality (Fry, 2006), which may complicate their interpretation in complex biological communities. To circumvent this limitation, we have developed a novel Trophic Behavior Index (TBI) which provides a trait-based framework that reduces reliance on isotopic signals alone by integrating body size and diel vertical migration amplitude with trophic position. This approach allows for a more robust interpretation of trophic structure in taxonomically diverse zooplankton assemblages.

A comprehensive understanding of the food web dynamics in the pelagic ecosystem thus requires an integrative approach considering the taxonomic and size structure of the plankton community along with the trophic interactions and DVM behaviors. However, the environmental variability may further modulate these biological traits (Décima, 2022). In the Humboldt Current upwelling system, sharp gradients in oxygen and temperature with a high-frequency (daily) variability in their water column properties (e.g., Aguirre et al., 2021) influence zooplankton distribution (Escribano et al., 2009; Ekau et al., 2010) and migration patterns (Gilly et al., 2013; Tutasi and Escribano, 2020), thus affecting predator–prey encounter rates (Roman et al., 2019) and potentially impacting the food web by modifying trophic pathways and reshaping the relative contribution of functional groups across depth strata. The magnitude of these ecological responses, however, may be attenuated by the high phenotypic plasticity of zooplankton (Frederick et al., 2024), which allows these organisms to cope with abrupt vertical gradients in the abiotic conditions (Childress and Seibel, 1998), raising the question of whether their trophic organization is primarily driven by environmental conditions or by intrinsic biological attributes.

To address this question and to disentangle the complex trophic ecology in dynamic marine environments, we propose the use of the TBI, a trophic index that integrates body size, diel vertical migration amplitude and trophic position of zooplankton taxa, as a tool to characterize the trophic structure of mesozooplankton communities. Specifically, this study aims to (i) develop and apply the TBI as a trait-based tool to describe the mesozooplankton trophic structure, (ii) to evaluate its performance across three stations with contrasting oceanographic conditions in the coastal upwelling region of the Southeast Pacific and (iii) to test the hypothesis that biological attributes, rather than environmental conditions, are the main drivers of the mesozooplankton trophic organization.

## 2. Material and methods

### 2.1. Field sampling

The study area includes three coastal stations, two of them located in the northern upwelling region off Chile and a third one at a further South upwelling location (Fig. 1). The stations at the northern upwelling zone appear close to each other on the map (Fig. 1); however, they represent contrasting hydrographic and ecological conditions. Station T3 is a relatively shallow site (ca. 1000 m) located over the shelf break, characterized by a shallower and more intense oxygen minimum zone (OMZ)

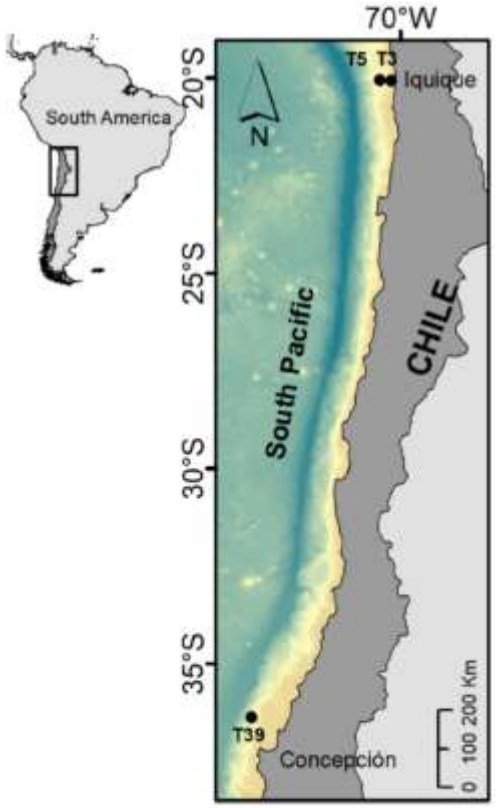


Fig. 1. The study area at the upwelling region off northern Chile, with the two sampling stations studied during the LowpHox II cruise and one sampling station at the southern upwelling region during the So296/2 cruise. The stations were represented by black dots.

near the surface and dominated by coastal copepod species (Tutasi and Escribano, 2020). In contrast, Station T5 is situated further offshore, influenced by a much deeper OMZ (>150 m) and hosting a zooplankton community composed of larger-sized taxa (Tutasi and Escribano, 2020). For comparison, Station T39, located in the central-southern upwelling region of Chile, represents an offshore temperate zone with lower productivity (Escribano and Schneider, 2007).

Both areas were sampled during the austral summer, onboard either the RV Cabo de Hornos in 2018 (St. T3 and St. T5 off Iquique, LowpHox II cruise) or the RV Sonne in 2023 (St. T39 off Concepción, So296/2 cruise) (see Fig. 1). In both cruises, the hydrographic data were obtained by deployment of a Seabird SBE-9 plus (conductivity, temperature and depth sensors, CTD), equipped with an SBE-43 oxygen sensor and a SeaTech fluorometer.

### 2.2. Zooplankton sampling and processing

Zooplankton samples were collected at each station during the daytime (08:00 to 18:00 Local time) and nighttime (21:00 to 04:00 h, local time) in February 2018 and January 2023 at the northern and southern region, respectively, by stratified vertical hauls of a Hydrobios Multinet Midi type (0.25 $m^2$ opening area and 200 µm mesh size) which collected zooplankton at 5-depth strata across the upper 900 m. These strata were defined according to the oxygen profile, such that each stratum could represent distinctive oxygen conditions from the highly oxygenated upper layer, covering the nearly anoxic OMZ core, and below the lower limit of the OMZ. Same strata were sampled at stations T3 and T5 and slightly different depth strata at T39. Details of sampling can be found in (Supplementary Material Table S1).

Samples were either divided into 2-halves with a Motoda splitter (T3 and T5) or taken in duplicate by consecutive Multinet hauls (T39). In the case of split samples, one-half was preserved in a 5 % formalin solution buffered with seawater for taxonomic analysis. The other half of the sample was fractionated in four size classes (200–500, 500–1000, 1000–2000, 2000–5000 µm) and frozen in liquid N for stable isotope analyses. These C and N isotope measurements were carried out in daytime and nighttime samples at stations T3 and T5, but only in nighttime samples at station T39 in the central-southern region. There were also missing measurements in T3 at 30, 90 and 150 m.

The quantitative and qualitative analyses of zooplankton were carried out by using digitized images obtained with a Hydroptic ZooScan digital imaging system. This method allowed us to identify 28 taxa (taxonomic units). Subsamples (1/4 of samples) were scanned and digitized at a resolution of 2400 dpi and analyzed by ZooProcess software (Gorsky et al. 2010). The biomass of each taxon (taxonomic unit) was estimated using estimates of the equivalent spherical diameter (ESD in mm) of each scanned object (individuals), and applying the empirical equation obtained by Medellín-Mora et al. (2019) to compute dry weight (DW, mg) as:

$$DW = 34.3\,ESD^{2.88} \quad (1)$$

Carbon biomass of individuals was then calculated by assuming the carbon content of dry biomass to be 40 % of the dry weight (Omori and Ikeda, 1984; Escribano and Schneider, 2007). The zooplankton abundances (ind. $m^{-3}$) were calculated considering the number of individuals in each taxonomic unit and standardized by the seawater volume filtered by the multinet ($m^3$).

The stable isotopes ($\delta^{13}C$ and $\delta^{15}N$) were determined on approximately 2 mg of freeze-dried (lyophilized) samples of each size class. The analyses were carried out in the Fish and Stable Isotope Ecology Laboratory of the Universidad de Antofagasta (Chile) and Servicio de Analisis Instrumental from the University of A. Coruña (Spain). The results were expressed relative to Vienna Pee Dee Belemnite (VPDB) and atmospheric $N_2$ for $\delta^{13}C$ and $\delta^{15}N$, respectively. To minimize potential effects caused by the lipid content, $\delta^{13}C$ values were corrected using the C: N mass ratios according to the empirical equation $\Delta\delta^{13}C = -3.32 + 0.99C: N$, where $\Delta\delta^{13}C$ is the depletion in $^{13}C$ caused by lipids (Post et al., 2007).

### 2.3. Data analysis

The mesozooplankton community was described in terms of abundance and vertical distribution of each taxonomic unit. Those units representing less than 5 % of total abundance were included in a category named "others". To describe the vertical distribution, the abundances were first $\log_{10}$ transformed. Among the taxonomic units, copepods were divided in two broad categories: large copepods (COP_L > 1000 µm) and small copepods (COP_S < 1000 µm). When possible, some copepods were further identified to the genus level by the ZooProcess software; however, when taxonomic identification was not possible, individuals were categorized solely based on their size.

The Weighted Mean Depth (WMD) of zooplankton for each taxonomic unit was calculated during both day and night, considering the width of each depth strata (Andersen, 2004):

$$WMD = \Sigma(ni \times si \times di)/\Sigma(ni \times si) \quad (2)$$

where $ni$ is the abundance (ind $m^{-3}$) of a given taxonomic group, $si$ is the width (m) of the strata, and $di$ is the mean depth of the strata (m). The Diel Vertical Migration amplitude (ΔDVM) was then calculated as the difference between the weighted mean depth during the day and night for each taxon. Positive values indicate normal vertical migration (upward migration at night), while negative values indicate inverse vertical migration, as explained in Tutasi and Escribano (2020). Only taxonomic groups with day and night data per period and a statistically significant sample size ($n > 3$) were included in the analysis. Resident taxa with very low or null ΔDVM were also considered, as the absence of vertical displacement provides ecologically relevant information. This allowed the TBI to capture the full range of trophic strategies, from migratory predators to non-migratory herbivores and omnivores.

To describe changes in the zooplankton size structure, we used the slope and linear fit of the logarithmic binning with a normalized biomass size spectrum (Mauríquez et al., 2012). The size spectrum analysis was conducted for each station and depth strata by considering fifteen biomass size classes in the range of 0.03 and 3145 µg C ($\log_{10}$ zooplankton biomass, µg C).

For the trophic position (TP) of each size fraction we assumed a constant trophic fractionation for $\delta^{15}N$ at each trophic step of 3.4 ‰, according to Post (2002). The calculations were as follows:

$$TP_{size\ fraction} = \left[\left(\delta^{15}N_{size\ fraction} - \delta^{15}N_{baseline}\right)/3.4\right] + \lambda \quad (3)$$

where the δ15Nsize fraction is the isotopic signature of a particular sample for each depth strata, the δ15Nbaseline is the isotopic value of the 200–500 µm size category in the epipelagic layer and the λ represents the TP of the δ15Nbaseline. These calculations assume that the 200–500 µm zooplankton in the epipelagic layer are primarily herbivores (TP = 2), serving as the δ15N baseline for larger size fractions. However, in deeper layers, this size-category may exhibit increased omnivory in absence of photosynthetically active phytoplankton, yielding TP > 2.

The relationship between size, trophic position and diel vertical migration was then integrated into a Trophic Behavior Index (TBI). This parameter integrates station-standardized values of zooplankton size (ESD) obtained from the ZooScan for each taxonomic unit, the estimated TP for each size fraction, and ΔDVM for each taxonomic unit at each depth strata. The index was computed as:

$$TBI_a = \frac{ESD_{ab}}{ESD_{Max}} + \frac{TP_{cb}}{TP_{Max}} + \frac{DVM_a}{DVM_{Max}} \quad (4)$$

where $a$ is a given taxon, ESD represents the mean size of each taxon at a given depth ($b$), TP is the mean trophic position for a corresponding size-fraction ($c$) and DVM is the amplitude of migration. All parameters (ESD,

TP and DVM) were divided by the maximum (Max) values from all taxa and size fractions found at the corresponding station for standardization purposes. Due to the difficulties in measuring TP for each specific taxonomic unit, the TP value for the corresponding size-fraction was used instead. If a value was missing for any of the variables, data was excluded for calculation of the index.

To associate the variation of TBI with the oceanographic conditions, we used all sampling conditions (stations, strata, day and night) and their corresponding oceanographic conditions for statistical purposes. The oceanographic conditions were represented by mean values of a given depth stratum. A 1-step stepwise multiple regression was applied to test the dependence of TBI with temperature, dissolved oxygen and Chlorophyll-a (Chl-*a*). Thereafter, we integrated the oceanographic variables into a principal components analysis (PCA) using the correlation matrix for 3 components. The first component (PC1), assumed as containing most of the variance of environmental conditions, was thus related to TBI through a linear model.

For a mesozooplankton community, the expected minimum organism size is approximately 0.2 mm (measured as ESD), the minimum TP would be 2 (corresponding to strict herbivory) and the minimum ΔDVM would be zero for non-migrating species. Conversely, maximum mesozooplankton sizes may exceed 2 mm, the TP may reach up to 5 for potential top predators, and ΔDVM can exceed 200 m in highly migratory taxa. Therefore, according to Eq. (4), the theoretical lower bound of TBI is approximately 0.4 when all parameters are at their minimum values, while the upper limit is 3.0 when all parameters reach up their maximum.

To classify the zooplankton community based on their TBI values, the expected full range (0.4–3.0) was divided into four equally spaced intervals (quartiles). The cut-off points correspond to the minimum (0.4) and maximum (3.0), and so resulting the following groups: G4 (0.4–1.04), G3 (1.5–1.69), G2 (1.70–2.34), and G1 (2.35–3). Therefore, zooplankton organisms were classified into four trophic levels: G1 as top predators (primarily carnivores), G2 as second level predators (secondary consumers), G3 as moderate predators (mainly omnivores), and G4 as low-level predators (primarily herbivores). The relative abundance of each group was used as an indicator of the food web structure, reflecting the degree of carnivory under a given condition. A high proportion of G1 + G2 suggests a predator-dominated (carnivory-driven) community, whereas their absence or low proportion indicates a system dominated by herbivores and omnivores (G3 and G4). Additionally, a correlation analysis was conducted to explore the relationships between the proportion of G1 + G2 groups and oceanographic variables, including temperature, chlorophyll-a concentration and dissolved oxygen. The relative abundance of G1 and G2 (top and secondary predators, respectively) was used as an indicator of the zooplankton food web structure, as these groups represent the higher trophic levels within the community and their dominance may indicate a stronger top-down control. In contrast, G3 (moderate predators, mainly omnivores) and G4 (low-level predators, primarily herbivores and omnivores) constitute the basal components of the food web and are generally expected to dominate in abundance. Therefore, an increased proportion of G1 + G2 reflects a shift toward a predator-dominated (carnivory-driven) community, whereas a low proportion indicates an assemblage dominated by herbivores and omnivores.

All statistical analyses and visualizations were conducted in R v 4.3.2 (Team and R. C, 2025), except for the student *t*-test, which was performed in Microsoft Excel. General linear models and ANOVAs were applied using functions from the stats package to evaluate the effects of depth and station on abundances, size fractions and trophic indicators. Model assumptions of normality and homoscedasticity were tested with the Shapiro–Wilk test and Levene's tests, respectively, the latter using the car package (Fox and Weisberg, 2019). Post hoc comparisons (Tukey's HSD) were conducted with the agricolae package (de Mendiburu & de Mendiburu, 2019). Size spectrum analyses were performed using size Spectra package (Edwards et al. 2017). Graphical representations, including bar plots, regression lines and facet visualizations, were generated using the ggplot2, cowplot and patchwork packages (Wickham, 2011; Pedersen, 2019; Wilke et al., 2019).

A Principal Component Analysis (PCA) was performed to examine multivariate patterns in environmental variables (temperature, dissolved oxygen and chlorophyll-a) and biological responses (body size and trophic position). The PCA was conducted using PAST v4.17 (Hammer et al., 2001) using standardized variables and a correlation-based ordination. The variables contributing most to the observed gradients were identified and interpreted to assess relationships among stations and depth strata.

## 3. Results

### 3.1. Oceanographic conditions

At the northern upwelling region (stations T3 and T5), the thermocline was located within the upper 40 m, showing strong differences between the two stations in the salinity (Fig. 2). Station T3 displayed a more mixed layer within the upper 20 m compared to Station T5, with salinity values of around 34.8 decreasing gradually with depth down to 30 m and increasing below 90 m. Conversely, T5 showed higher salinity values (>35.2) in the upper 20 m and a clear halocline between 20–40 m. It is noteworthy that the oxycline in T3 was shallower than in T5, with oxygen depletion occurring between the first 90 m in both cases. The subsurface peak of Chl-*a* was also shallower in the thinner euphotic zone from T3 (Fig. 2).

Station T39 (in the southern region) showed a more mixed water column, with colder conditions (<14 °C) and a lower salinity in the upper layer. A near-surface (−45 m) chlorophyll-a peak exceeding 4 mg $m^{-3}$ coincided with the thermocline, the oxycline and the presence of higher-salinity waters associated with the Equatorial Subsurface Water mass, reflecting the influence of upwelling in this region, although with lower intensity compared to the northern stations. The OMZ core was identified between 100 m and 300 m, with oxygen concentrations increasing again at greater depths to get relatively stable below 600 m (Fig. 2).

### 3.2. Taxonomic assemblages

The identified taxonomic units, their mean abundance and their mean size are summarized in Table S2 for each station. Zooplankton abundance showed significant differences between stations (one-way ANOVA, $p < 0.001$), although the depth effects varied with the station (Fig. 3) (Table S3). The Tukey post hoc test revealed significant differences for the station factor, only the T5–T3 comparison. These results emphasize the effect of spatial variability on zooplankton abundance across a horizontal scale of approximately 50 km. For the depth strata factor, we could identify particularly difference between the oxygenated surface waters (0–30 m and 0–100 m in the northern and southern upwelling regions, respectively) and the upper layer of their respective OMZ (90–150 m and 100–200 m in the northern and southern upwelling regions, respectively). There were also differences in the abundances between the two upwelling regions when comparing strata with similar dissolved oxygen conditions (e.g. between the 90–150 m and 100–200 m from the northern and southern upwelling region, respectively). However, the one-way ANOVA test did not show significant differences in the zooplankton abundances between day and night conditions when separated by stations (Table S3).

### 3.3. Diel vertical migration

Migration amplitudes were larger in stations T5 and T39 compared with T3 (Fig. 4) with *Corycaeus*, ostracods, *Oncaea*, annelids, foraminifera and chaetognaths having the highest amplitude of migration (ΔDVM: > 200 m). However, organisms with low amplitude of

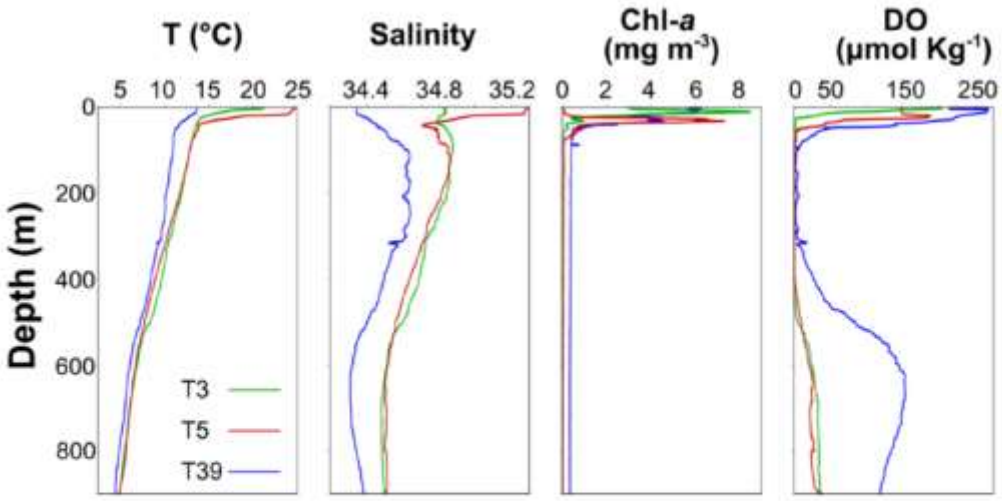


Fig. 2. Vertical profiles of temperature (T, °C), salinity, chlorophyll-a (Chl-a, mg $m^{-3}$), and dissolved oxygen (DO, µmol $Kg^{-1}$), in stations T3 and T5 at the northern upwelling region (February 2018), and station T39 at the southern region of Chile (January 2023).

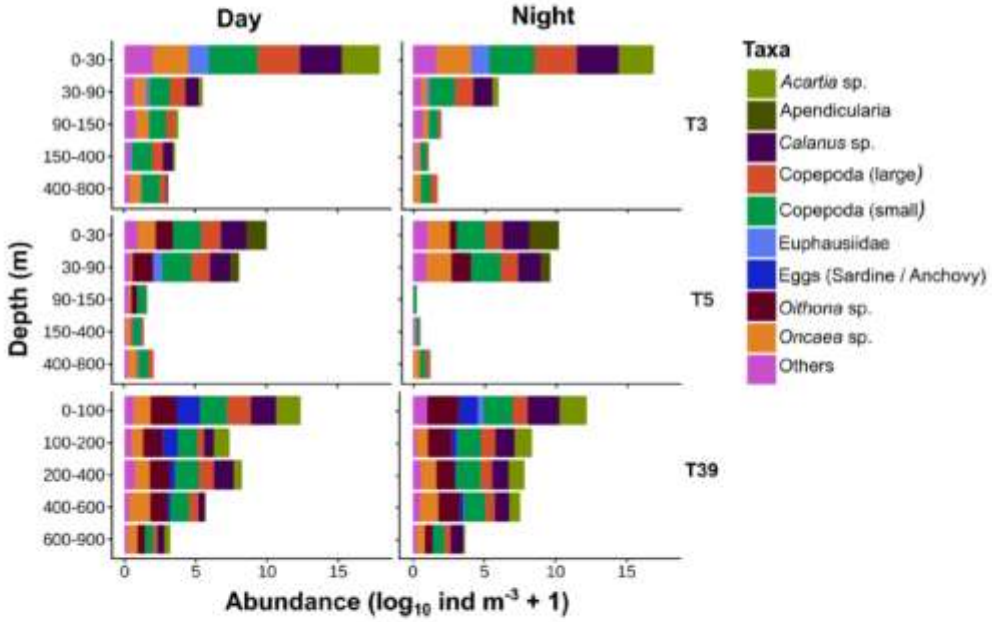


Fig. 3. Zooplankton abundance found at the northern upwelling region (Stations T3 and T5) and the southern region (station T39) during the daytime (left column) and nighttime (right column). Taxa represent major groups (taxonomic units) identified by ZooScan analysis.

migrations (ΔDVM: < 50 m) were identified across all three stations, including *Calanus* and small copepods. In the case of *Oitona*, large copepods, and siphonophores showed low migration too in at least two stations. Notably, some taxa such as *Acartia* did not exhibit vertical migration at the T3.

### 3.4. Size spectra

The size spectra (Fig. 5) showed that Station T39 had a biomass distribution in the size range of $2 \times 10^{-3}$ to 1.7 (µg C) on the surface which is smaller than the size range found in the northern region (> 2 µg C in the surface strata of T5 and T3).

In all situations, the size spectra of the upper layer exhibited a more uniform distribution and displayed larger size classes. The slopes became consistently more negative with water depth, indicating a greater dominance of the smaller size classes at depth (Fig. 5). There were no statistical differences in the slopes between day and night (pairwise Student *t*-test, $p > 0.05$). Significant differences, however,

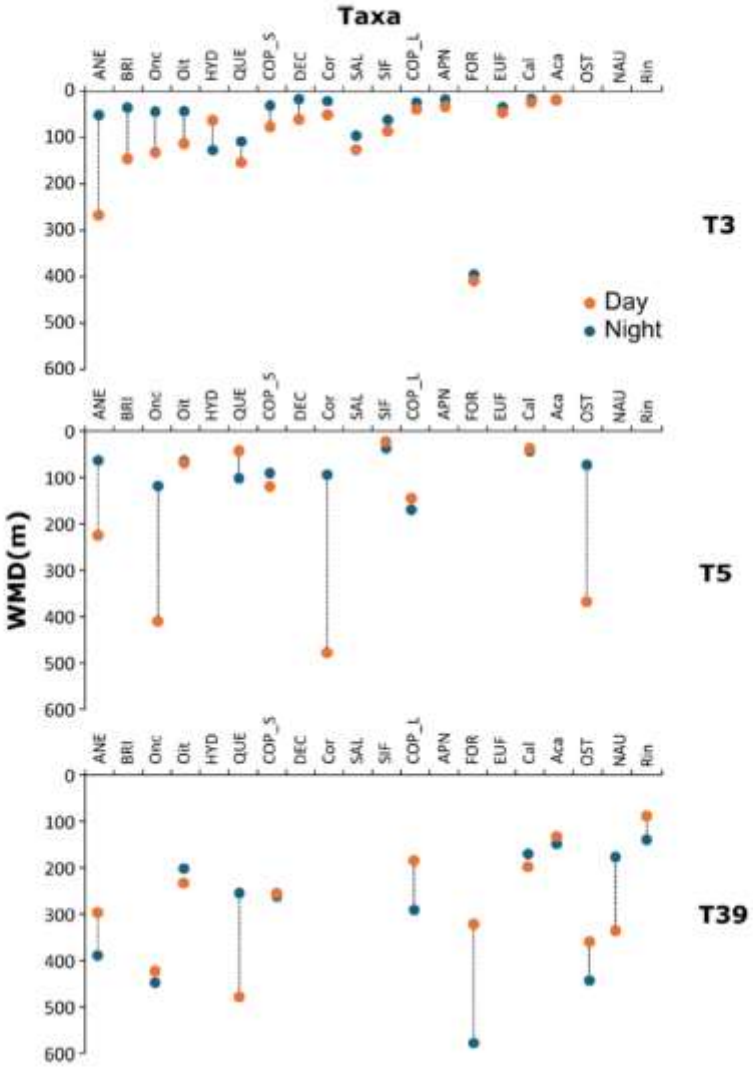


Fig. 4. Amplitude of zooplankton diel vertical migration at the three study sites. Dots indicate the weighted mean depth (WMD) during the day (orange) and night (blue), while the vertical arrows represent the differences in WMD, i.e. the migration amplitude. Taxa names are provided in Table S2.

were found between stations T5 and T39 (Student *t*-test, $p = 0.01$) and between the upper oxygenated layer (0–30 m and 0–100 m in the northern and the southern regions, respectively) and the upper OMZ (90–150 m and 100–200 m in the northern and the southern regions, respectively) (see Table S4).

### 3.5. Stable isotope composition and trophic position of zooplankton

Although no strong vertical trend was observed in the carbon and nitrogen stable isotope composition, a slight increase in $\delta^{15}N$ with depth was evident (reaching maximum values of ~ 19.4 ‰ at T5), while $\delta^{13}C$ generally decreased with depth (Fig. 6). Overall, isotopic values at station T5 showed greater variability compared to the other stations, whereas $\delta^{13}C$ values at station T39 were consistently lower compared to those found in the northern region.

Nitrogen isotopes varied significantly between stations and depth in both regions (one-way ANOVA, Table S5). In the northern region, $\delta^{15}N$ values differed between the surface (30–0 m) and mid-depth layers (150–90 m) compared to the deeper strata (800–400 m), while in the southern region the upper layer (0–100 m) was significantly different from all other strata (Table S5 and Fig. 6). No significant differences in $\delta^{15}N$ were detected among size classes at station T3 (Student *t*-test test, $p > 0.05$), whereas $\delta^{13}C$ differed between the 200–500 µm and 500–1000 µm size categories ($p < 0.05$). At station T5, significant differences in both isotope signatures were found between the 200–500 µm size fraction and all other size fractions ($p < 0.05$), while station T39 showed a pattern similar to station T3, with statistically indistinguishable $\delta^{15}N$ values ($p > 0.05$) but significant $\delta^{13}C$ differences between the 200–500 µm and 500–1000 µm fractions ($p < 0.05$).

Trophic position (TP) estimates ranged from 1.8 to 4, indicating a

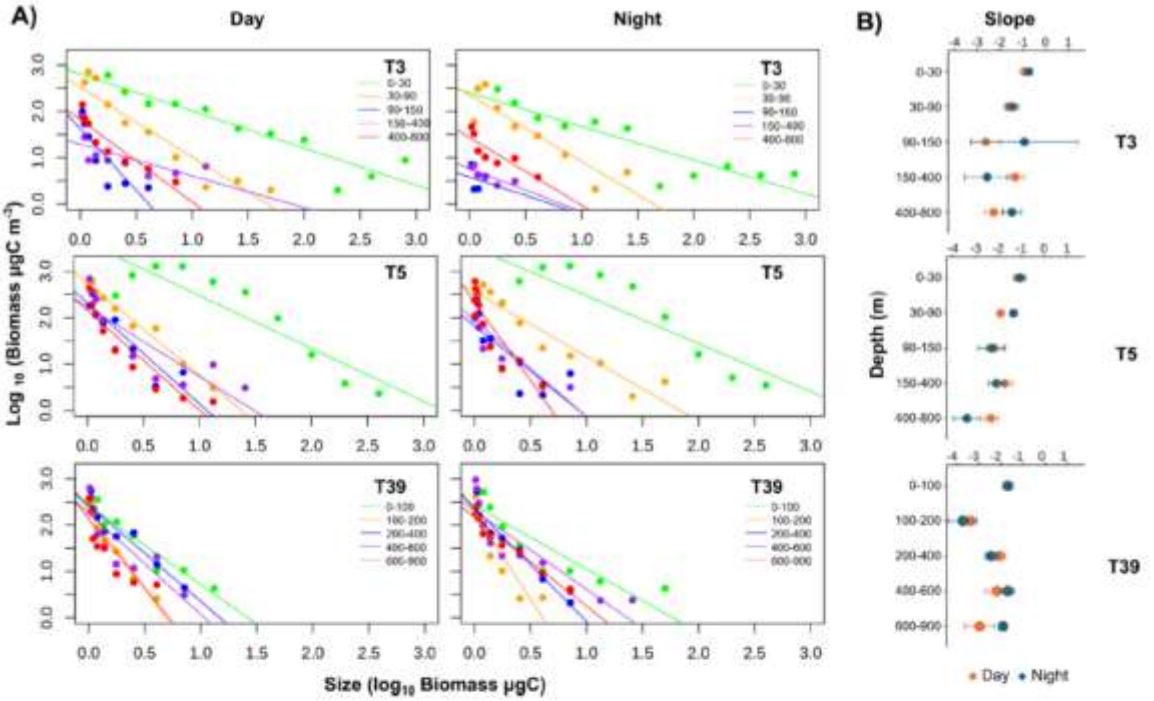


Fig. 5. (A) Normalized zooplankton size spectrum during day and night conditions at three sampling sites (T3, T5, T39) in upwelling zone of Chile. (B) Vertical distribution of the slopes of the size spectra at each sampling site. The error bars in the slope are standard errors derived from the linear regressions.

wide range of feeding modes, from herbivores (TP = 2) to carnivores (TP = 3–4). During the daytime, TP values tended to increase with depth, particularly at T5, where organisms from deeper strata (400–150 m, 800–400 m) reached TP values up to 4 (see Table 1). At night, TP values increased in surface waters compared to daytime, suggesting trophic shifts associated with diel vertical migrations. In contrast, stations T3 and T39 exhibited less pronounced vertical variation, with only a slight TP increase in deeper layers. It is important to note, however, that no nighttime isotope measurements were obtained at T3 below 90 m due to logistical constraints during sampling. Consequently, some depth comparisons, especially in deeper layers, rely exclusively on daytime data. This limitation should be considered when interpreting vertical patterns, although statistical analyses (ANOVA, Table S5) were conducted separately for day and night samples to minimize potential biases.

### 3.6. The trophic behavior index and environmental variability

The TBI, estimated according to Eq. (4) (see Methods), ranged from 0.5 to 2.4 across all samples, with each value corresponding to a specific taxonomic unit at a given station and depth strata. A total of 17 taxa were evaluated at station T3, 10 at T5, and 12 at T39 (Fig. 7). Mean TBI values, pooled by station and depth, revealed consistent patterns in the vertical distribution of zooplankton, with a general trend of increasing TBI values with depth (Fig. S6).

To assess potential influences of environmental variables (temperature, dissolved oxygen and Chl-a) on TBI, a stepwise (1-Step) multiple regression was first applied. This regression revealed that only temperature had a significant correlation to TBI (Table S7). Since the independent variables were strongly correlated to each other ($F_{2,236} > 7.1$, $p < 0.01$), a principal component analysis (PCA) was conducted to synthetize environmental effects on a single axis (Fig. S8). Thereafter, the first component (PC1) was contrasted and tested against TBI. PC1 was also significantly correlated to TBI. The correlations between TBI and temperature and PC1 and illustrated in Fig. S9.

The taxa associated with the classification of the 4 trophic functional groups present at each sampling stations are shown in Fig. 7. For instance, G4 present at both northern (T3 and T5) and southern area (T39) included *Acartia*, appendicularians, foraminiferans, small and mid-size copepods (e.g., *Oithona* and *Calanus*), some chaetognaths, siphonophores and large copepods. At the coastal station (T3), bryozoans, small-sized copepods (e.g., *Oncaea*), decapod larvae, euphausiids, and gelatinous organism (chaetognaths, salps, hydrozoas and siphonophores) were dominant in G3. Small copepods, (*Oithona*, and *Oncaea*) were present at both the northern (T3 and T5) and the southern station (T39), while annelids and ostracods were found at T5 and T39 in the same trophic group (G3). In group G3, *Calanus*, *Rincalanus*, nauplii and large copepods were predominant at Station T39. In group G2, foraminifera and chaetognaths were found at Station T39, *Corycaeus* at T5, and annelids at T3. Group G1 was not represented at any station when considering averaged TBI values (Fig. 7); however, some taxa classified as G1 were found at Station T39 when considered individually.

The vertical distribution of the relative abundance of the four trophic functional groups across the three stations is shown in Fig. 8. The presence of top predators (G1) was particularly notable at station T39, where they accounted for 4 % of the community below the OMZ, in the deeper layer (400–600 m). Second-level predators (G2) showed their highest relative abundances at T3 (38 and 46 %) within the OMZ (30–90 m and 90–150 m), and in the deep layer (400–800 m) at T5 (43 %). In contrast, G2 was less abundant throughout the water column at T39 (1–7 %), with values ranging from 1 % to 7 %. Moderate predators (G3) and low-level predators (G4) dominated at both northern stations (T3 and T5) and at the southern station (T39), with G4 displaying a decrease in relative abundance with depth. At T39, G4 predominated throughout the water column.

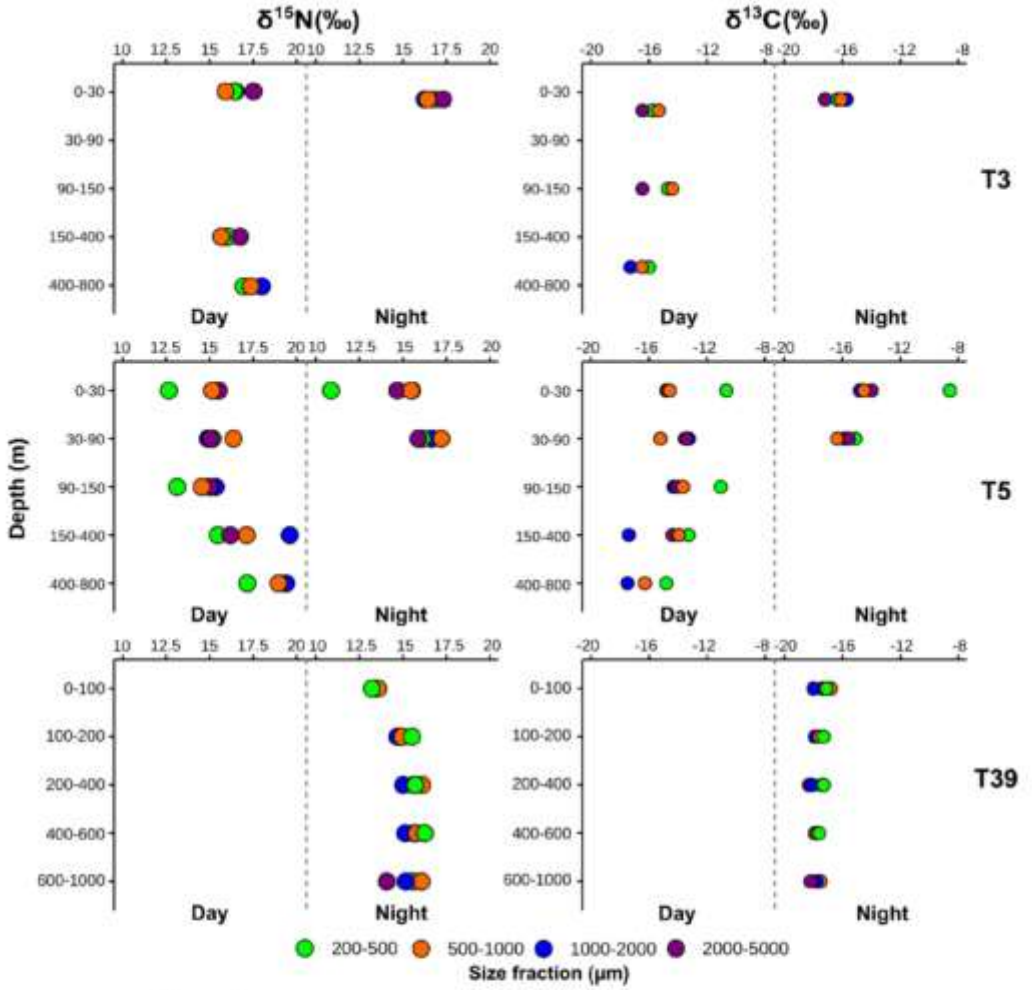


Fig. 6. Vertical distribution of $\delta^{15}N$ and $\delta^{13}C$ ratios in four zooplankton size fractions in the sampling stations during the austral summer in the northern upwelling zone (T3 and T5) and south-central zone (T39) of Chile. Replicated samples were obtained in 5 depth strata at daytime and nighttime conditions, except at T39 in which only nighttime samples were available.

To compare the food web structure and its relationship with the environmental conditions, the proportion of predator levels 1 and 2 (i.e., strict carnivores) (G1 + G2) with respect to the entire community (Fig. 9) was calculated and associated with oceanographic conditions. Percentage values above 10 % would be indicative of increased predatory behavior within the community. Although carnivorous zooplankton typically represent a minor fraction of the community in upwelling ecosystems, values exceeding this threshold could potentially indicate an unusually high presence of predators, which can exert significant top-down control. The proportion of G1 + G2 (carnivorous predators) revealed three distinct patterns: (i) an increase in abundance at night associated with vertical migration, as observed at station T5 in the upper limit of the OMZ (90–30 m) (Fig. 9); (ii) a higher proportion of these strong predators near the core of the OMZ (30–150 m), as seen at station T3; and (iii) a more uniform distribution of G1 and G2 throughout the water column, with a slight increase in abundance with depth, as observed in station T39. Additionally, an abrupt increase in G1 + G2 abundance in the deep layer (400–800 m) during the day at T5 may reflect a diurnal ascent of carnivores from deeper layers, not fully captured within our sampling scheme.

## 4. Discussion

### 4.1. Environmental changes and community structure

The distinct oceanographic settings observed at the three sampled stations highlighted the strongly variable conditions of the upwelling zone when comparing coastal vs offshore stations and northern vs southern regions. Although both northern stations (T3 and T5) shared some common conditions, such as a marked thermocline, and a sharp oxycline caused by the shallow OMZ, the vertical distribution of these variables changed markedly in depth. By contrast, the southern region (T39) was clearly different from T3 and T5, both in the magnitude of the oceanographic variables as well as in the vertical structure characterized by a much more mixed water column and weaker thermocline (also oxycline). These gradients were associated with distinct vertical stratification (zonation) in zooplankton abundance, particularly between the surface oxygenated layers and the upper boundaries of the OMZ in the

**Table 1**
Trophic position (TP) of zooplankton across different size fractions (μm) and depth strata (m) at three sampling stations (T3, T5 and T39) in the southeastern Pacific Ocean. n.d. indicates no data available for that category.

| Time | Station | Depth strata (m) | Size fraction (μm) | | | |
|---|---|---|---|---|---|---|
| | | | 200–500 | 500–1000 | 1000–2000 | 2000–5000 |
| Day | T3 | 30–0 | 2.0 | 1.9 | 2.0 | 2.3 |
| | | 90–30 | n.d | n.d | n.d | n.d |
| | | 150–90 | n.d | n.d | n.d | n.d |
| | | 400–150 | 1.9 | 1.8 | 1.9 | 2.1 |
| | | 800–400 | 2.2 | 2.3 | 2.5 | n.d |
| | T5 | 30–0 | 2.0 | 2.7 | 2.8 | 2.8 |
| | | 90–30 | 2.0 | 2.7 | 2.8 | 2.8 |
| | | 150–90 | 2.1 | 2.6 | 2.8 | 2.7 |
| | | 400–150 | 2.8 | 3.3 | 4.0 | 3.0 |
| | | 800–400 | 3.3 | 3.9 | 4.0 | n.d |
| Night | T3 | 30–0 | 2.0 | 2.0 | 2.0 | 2.3 |
| | | 90–30 | n.d | n.d | n.d | n.d |
| | | 150–90 | n.d | n.d | n.d | n.d |
| | | 400–150 | n.d | n.d | n.d | n.d |
| | | 800–400 | n.d | n.d | n.d | n.d |
| | T5 | 30–0 | 2.0 | 3.4 | 3.4 | 3.1 |
| | | 90–30 | 3.5 | 3.9 | 3.7 | 3.5 |
| | | 150–90 | n.d | n.d | n.d | n.d |
| | | 400–150 | n.d | n.d | n.d | n.d |
| | | 800–400 | n.d | n.d | n.d | n.d |
| | T39 | 100–0 | 2.0 | 2.1 | 2.1 | 2.1 |
| | | 200–100 | 2.7 | 2.5 | 2.5 | 2.0 |
| | | 400–200 | 2.8 | 2.9 | 2.6 | 2.7 |
| | | 600–400 | 2.9 | 2.8 | 2.6 | 2.8 |
| | | 900–600 | 2.7 | 2.9 | 2.6 | 2.3 |

northern region. In contrast, the southern station (T39) with a more homogeneous water column with deeper oxygen depletion, possibly contributed to a relatively uniform vertical distribution of taxa. These contrasting conditions may impact the taxonomic composition of the zooplankton community; for example, a decrease in the zooplankton abundances and biomass with depth was likely caused by the oxygen depletion in the OMZ, which is known to limit the vertical distribution and migration of some species (Escribano et al., 2009; Tutasi and Escribano, 2020). Regarding community size structure, the biomass size spectra revealed a shift in community structure with depth, where larger size classes were more abundant in the surface layers and smaller organisms dominating the deeper strata judging by a steeper slope. This pattern was consistent across the stations, suggesting a size-selective structuring of the water column. The significant differences in size spectra between stations T5 and T39 may further underscore the influence of local environmental conditions on community composition (size structure).

### 4.2. DVM behavior and size dependence

The observed diel vertical migration patterns in our study highlight the complexity and taxon-specific nature of this behavior across different environmental settings. Migration amplitudes were notably higher in stations T5 and T39, where environmental stratification was weaker and the oxycline deeper than at station T3, possibly allowing broader vertical movements. In contrast, station T3 exhibited reduced DVM amplitudes, likely constrained by a shallower and more intense OMZ, and stronger salinity and temperature stratification. These physical and chemical gradients can act as vertical ecological barriers, selectively filtering migratory capacity based on the species' physiological tolerance to hypoxia and energy availability (Donoso and Escribano, 2014).

Body size emerged as a significant, although not exclusive factor influencing DVM behavior. Larger zooplankton taxa, such as chaetognaths, annelids, and large copepods, exhibited the greatest migration amplitudes, often spanning > 200 m and eventually intruding the OMZ core (ca. 250 m). This is consistent with prior observations that larger organisms can better withstand low oxygen levels due to their higher energy reserves, lower surface-to-volume ratios, and often more efficient anaerobic metabolisms (Ekau et al., 2010; Wishner et al., 2018). Nevertheless, it should be noted that, although some taxa classified as strong migrators exhibited high TBI values due to their large size and active DVM behavior, their contribution to total abundance was low (<5%), indicating a limited influence on the overall community structure. Our results also revealed substantial DVM in relatively small taxa such as *Corycaeus*, *Oncaea* and *Acartia*, suggesting that factors such as life history strategies and predator avoidance also play critical roles in shaping DVM (Gilly et al., 2013; Frederick et al., 2024). Ecologically, DVM has far-reaching consequences. It not only structures predator–prey interactions by altering the spatial overlap between trophic levels but also contributes to the biological carbon pump through active transport of organic matter to depth (Pinti, et al., 2019; Steinberg and Landry, 2017). Although our results indicate that many taxa exhibit DVM, several species appeared to be largely resident, showing minimal or negligible vertical displacement. This pattern is consistent with previous findings in the northern Chilean upwelling system, where abundant copepod species such as *Paracalanus indicus*, *Calanus chilensis* and some cyclopoids were reported to remain restricted to the upper oxygenated layers without performing substantial DVM, likely constrained by the shallow oxycline (Escribano et al., 2009). Similarly, deeper layers may harbor species adapted to hypoxic conditions that remain resident within or near the OMZ. Acknowledging the presence of these non-migratory communities is important, as their vertical stability also plays a key role in structuring trophic interactions and carbon cycling within the upwelling system.

Overall, there is a clear need to consider both size and species identity when evaluating the ecological impacts of DVM. While body size is a useful proxy for migratory capacity, it does not fully explain the variability observed. A more nuanced understanding, incorporating traits such as metabolism, feeding strategy and vertical distribution of prey and predators is essential for accurately modeling zooplankton-mediated processes in upwelling ecosystems.

This size-dependent DVM behavior is the result of physiological and behavioral adaptations, with smaller organisms often having different ecological roles and predator avoidance strategies compared to the larger ones (Ringelberg, 2010). The size of zooplankton thus plays a

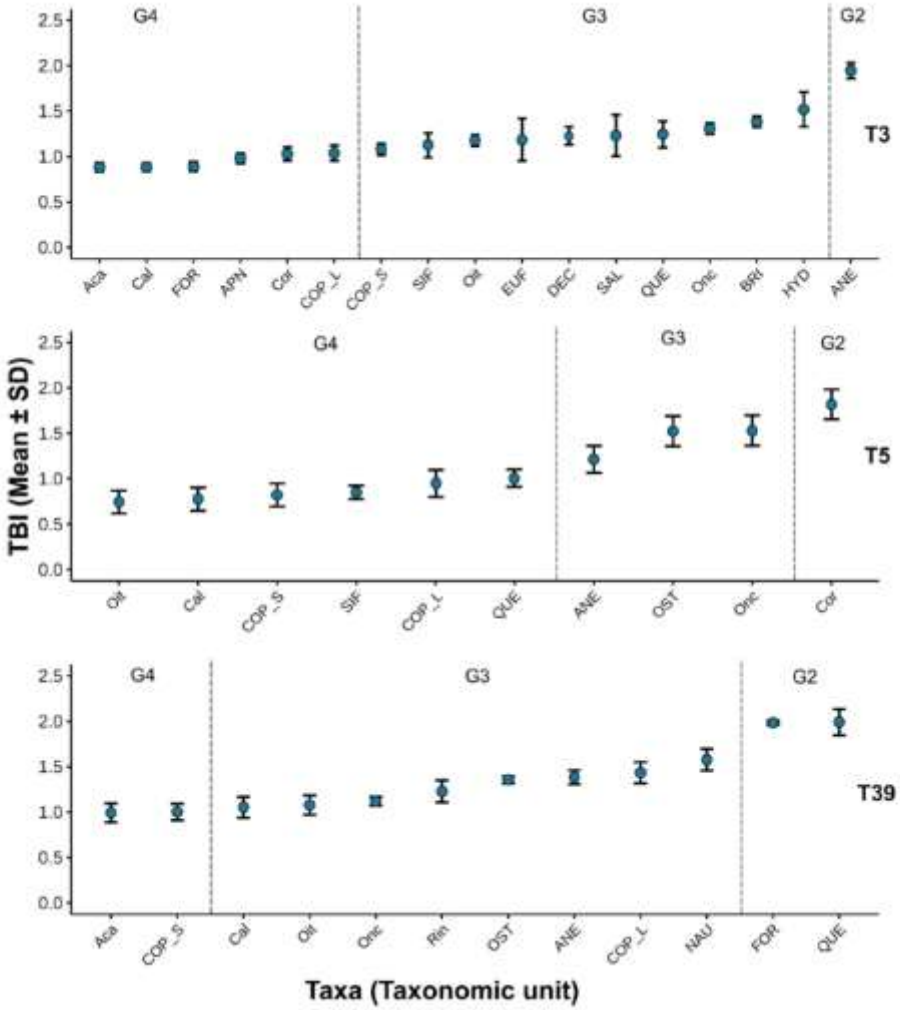


Fig. 7. Trophic Behavior Index (TBI) of zooplankton in the upwelling zones off northern and southern Chile. TBI are mean values and standard deviation (SD) of pooled data from different depth strata. Each taxonomic unit is shown along the x-axis. Acronyms for the taxonomic groups are detailed in Table S2. G1 to G4 define four trophic functional groups according to TBI values ranged uniformly in quartile values from the entire expected TBI range.

crucial role in determining their migration patterns, highlighting the importance of understanding size variations within these communities. Furthermore, there are ontogenetic changes in DVM patterns within species. For instance, small-bodied juvenile zooplankton, such as copepod nauplii, do not exhibit the same migratory behaviors as their larger adult counterparts (Escribano et al., 2009).

### 4.3. Isotopic composition and trophic position

The isotopic composition also pointed out the differential distribution of trophic functional groups across the water column. The differences related to size fractions and DVM between stations were mainly attributed to the number of taxa that exhibited high DVM, while most taxa presented an averaged DVM of ~40 m in station T3 (Fig. 4), with minimal differences in the $\delta^{15}N$ and $\delta^{13}C$ values between depth layers (Fig. 6). However, the community composition was more diverse in other stations (Table S2), generally when exhibiting more extensive amplitude of DVM (mean = 106.3 m) and higher variability in the isotopic signatures. Differences between the strata could be mostly attributed to composition and size structure variations, leading to distinct $\delta^{15}N$ and $\delta^{13}C$ values. For instance, the noticeably high $\delta^{13}C$ and low $\delta^{15}N$ values observed in the smaller size fraction in the upper layers of station T5 likely reflect a greater contribution of herbivorous suspension feeders, such as foraminifera and pteropods, which are typically associated with phytoplankton-based diets and, in many species, possess carbonate skeletons (Table S2).

The $\delta^{15}N$ increase with depth suggests a shift in the feeding behavior across the water column, as also reported by Hannides et al. (2013) for zooplankton in the oligotrophic North Pacific Subtropical Gyre at station ALOHA. Using compound-specific amino acid analysis, these authors demonstrated that this enrichment resulted from both an increase in trophic position (up to 0.6 TP-units) and a $^{15}N$ enrichment at the base of the food web. Although our study is based on bulk isotope analysis, the observed depth-related increase in $\delta^{15}N$ in our samples could also reflect

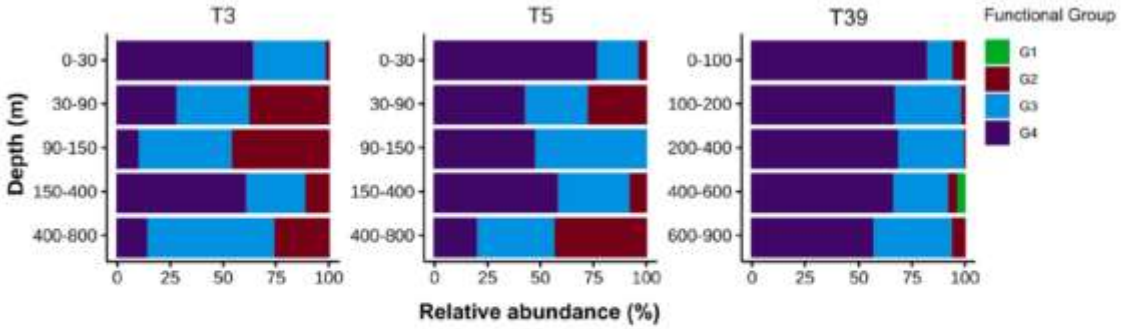


Fig. 8. Vertical distribution of the relative abundance of four trophic functional groups of zooplankton taxa at three stations (T3, T5 and T39) in the upwelling zone of the Southeast Pacific. G1, G2, G3, G4 were assigned according to a trophic behavior index (TBI values) estimated from body size, vertical migration behavior and trophic position of zooplankton assemblages.

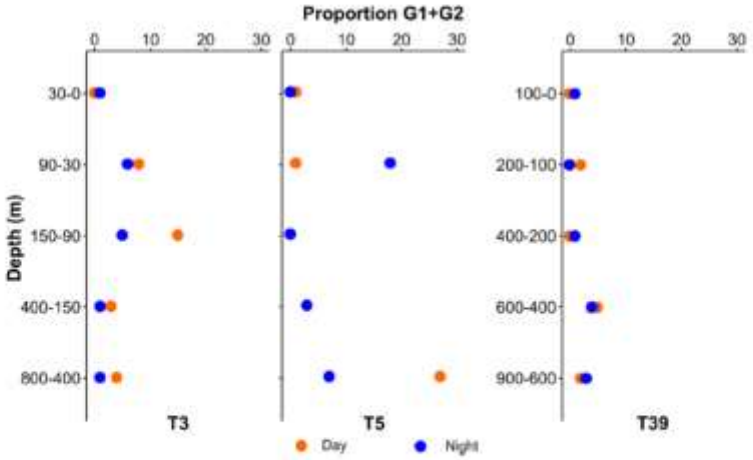


Fig. 9. Proportion (%) of levels 1 and 2 predators (functional groups G1 + G2) relative to the entire zooplankton community, separated by stations (T3, T5, T39), depth strata and day (orange) and night (blue) conditions. Functional groups defined as shown in Fig. 7.

a combination of these processes, with deeper zooplankton feeding at higher trophic levels and on food resources that are progressively enriched in $^{15}N$ through degradation and microbial reworking. Furthermore, the increased $\delta^{15}N$ values may also be accompanied by a variation in the isotopic signature of the source nitrogen resulting from denitrification processes (Dalsgaard et al., 2012). The higher TPs found in the northern upwelling zone (TP > 3) compared to the southern region (with TP values between 2 and 2.9) indicates the dominance of carnivores within the zooplankton community from the northern region than in the southern upwelling region, where the zooplankton was primarily omnivore. In upwelling ecosystems, $NO_3^-$ is typically the main source of new nitrogen and, therefore, changes in the $\delta^{15}N$ of the N-species (e.g. polypeptides) sustaining the food web is expected to be negligible, and thus the increased $\delta^{15}N$ values may be rather explained by trophic shifts. Understanding the finer-scale and time-integrated effects of upwelling is, however, essential for grasping the lengthening of coastal planktonic food webs. Using $\delta^{15}N$ measurements in amino acids, García-Seoane et al. (2023) found that in the NW Iberian Peninsula, microbial contributions to the food web decreased linearly with upwelling strength, indicating that microbial and metazoan food webs reach optimal coupling at low to moderate upwelling intensities. This suggests a shortening of food webs in more productive ecosystems, with increased complexity when considering microbial trophic steps. Similarly, Fernández-Urruzola et al. (2023) observed that, under mesotrophic or post-bloom conditions in the Southeast Pacific, zooplankton were predominantly omnivorous to carnivorous, and the microbial food web played a particularly important role in the energy transfer to larger zooplankton (> 1000 μm). These findings challenge the classical oceanic food web paradigm that traditionally considers highly productive environments dominated by large phytoplankton cells and stress the importance of predation on protozoa in sustaining oceanic food webs at intermediate productivities (Décima, 2022). However, in the absence of specific measurements of the microbial (or protozoan) contribution to the zooplankton diet the use of bulk $\delta^{15}N$ isotopic signatures, in combination with body size and DVM, allows for an integrated description of the trophic interactions and energy flow through the water column.

### 4.4. Integrating DVM, body size, and trophic position into a trophic behavior index

The integration of body size, DVM amplitude, and TP into a unified Trophic Behavior Index allowed us to move beyond taxonomic resolution and assess the functional structure of the mesozooplankton community across different upwelling regimes. This trait-based approach

proved effective in capturing the ecological strategies of dominant taxa and their contribution to vertical and horizontal trophic organization. Under this approach, a key finding is the encountered correlation between TBI and environmental variability, either with the principal component PC1, or with temperature. However, these correlations, although statistically significant, only explain a very low fraction of TBI variability (Fig. 5B). Furthermore, as TBI depends on size, DVM and trophic position, a negative correlation with temperature can be expected since small animals with limited DVM are mostly herbivores (i.e., with low TP) and tend to prevail in the upper layer with warm conditions. Variation of TBI across stations (i.e., among contrasting conditions) can thus occur independently from changes in temperature, oxygen and Chl-*a*. This interpretation is also supported by the absence of significant correlation between TBI and oxygen. It has frequently been suggested that the oxygen gradient can limit DVM in the upwelling zone (e.g. Tutasi and Escribano, 2020) and in that case low-oxygen conditions, such as in shallow strata of station T3, are expected to strongly prevent zooplankton DVM. While zooplankton biomass is closely linked to primary production (Hernández-León et al., 2020), the low correlation of TBI with Chl-*a* suggests that availability of the primary food sources is not the only factor affecting migration patterns and the structure of the food web within the zooplankton community. It should be noted that TBI value may represent different taxonomic units (or taxa) at variable locations, although they might indeed correspond to distinct species which cannot be properly resolved by ZooScan analysis.

### 4.5. TBI as a community descriptor

Our arbitrary classification into four trophic functional groups (G1 to G4) based on TBI revealed ecologically meaningful patterns. Groups G1 and G2, representing level 1 and 2 predators (mostly carnivores), were associated with deeper layers and with nighttime samples, where active migrators were more abundant (e.g., station T5). In contrast, G4 taxa, composed mainly of small suspension feeders, dominated surface waters and were more prevalent in stratified, oxygenated zones. The intermediate group (G3) was the most broadly distributed, potentially serving as a trophic link between producers and higher-level consumers. These patterns can be further illustrated by the trophic functional composition at each station (Fig. 10) which shows the relative abundance of each trophic group (G1 to G4) across different oceanographic zones — Subtropical Coastal, Subtropical Offshore in the northern region, and temperate conditions at the Coastal Transition Zone (CTZ) in the southern region. Distinct community structures were observed: intermediate and primary consumers (G3 + G4) prevailed across all zones, while predator-dominated groups (G1 + G2) were relatively more abundant (>10 %) in the offshore and CTZ zones. Notably, the latter was the only zone where G1 taxa were present.

Ecologically, the shifts in trophic composition, as those shown in Fig. 10, can have important implications. Predator-rich communities (high G1 + G2), characterized by strong migrators, may enhance vertical carbon flux through active transport, while G4-dominated systems may likely promote retention of freshly produced organic C near the surface. Moreover, a minor presence of G4 taxa in station T39 suggests a more heterotrophic food web structure upon low abundance of primary consumers (exclusively herbivores). Therefore, by synthesizing three key biological attributes into a single metric, TBI can offer a valuable tool to assess the trophic structures and their consequent ecological implications in the strongly heterogeneous and dynamic upwelling zone inhabited by a taxonomically complex zooplankton community. In this context, TBI may thus be considered an ecological indicator and a community descriptor with fundamental biological bases. For instance, organisms' size has long been recognized as one of the fundamental properties of biological communities regarding trophic ecology and the energy flow in any ecosystem (Peters, 1983; Décima, 2022). Diel vertical migration, on the other hand, is known to be closely related to prey-predator relationships (Kelly et al., 2019; Tutasi and Escribano, 2020), whereas $\delta^{15}N$ from bulk stable isotopic analyses has long been used to assess trophic roles of individual components within the food webs (e.g., Post, 2002; Massing et al., 2022). These combined ecological attributes can thus provide a suitable index to distinguish functional groups

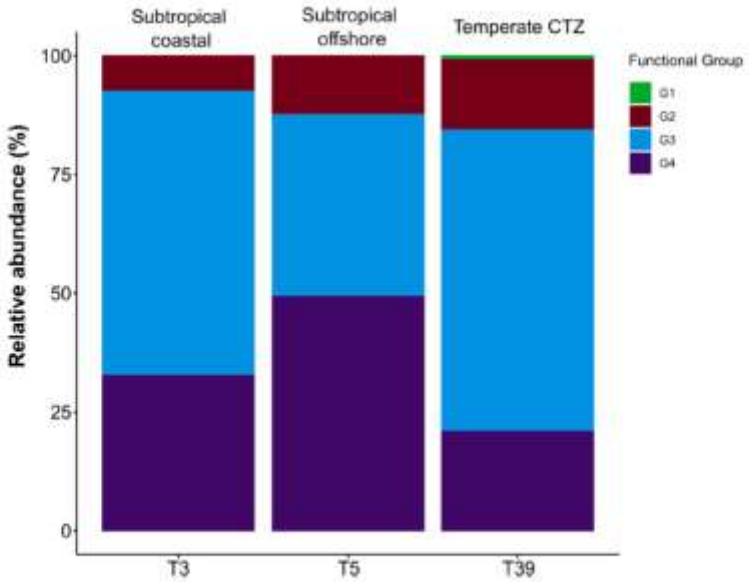


Fig. 10. Trophic functional composition of the zooplankton community across different oceanographic zones: Subtropical Coastal, Subtropical Offshore, Temperate Coastal Transition Zone (CTZ) in the upwelling zone of the southeast Pacific (Chile). The proportion of each trophic functional group (G1: Top predators, G2: Predators second level, G3: Moderate predators, G4: Low-level predators) is shown to illustrate the spatial patterns in food web structure upon different oceanographic conditions.

(beyond species), in terms of predation intensity, from zooplankton qualified as low-predators to strong-predators in different plankton communities conformed by a wide variety of consumers.

## 5. Conclusions

Variability in oceanographic conditions in the upwelling zone influences zooplankton community composition through differential responses to temperature, dissolved oxygen levels and water column stratification. However, our findings suggest that the trophic structure of zooplankton assemblages is primarily shaped by key ecological attributes of functional groups, including body size, diel vertical migration behavior and trophic position. These traits can be effectively integrated into the Trophic Behavior Index (TBI), which has been demonstrated to serve as a robust ecological indicator of zooplankton food web structure in upwelling systems. TBI thus provides a trait-based framework for meaningful comparisons across contrasting environmental conditions, as it accounts not only for the occurrence of specific functional groups but also for their relative contributions to community organization, offering a more integrative perspective than single-trait approaches.

## 6. Data availability

Oceanographic and data on zooplankton abundance and isotope composition of Carbon and Nitrogen are available at public repository Zenodo: https://doi.org/10.5281/zenodo.15397049.

## CRediT authorship contribution statement

**Cabrera-Núñez Susana:** Writing – original draft, Writing – review & editing, Methodology, Validation, Software, Data curation, Investigation, Conceptualization. **Fernández-Urruzola Igor:** Writing – review & editing, Visualization, Validation, Supervision, Investigation, Methodology, Conceptualization, Funding acquisition. **Bode Antonio:** Writing – review & editing, Visualization, Validation, Supervision, Methodology, Investigation, Funding acquisition, Conceptualization. **Hernández-Trujillo Sergio:** Writing – review & editing, Visualization, Supervision. **Hidalgo Pamela:** Supervision, Validation, Writing – review & editing, Investigation. **Escribano Ruben:** Writing – original draft, Writing – review & editing, Funding acquisition, Investigation, Visualization, Validation, Supervision, Formal analysis, Conceptualization.

## Funding

This work has been funded by the National Agency of Research and Development of Chile ANID AIM23_0003, FONDECYT 11221079 and Scholarship 21211977. Additional funding has been provided by the Millennium Nucleus DEOXS NCN2024_113 and by the IN607A 2022/05 grant to IEO by Xunta de Galicia (Spain). The LowPhox-2 cruise was funded by ANID grant AUB 150006/12806 and the Sonne cruise So296/2 by BMBF, Germany.

## Declaration of competing interest

The authors declare that they have no known competing financial interests or personal relationships that could have appeared to influence the work reported in this paper.

## Acknowledgements

We are grateful to two anonymous reviewers and the Associate Editor for their very thoughtful comments and corrections that helped to improve our work. We are also grateful to Natalia Osma who helped us to obtain and process samples for isotopes analyses and Daniel Toledo for scanning and processing zooplankton samples.

## Appendix A. Supplementary material

Supplementary data to this article can be found online at https://doi.org/10.1016/j.pocean.2025.103500.

## Data availability

Data will be made available on request.

## References

Aguirre, C., Garreaud, R., Belmar, L., Farías, L., Ramajo, L., Barrera, F., 2021. High-frequency variability of the surface ocean properties off central Chile during the upwelling season [original research]. Front. Mar. Sci. 0–2021. https://doi.org/10.3389/fmars.2021.702091.

Andersen, V., 2004. Vertical distributions of zooplankton across the Almeria-Oran frontal zone (Mediterranean Sea). J. Plankton Res. 26 (3), 275–293. https://doi.org/10.1093/plankt/fbh036.

Childress, J.J., Seibel, B.A., 1998. Life at stable low oxygen levels: adaptations of animals to oceanic oxygen minimum layers. J. Exp. Biol. 201 (8), 1223–1232. https://doi.org/10.1242/jeb.201.8.1223.

Dalsgaard, T., Thamdrup, B., Farías, L., Revsbech, N.P., 2012. Anammox and denitrification in the oxygen minimum zone of the eastern South Pacific. Limnol. Oceanogr. 57 (5), 1331–1346. https://doi.org/10.4319/lo.2012.57.5.1331.

de Mendiburu, F., de Mendiburu, M.F., 2019. Package 'agricolae'. R Package, Version 1 (3), 1143–1149.

Decima, M., 2022. Zooplankton trophic structure and ecosystem productivity. Mar. Ecol. Prog. Ser. 692, 23–42. https://doi.org/10.3354/meps14077.

Donoso, K., Escribano, R., 2014. Mass-specific respiration of mesozooplankton and its role in the maintenance of an oxygen-deficient ecological barrier (BEDOX) in the upwelling zone off Chile upon presence of a shallow oxygen minimum zone. J. Mar. Syst. 129, 166–177. https://doi.org/10.1016/j.jmarsys.2013.05.011.

Edwards, A.M., Robinson, J.P., Plank, M.J., Baum, J.K., Blanchard, J.L., 2017. Testing and recommending methods for fitting size spectra to data. Methods Ecol. Evol. 8 (1), 57–67.

Ekau, W., Auel, H., Pörtner, H.O., Gilbert, D., 2010. Impacts of hypoxia on the structure and processes in pelagic communities (zooplankton, macro-invertebrates and fish). Biogeosciences 7 (5), 1669–1699. https://doi.org/10.5194/bg-7-1669-2010.

Escribano, R., Hidalgo, P., Krautz, C., 2009. Zooplankton associated with the oxygen minimum zone system in the northern upwelling region of Chile during March 2000. Deep Sea Res. Part II 56 (16), 1083–1094. https://doi.org/10.1016/j.dsr2.2008.09.009.

Escribano, R., Schneider, W., 2007. The structure and functioning of the coastal upwelling system off central/southern Chile. Prog. Oceanogr. 75 (3), 343–347. https://doi.org/10.1016/j.pocean.2007.08.020.

Fernández-Urruzola, I., Bode, A., Loick-Wilde, N., Schneider, W., Lindsay, D., Escribano, R., 2023. Trophic ecology of midwater zooplankton along a productivity gradient in the Southeast Pacific. Front. Mar. Sci. 10:1057502. https://doi.org/10.3389/fmars.2023.1057502.

Fox, J., Weisberg, S., 2019. Using car functions in other functions. CRAN R.

Franks, P.J.S., 2002. NPZ models of plankton dynamics: their construction, coupling to physics, and application. J. Oceanogr. 58 (2), 379–387. https://doi.org/10.1023/A:1015874028196.

Frederick, L., Urbina, M.A., Jorquera, E., Escribano, R., 2024. Adjusting metabolic rates and critical oxygen tension in planktonic copepods under increasing hypoxia in highly productive coastal upwelling zones. Limnol. Oceanogr. https://doi.org/10.1002/lno.12556.

Fry, B., 2006. Stable Isotope Ecology. Springer Science+Business Media LLC.

García-Seoane, R., Vieira, L.G., Bode, A., 2023. Seasonal upwelling influence on trophic indices of mesozooplankton in a coastal food web estimated from δ15N in amino acids. Prog. Oceanogr. 219. https://doi.org/10.1016/j.pocean.2023.103149.

Gilly, W.F., Beman, J.M., Litvin, S.Y., Robison, B.H., 2013. Oceanographic and biological effects of shoaling of the oxygen minimum zone. Ann. Rev. Mar. Sci. 5, 393–420. https://doi.org/10.1146/annurev-marine-120710-100849.

Gorsky, G., Ohman, M.D., Picheral, M., Gasparini, S., Stemmann, L., Romagnan, J.-B., Cawood, A., Pesant, S., García-Comas, C., Prejger, F., 2010. Digital zooplankton image analysis using the ZooScan integrated system. J. Plankton Res. 32 (3), 285–303. https://doi.org/10.1093/plankt/fbp124.

Hammer, Ø., Harper, D., Ryan, P., 2001. PAST: paquete de programas de estadística paleontológica para enseñanza y análisis de datos. Palaeontol. Electron 4 (1), 4.

Hannides, C.C.S., Popp, B.N., Choy, C.A., Drazen, J.C., 2013. Midwater zooplankton and suspended particle dynamics in the North Pacific subtropical gyre: a stable isotope perspective. Limnol. Oceanogr. 58 (6), 1931–1946. https://doi.org/10.4319/lo.2013.58.6.1931.

Hernández-León, S., Koppelmann, R., Fraile-Nuez, E., Bode, A., Mompeán, C., Irigoien, X., Olivar, M.P., Echevarría, F., Fernandez de Puelles, M.L., González-Gordillo, J.I., Cozar, A., Acuna, J.L., Agusti, S., Duarte, C.M., 2020. Large deep-sea zooplankton biomass mirrors primary production in the global ocean. Nat. Commun. 11 (1), 6048. https://doi.org/10.1038/s41467-020-19875-7.

J. Kämpf P. Chapman 2016 The peruvian-chilean coastal upwelling system Upwelling Systems of the World 161 201 10.1007/978-3-319-42524-5_5.

Kelly, T.B., Davison, P.C., Goericke, R., Landry, M.R., Ohman, M.D., Stukel, M.R., 2019. The importance of mesozooplankton diel vertical migration for sustaining a

mesopelagic food web. Front. Mar. Sci. 6. https://doi.org/10.3389/fmars.2019.00506.
Manriquez, K., Escribano, R., Riquelme-Bugueño, R., 2012. Spatial structure of the zooplankton community in the coastal upwelling system off central-southern Chile in spring 2004 as assessed by automated image analysis. Prog. Oceanogr. 92–95, 121–133. https://doi.org/10.1016/j.pocean.2011.07.020.
Manning, J. C., Schukat, A., Auel, H., Auch, D., Kittu, L., Pinedo Arteaga, E. L., J., C. A., & W., H. (2022). Toward a Solution of the "Peruvian Puzzle": Pelagic Food-Web Structure and Trophic Interactions in the Northern Humboldt Current Upwelling System Off Peru. Frontiers in Marine Science, 8, 759603. https://doi.org/10.3389/fmars.2021.759603.
Medellín-Mora, J., Atkinson, A., Escribano, R., 2019. Community structured production of zooplankton in the eastern boundary upwelling system off central/southern Chile (2003–2012). ICES J. Mar. Sci. https://doi.org/10.1093/icesjms/fsz193.
Omori, M., Ikeda, T., 1984. Methods in Zooplankton Ecology. Wiley.
Pedersen, T. L. (2019). Package 'patchwork'. R package http://CRAN. R-project. org/package= patchwork. Cran.
Peters, R.H., 1983. Te Ecological Implications of Body Size. Cambridge Univ. Press, Cambridge, UK.
Pinti, J., Kiørboe, T., Thygesen, U.H., Visser, A.W., 2019. Trophic interactions drive the emergence of diel vertical migration patterns: a game-theoretic model of copepod communities. Proc. Biol. Sci. 286 (1911), 20191645. https://doi.org/10.1098/rspb.2019.1645.
Post, D.M., 2002. Using stable isotopes to estimate trophic position: models, methods, and assumptions. Ecology 83 (3). https://doi.org/10.1890/0012-9658(2002)083[0703:Usitet]2.0.Co;2.
Post, D.M., Layman, C.A., Arrington, D.A., Takimoto, G., Quattrochi, J., Montana, C.G., 2007. Getting to the fat of the matter: models, methods and assumptions for dealing with lipids in stable isotope analyses. Oecologia 152 (1), 179–189. https://doi.org/10.1007/s00442-006-0630-x.
Ringelberg, P., 2010. In: Diel Vertical Migration of Zooplankton in Lakes and Oceans. Springer. https://doi.org/10.1007/978-90-481-3093-1.
Roman, M.R., Brandt, S.B., Houde, E.D., Pierson, J.J., 2019. Interactive effects of hypoxia and temperature on coastal pelagic zooplankton and fish [Review]. Front. Mar. Sci. 6. https://doi.org/10.3389/fmars.2019.00139.
Steinberg, D.K., Landry, M.R., 2017. Zooplankton and the ocean carbon cycle. Ann. Rev. Mar. Sci. 9, 413–444. https://doi.org/10.1146/annurev-marine-010814-015924.
Team, R. C. (2025). R language definition. Vienna, Austria: R foundation for statistical computing.
Tutasi, P., Escribano, R., 2020. Zooplankton diel vertical migration and downward C flux into the oxygen minimum zone in the highly productive upwelling region off northern Chile. Biogeosciences 17 (2), 455–473. https://doi.org/10.5194/bg-17-455-2020.
Vinogradov, M. E. e. (1970). Vertical distribution of the oceanic zooplankton (Vol. 1). Israel Program for Scientific Translations.
Wickham, H., 2011. ggplot2. Wiley Interdiscip. Rev. Comput. Stat. 3 (2), 180–185.
Wilke, C. O., Wickham, H., & Wilke, M. C. O. (2019). Package 'cowploc'. Streamlined plot theme and plot annotations for 'ggplot2', 1.
Wishner, K.F., Seibel, B.A., Roman, C., Deutsch, C., Outram, D., Shaw, C.T., Birk, M.A., Minlan, K.A.S., Adams, T.J., Moore, D., Riley, S., 2018. Ocean deoxygenation and zooplankton: very small oxygen differences matter. Sci. Adv. 4 (12), eaau5180. https://doi.org/10.1126/sciadv.aau5180.
Zhou, M., 2006. What determines the slope of a plankton biomass spectrum? J. Plankton Res. 28 (5), 437–448. https://doi.org/10.1093/plankt/fbi119.

## 4.2 Capítulo 2: "Procesos biológicos y físicos que controlan el flujo de carbono mediado por el zooplancton y el micronecton en el sistema de surgencia frente al centro-sur de Chile"

Articulo científico enviado para publicación en la revista "Deep sea research Part I". FECHA


### Resumen

El flujo de carbono orgánico representa un componente esencial de la bomba biológica del océano y puede intensificarse mediante el transporte activo asociado a la migración vertical diaria (DVM) del zooplancton y los peces. En los sistemas de surgencia costera, la mayor parte de la producción biológica ocurre en aguas someras, donde los procesos físicos y biológicos interactúan promoviendo el transporte de carbono hacia las capas profundas. En este estudio se analizan las interacciones tróficas del zooplancton y el micronecton, sus patrones de DVM y el efecto de la surgencia que favorece el transporte costa-océano de biomasa planctónica, contribuyendo conjuntamente al transporte activo de carbono hacia aguas profundas en la zona de surgencia del centro-sur de Chile durante el verano austral de 2023.

Se obtuvieron muestras estratificadas en profundidad de zooplancton y micronecton bajo condiciones diurnas y nocturnas mediante los sistemas Multinet y MOCNESS-10, junto con mediciones hidrográficas. Los datos satelitales se emplearon para estimar el transporte de Ekman y la producción primaria neta (PPN). Durante eventos de surgencia activa, el transporte de Ekman podría movilizar aproximadamente 1.4 g C $m^{-3}$ $d^{-1}$ de biomasa de mesozooplancton dentro de la capa superficial. Adicionalmente, se analizaron las composiciones isotópicas de carbono y nitrógeno, incluyendo los isótopos de nitrógeno en aminoácidos, en cuatro clases de tamaño, para identificar la

fuente biogeoquímica y evaluar las posiciones tróficas a lo largo del gradiente costa-océano. La baja variabilidad en los valores de $\delta^{13}C$ y $\delta^{15}N$-fenilalanina indicó una fuente biogeoquímica común derivada de la producción costera. Las posiciones tróficas tendieron a aumentar hacia zonas oceánicas, identificando zooplancton herbívoro, así como zooplancton y micronecton carnívoros.

El transporte activo de carbono estimado en cinco estratos de profundidad hasta los 1000 m mostró un incremento a profundidades intermedias en la zona oceánica, con un promedio de 38.3 mg C $m^{-2}$ $d^{-1}$, lo que representa el 2.7% de la PPN oceánica y el 2.1% de la PPN costera. Los resultados indican que la advección costa-océano, combinada con las interacciones tróficas y la migración vertical, constituye un mecanismo eficiente que potencia el flujo descendente de carbono hacia aguas profundas, fortaleciendo la conexión entre la productividad superficial y los procesos de secuestro de carbono en el océano profundo.

# Biological and Physical Drivers of the Downward Carbon Flux Mediated by Zooplankton and Micronekton in the Upwelling System Off Central-Southern Chile

S. Cabrera-Núñez[1, 2], I. Fernández-Urruzola[2,3], A. Bode[4], N. Osma[2,3], V. Mohrholz[5], and R. Escribano[2,6]

[1]Programa de Postgrado en Oceanografía, Departamento de Oceanografía, Facultad de Ciencias Naturales y Oceanográficas, Universidad de Concepción, Casilla 160-C, Concepción, Chile.

[2]Millennium Institute of Oceanography, Universidad de Concepción, Concepción, Chile.

[3]Instituto de Ciencias Naturales Alexander von Humboldt, Universidad de Antofagasta, Antofagasta, Chile.

[4]Centro Oceanográfico de A Coruña, Instituto Español de Oceanografía, CSIC, A Coruña, España.

[5] Leibniz-Institute for Baltic Sea Research Warnemünde, Seestraße 15, 18119 Rostock, Germany

[6]Departamento de Oceanografía, Universidad de Concepción, Concepción, Chile.

Corresponding author: Ruben Escribano (rescribano@udec.cl)

## Key Points:

- Cross-shelf transport of zooplankton biomass produced in the upwelling zone can fuel the offshore deep-water ecosystem.
- Vertical migration and trophic interactions among zooplankton and micronekton promote the downward flux of C originating in the upwelling zone.

## Abstract

The downward flux of organic carbon is crucial in the ocean, and it can be promoted by active transport mediated by diel vertical migration (DVM) of zooplankton and fishes. In upwelling systems, most biological production occurs inshore, where physical and biological processes interact to promote C transport to depth. Here, we assess the trophic interactions of zooplankton and micronekton, their DVM behaviors, and the effect of upwelling circulation favoring inshore-offshore transport of zooplankton biomass, together promoting active C flux to deep waters in central-southern Chile during the Austral summer 2023. Depth-stratified zooplankton and micronekton samples under day-night conditions were collected with multinet and MOCNESS-10 systems, along with hydrographic measurements. Satellite data were used to estimate daily Ekman advection and net primary production (NPP). Ekman transport during active upwelling advected about 1.4 g C $m^{-3}$ $d^{-1}$ of mesozooplankton biomass within the Ekman layer. We also analyzed carbon and nitrogen isotope composition, including nitrogen isotopes in amino acids, in four size classes of zooplankton to trace elemental sources and assess their trophic positions. Low variability in phenylalanine $\delta^{15}N$ and $\delta^{13}C$ indicated a single elemental source from the upwelling region. Trophic positions increased offshore from herbivory to carnivory. Active C transport across five depth layers to 1000 m increased at mid-depth in the offshore, averaging 38.3 mg C $m^{-2}$ $d^{-1}$, representing 2.7% of offshore and 2.1% of inshore NPP. We conclude that cross-shelf advection combined with trophic interactions and DVM efficiently promotes C flux to deep waters.

**Plain Language Summary**

In the ocean off central-southern Chile, small drifting organism called zooplankton and mid-water fishes known as micronekton move up and down between surface waters that have plenty of oxygen and deeper layers with very little oxygen. As these migrate and as water flows from the productive coast out to the open ocean, carbon from the surface is carried down into the deep sea. We found that larger organisms higher up the food web, such as predators, are the main contributors to this active transport of carbon. Understanding how coastal productivity, organism movement, and water circulation work together to move carbon into the deep ocean is important because it helps us learn how the ocean stores carbon, especially as the climate changes.

# 1 Introduction

Pelagic organisms have a critical role in the downward flux of organic matter affecting ecological processes involved in the function of the biological carbon pump and its contribution to carbon sequestration to the deep ocean (Cook et al., 2023; Davison et al., 2013; Steinberg & Landry, 2017). As widely recognized, the biological carbon pump and the factors influencing its efficiency are key issues for assessing the global carbon budget upon ongoing climate variability (Siegel et al., 2023; Wang et al., 2023).

An important pathway for carbon sequestration to deep waters involves the dual contribution of pelagic organisms to both passive and active C fluxes. Among these, zooplankton and micronekton are recognized as key biological components, not only due to their production of fast-sinking fecal pellets, but also through their diel vertical migration (DVM) by which they can release organic C at depth through respiration, excretion, and mortality after feeding in the productive photic zone and then migrating downward (Ariza et al., 2015; Hidaka et al., 2001; Kwong et al., 2020). Although DVM is a behavioral response to the predator-prey dynamics (Ringelberg, 2010) its implications for carbon export are increasingly recognized, particularly in highly productive upwelling zones with oxygen minimum zones (OMZs), where migrant organisms often descend through or stay within the hypoxic layers (Kiko & Hauss, 2019; Massing et al., 2022; Tutasi & Escribano, 2020).

In coastal upwelling zones, strong gradients in oxygen and temperature may favor the C export and retention at depth. These gradients not only occur in the vertical axis, but also horizontally over the cross-shelf dimension (Escribano & Schneider, 2007). When coupled with physical forcing such as advection and convection processes, these gradients promote both vertical and lateral transport of organic matter produced in the upwelling zone, thereby fueling the deep ocean ecosystem with organic C (Flores et al., 2023; González et al., 2023). While such environmental gradients are commonly associated with changes in the zooplankton and micronekton communities, both vertically and horizontally, it is also essential to consider the trophic behavior of these organisms which can vary independently from the environmental gradients. For instance, omnivorous taxa tend to dominate surface layers, whereas deeper strata are often inhabited by more carnivorous

species (Fernández-Urruzola et al., 2023; Hannides et al., 2013; Hernández-León et al., 2019; Massing et al., 2022). These trophic shifts are not only a consequence of community diversity, but they also reflect evolved behavioral strategies such as dietary flexibility or vertical migration, both influencing the efficiency of carbon transfer through the water column.

Understanding the trophic behavior of the community is a necessary step to evaluate its functional role in vertical and lateral carbon export. The variety of trophic behaviors is not only reflected in the community composition, but also in the isotopic signatures of the species. In particular, the nitrogen stable isotope composition ($\delta^{15}N$) of the bulk biomass of zooplankton usually increases with depth due to a trophic enrichment and a more reworked sinking organic matter (Bode & Hernández-León, 2018; García-Seoane et al., 2023; Koppelmann et al., 2003). However, ecological inferences based on bulk $\delta^{15}N$ values require concurrent analyses of the isotopic signatures of both prey and consumers and are additionally influenced by artifacts arising from temporal decoupling between their isotopic baselines due to differences in turnover rates, growth, and life cycles. To overcome these issues, the compound-specific isotope analysis of nitrogen in amino acids (CSIA-AA) provides a more reliable approach to disentangle trophic enrichment from baseline variability. In this case, the N source represents the isotopic signature of nitrogen at the base of the food web, reflecting the $\delta^{15}N$ values of primary producers or the nitrogen source. Because amino acids such as phenylalanine have minimal trophic enrichment during assimilation, their $\delta^{15}N$ values are conserved across trophic transfers used as indicators of the nitrogen baseline. Thus, comparing the $\delta^{15}N$ of phenylalanine with that of trophic fractionating amino acids (e.g., glutamic acid) allows baseline isotopic variation from true trophic enrichment effects (Gloeckler et al., 2017; McCarthy et al., 2007; McClelland & Montoya, 2002). This approach has proven useful in identifying the feeding depth and trophic structure of vertically migrating organisms, offering insights into the ecological pathways that underpin carbon transfer to the deep ocean (Bode & Hernández-León, 2018; Hernandez-Leon et al., 2020).

At the coastal upwelling zone of Central Chile, González et al. (2023) suggested that deep waters of the Atacama Trench located offshore may receive plankton from the inshore upwelling zone which is being transported by mesoscale process farther offshore

and taken to depth by passive sinking and vertical migration. This may be a very efficient mechanism to fuel the deep ocean ecosystem with freshly produced organic C. However, the ecological processes linking the original sources of C produced in shallow coastal waters and the downward flux of C into deep waters remain unclear. In a first step, the organic matter in the form of fresh plankton biomass must be transported from shallow waters (<200 m) to deep layers (>1000 m), and this process can be controlled by advective forces including mesoscale eddies (Hormazabal et al. 2013; Morales et al. 2010) and near-surface cross-shelf advection due to Ekman transport (Giraldo et al. 2001). A second step may involve the incorporation of this plankton into the food web which can be accomplished by predation by larger zooplankton and micronekton at the coastal transitional zone and offshore region. Thereafter, passive sinking of organic matter such as fecal pellets and active transport by DVM might control the downward flux below the thermocline and down to mesopelagic or deeper layers. In this study, we investigate how cross-shelf advection and biological processes together drive the transfer of organic matter from the coastal upwelling zone toward deeper and offshore regions along the central-southern Chilean margin. Specifically, we examine the lateral transport of organic material and the trophic and migratory behaviors of zooplankton and micronekton that facilitate vertical carbon export. Using the CSIA-AA technique, we trace the sources of organic matter supporting these consumers and assess their trophic linkages and predator–prey interactions through which planktonic biomass is incorporated into the food web and ultimately exported to depth via active migration. By integrating DVM with trophic relationships across environmental gradients, our aim is to uncover the ecological mechanisms that couple coastal productivity with deep-ocean carbon sequestration in upwelling ecosystems.

# 2 Materials and Methods

## 2.1 Study area

The sampling was carried out in the upwelling area over the continental shelf off Concepción in four oceanographic stations, as show in Fig. 1a, during the So296/2-Leg 1 cruise, onboard the German R.V. SONNE. The cruise was carried out during the austral summer (late January 2023), when intense and constant winds sustain regular upwelling events in the coastal region (Escribano and Schneider, 2007). The hydrographic data were

obtained by deployment of a Seabird SBE-911 plus Conductivity, Temperature, and Pressure sensor (CTD) equipped with an oxygen sensor (SBE 43) and a SeaTech Fluorometer to estimate Chlorophyll-a (Chl-a).

Environmental information was complemented with satellite derived Net Primary production (NPP) as a product of the Global Ocean Color (Copernicus-GlobColour), Bio-Geo-Chemical data (L4 monthly and interpolated) from Satellite Observations (1997-ongoing). provided by the Copernicus Marine Environment Monitoring Service (CMEMS, 2023). These data cover a monthly average period from January 01to January 31, 2023, with a spatial resolution of approximately 4 km.

We also estimated the Ekman transport, which was calculated using a hourly sea surface wind data obtained from the Global Ocean Level-4 product (CMEMS, 2024). This dataset consists of stress-equivalent wind at a spatial resolution of 0.125°, derived from a combination of satellite scatter-meter observations and ERA5 reanalysis data from the European Centre for Medium-Range Weather Forecasts. The data corresponding to the temporal (01/21/2023 to 01/27/2023) and spatial domain (sample station) of interest were extracted using the tidync and ncdf4 packages in R. The northward component of the wind was used to calculate the meridional Ekman transport ($M_x$) at each station, following the equation:

$$M_x = \tau_y / f \quad Eq.1$$

Where $M_x$ represents Ekman transport ($m^3\ d^{-1}\ km^{-1}$), f is the Coriolis parameter and τy denotes the alongshore wind stress (Pa). $M_x$ is positive four south winds and negative for north winds, and tau (τy) was estimated as:

$$\tau_y = \rho_a\ C_d \left(V_y\ |V_y|\right) \quad Eq.2$$

Where $\rho_a$ is the air density (1.2 kg $m^{-3}$), $C_d$ is the drag coefficient (0.0013) and $V_y$ is the velocity of the alongshore component of the wind (m $s^{-1}$). The stations and dates grouped the resulting daily transport values to assess temporal patterns in wind-driven transport.

## 2.2 Field sampling

Mesozooplankton samples were collected by stratified obliques hauls of a Hydrobios Multinet midi type (Kiel, Germany) with a 0.25 $m^2$ opening area and 200 µm mesh size. Up to five depth-strata were defined according to the oxygen concentrations in the water

column (Table 1): in the coastal stations (St. 18, 26 and 31) above the costal shelf 2 or 3 depth-strata were considered between the surface and 200 m, whereas in the oceanic station (St. 39, day and night hauls) 5 depth-strata were sampled between the surface and 1000 m. The towing speed of the net was 0.3 m $s^{-1}$. Samples were collected for both taxonomic and isotopic analyses. Those intended for taxonomic identification were preserved in a 5% buffered formalin-seawater solution. Samples for elemental and isotopic composition analysis were first fractionated in four size classes (200-500, 500-1000, 1000-2000, 2000-5000 μm) and subsequently frozen in liquid nitrogen.

Micronekton samples were obtained by means of a MOCNESS-10 net (Multiple Opening-Closing Net and Environmental Sensing System) deployed during the day (16:00 h) and night (23:00 h) down to 1000 m to collect micronekton samples (2-20 cm), with the depth strata being the same as those sampled by the Multinet (Table 1). The net-frame had a 10 $m^2$ mouth opening, equipped with 6 nets of 3 mm mesh size each. The MOCNESS net worked in real time through a conductive cable and a deck unit, allowing us to monitor the angle and to close each net at the selected depths. The net was trawled at a speed between 2-3 knots and recovered at 0.5 m $s^{-1}$. From the samples, individual organisms, mainly fish, were sorted, measured and frozen in liquid nitrogen.

Table 1. Depth distribution of oxygen layers at each station. These layers were determined based on dissolved oxygen concentration across stations. Surface saturated oxygen layer (Upper-Oxy), the oxygen minimum zone (OMZ), and the suboxic layer (Lower-Oxy).

| Station | Depth strata (m) | Oxygen layer |
|---|---|---|
| **18** | 20-0 | Upper-Oxy |
| | 60-20 | OMZ |
| **26** | 20-0 | Upper-Oxy |
| | 80-20 | OMZ |
| **31** | 25-0 | Upper-Oxy |
| | 80-25 | Upper-Oxy |
| | 200-80 | OMZ |
| **39** | 100-0 | Upper Oxy |
| | 200-100 | OMZ |
| | 400-200 | OMZ |
| | 600-400 | Lower-Oxy |
| | 1000-600 | Lower-Oxy |

## 2.3 Zooplankton and micronekton samples processing

The taxonomic identification of mesozooplankton groups was carried out by digitized image analysis using the Hydroptic ZooScan digital imaging system. Samples were first scanned and digitized at a resolution of 2400 Dpi and then analyzed by the ZooProcess software. The biomass of each taxa identification was estimated from the equivalent spherical diameter (ESD), converted to carbon units (mg C), after calculating the dry weight per individual as 34.3*ESD (mm)^2.38 (Medellín-Mora et al., 2020), and assuming the carbon content of dry biomass to be a constant 40% by weight (Escribano & Schneider, 2007; Omori & Ikeda, 1984). The zooplankton abundances (ind. $m^{-3}$) were calculated considering the number of individuals in each group, the fraction used for the ZooScan analysis, and the filtered volume by the net ($m^3$). The community structure was described in terms of relative abundances and the vertical distribution of each taxon. Copepods were identified as large copepods (COP_L) or small copepods (COP_S) according to their ESD (mm).

The differences in zooplankton abundances across depths and size-classes were evaluated using the Kruskal-Wallis test, since the data did not meet the assumptions of normality and homoscedasticity required for parametric tests. All statistical analyses and visualizations were conducted in R v 4.3.2 (Team and R. C, 2025). Multivariate analysis was used to evaluate differences in the taxonomic composition of zooplankton across oxygen layers along the transect and between stations. This analysis of similarities (ANOSIM) was performed using Bray-Curtis similarity on logarithm-transformed data of abundance, separately. Samples were grouped according to their position relative to the OMZ, categorizing depth strata as: (i) saturated and oxycline conditions (Upper- Oxy); (ii) the OMZ core (OMZ), with dissolved O2 stratum) concentrations < 20 µmol O2 $kg^{-1}$ (Tutasi & Escribano, 2020); and (iii) increased oxygenated conditions in deeper waters below the OMZ (lower-Oxy) stratum (only found at the oceanic station, St. 39) (Table 1). Similarity Percentage Analysis (SIMPER) was also conducted to identify the taxa contributing the most to the observed dissimilarities among depth layers. ANOSIM and SIMPER analysis were performed in PRIMER-6 v.6.1.5 (Clarke & Gorley, 2006).

The micronekton taxa were identified usually down to family level, weighted (wet mass, g) and measured in length (cm). Approximately 1 mg of dorsal muscle was obtained,

avoiding bones, skin and internal organs, for subsequent isotopic analyses. These subsamples were freeze-dried and stored in dry conditions until further analyses. Carbon biomass was estimated by converting wet mass (WM) to dry mass (DM), and subsequently DM to carbon biomass. The water content was assumed 75% for fish and crustaceans based on values reported by Cotté et al. (2022). The percentage of carbon in dry mass (%C in DM) was derived from our own bulk stable isotope analyses performed on representative taxa from each group (Table S1). These values were then averaged per group and used to convert DM to carbon biomass for trophic and carbon flux analyses. The abundance was estimated by the number of individuals of each family or taxonomic group from each net; these counts were then standardized to individuals per cubic meter (ind. $m^{-3}$) using the filtered water volume in each haul. This allowed for a consistent comparison of micronekton abundance across depth strata and stations.

## 2.4 Stable isotope analyses

Nighttime samples were used for isotopic analyses, considering the negligible differences in the isotopic composition of size-fractions (zooplankton) or species (micronekton) over the daily cycle (Bode et al., 2021). For micronekton, we chose 3 individuals of each family at all depth-strata. All dried samples were ground to fine powder using a mortar and pestle.

We packed ca. 1 mg of dry material into tin capsules for bulk measurements of $\delta^{15}N$ and $\delta^{13}C$ in the samples. The determination of $\delta^{15}N$ and $\delta^{13}C$ was performed via combustion in a Flash IRMS analyzer coupled through a Conflo IV interface to a DeltaV Advantage isotope ratio mass spectrometer (Thermo Scientific). The results are expressed in ‰ relative to atmospheric air and VPDB (Vienna Pee Dee Belemnite), respectively. In each analytical sequence, the following secondary standards were used for $\delta^{15}N$: USGS 40 (-4.52‰), USGS 41a (+47.55‰), IAEA-N-1 (+0.4‰), IAEA-N-2 (+20.3‰), and USGS-25 (-30.4‰). For $\delta^{13}C$, the standards used were: USGS 40 (-26.39‰), USGS 41a (+36.55‰), NBS 22 (-30.031‰), and USGS 24 (-16.049‰). To evaluate precision (standard deviation), acetanilide was used as a reference material, yielding ± 0.15‰ (n=10). $\delta^{13}C$ values were corrected for the depletion caused by variable lipid content using the C:N ratio measured concurrently. This correction was made using the equation provided by Post et al. (2007) for aquatic invertebrates.

Compound specific isotope analyses of $\delta^{15}N$ in individual amino acids (CSIA-AA) was additionally performed in subsamples following Bode et al. (2021). Samples were first derivatized to improve the chromatographic behavior of the single amino acids; in short, the procedure included a hydrolysis step with 2 mL 6N HCl (20 h, 110 ◦C), followed by filtration (0.2 μm hydrophilic filters) and evaporation under $N_2$ at 60 ◦C. Extracts were further esterified with a mixture of 2.5 mL acetyl chloride:2-propanol (1:5) (60 min, 110 ◦C), and derivatized with a mixture of 0.9 mL diclomethane:trifluoracetic anhydride (DCM:TFAA, 3:1) (15 min, 110 ◦C). The resulting derivatized AAs were purified by solvent extraction using 3 mL of chloroform:phosphate buffer (1:2) ($Na_2HPO_4$ + $NaH_2PO_4$ in Milli-Q water, pH = 7.4) after centrifugation (13200 rpm, 10 min) and evaporation at room temperature under $N_2$. Finally, acyl-derivatives were re-dissolved in 0.25 mL of DCM and stored in vials at −20 ◦C until CSIA-AA.

The analysis of derivatized amino acid extracts was performed using a DeltaV Advantage isotope ratio mass spectrometer (Thermo Scientific), coupled via a Conflo IV continuous flow interface to a Trace1310GC gas chromatograph (Thermo Scientific) and a GC Isolink combustion module (Thermo Scientific). The TFA derivatives of the amino acids were separated by gas chromatography using a TG-5MS column (60 m, 0.32 mm × 1.0 μm); after separation, the different species underwent combustion to generate $N_2$ gas, which was subsequently analyzed via electron ionization.

The method allows for the analysis of the following individual amino acids: alanine (Ala), glycine (Gly), threonine (Thr), serine (Ser), valine (Val), leucine (Leu), isoleucine (Ileu), proline (Pro), methionine (Met), phenylalanine (Phe), and lysine (Lys). Considering that acid hydrolysis of the sample converts glutamine (Gln) into glutamic acid (Glu) and asparagine (Asn) into aspartic acid (Asp), the isotopic nitrogen abundance was determined by the combinations Gln+Glu (Glx) and Asn+Asp (Asx). The $\delta^{15}N$ results are expressed in ‰ relative to atmospheric air. All isotopic analyses were conducted at the Servicio de Analisis Instrumental from the University of A Coruña (Spain).

## 2.5 Trophic Ecology

The zooplankton and micronekton trophic positions (TP) were then calculated as follows:

$$TP_{Tr} = [(\delta^{15}N_{Tr} - \delta^{15}N_{PheC} - \beta)/(TDF)] + 1 \quad Eq.3$$

where $Tr$ is the trophic AA, either Glx or Ala, $\beta$ stands for the difference between *Tr* and Phe at the base of the food web. In the case of zooplankton, $\beta$ was assumed to be 3.4‰ and 3.2 ‰ for Glx and Ala, respectively, while the $^{15}$N enrichment of $Tr$ in each trophic step ($TDF$) was assumed to be 7.6‰ and 4.5‰ for Glx and Ala, respectively, after Fernández-Urruzola et al. (2023). In the case of micronekton, $\beta$ values were 3.6‰ and 3.2‰ for Glx and Ala, respectively, and $TDF$ being 5.7‰ and 6.1 for Glx and Ala, respectively following Bode et al. (2021).

The effect of trophic discrimination in the source AA Phe ($\delta^{15}N_{Phe}$) was corrected ($\delta^{15}N_{PheC}$) (Xi et al. 2020) by assuming a 0.4‰ enrichment at each trophic level according to Chikaraishi et al. (2009):

$$\delta^{15}N_{PheC} = \delta^{15}N_{Phe} - 0.4 \text{ x } (TP_{Glx} - 1) \quad \text{Eq. 4}$$

The fractional contribution of the microbial loop into the metazoan food web was calculated using the difference between the $TP_{Ala}$ and $TP_{Glx}$ after (Fernández-Urruzola et al., 2023):

$$\%\ Microbial\ contribution = 100 \text{ x } \frac{TP_{Ala} - TP_{Glx}}{TP_{Ala}} \qquad Eq. 5$$

Significant differences in $\delta^{15}N_{PheC}$, TP and contribution of the microbial either between groups or depth-strata were assessed using a one-way analysis of variance (ANOVA). Data normality and homoscedasticity were first confirmed using the Shapiro-Wilk and Levene's tests, respectively.

## 2.6 Carbon Flux Estimation

The amplitude of the diel vertical migration (ΔDVM) was calculated only in the oceanic station (St. 39) for the identified zooplankton and micronekton migrators (having a ΔDVM >100 m). ΔDVM is the difference between the weighted mean depth (WMD) during the day and night for each taxa considering the width of each depth strata (Andersen, 2004; Tutasi & Escribano, 2020):

$$\text{WMD} = \Sigma\,(ni \times zi \times di)/\,\Sigma\,(ni \times zi) \qquad \text{Eq. 6}$$

where *n*i is the biomass (mg C m$^{-3}$) of a given taxonomic group, *z*i is the width (m) of the strata and *d*i is the mean depth of the strata (m). In one case, the haul corresponding

to the 100-200 m stratum was missed; therefore, we estimated its value using data from the adjacent strata above and below. This adjustment was applied only to myctophid fish, which dominated among migrators.

In addition, we estimated the TP for each selected migrating taxa of zooplankton. This TP was assumed from the corresponding TP of the size fraction of which the taxa belonged to. In the case of micronekton we used the TP corresponding to each taxon.

To estimate the downward flux of C (*C flux*), we first quantified the carbon biomass of the migratory zooplankton and micronekton (mg C $m^{-2}$) across depth strata sampled during day and night. This migratory biomass was determined as the difference in carbon biomass between nighttime and daytime samples in each depth strata. The *C flux* was calculated using the formula:

$$C\ flux = MB\ \times \left(\frac{R + E + M}{2}\right) \qquad Eq.7$$

where MB is the migratory biomass, *R* was the respiration rate estimated for zooplankton following Ikeda (2014), and for micronekton following Belcher et al. (2020) and Ikeda (2016). *E* is the excretion rate obtained from published literature and assumed as 30% of the respiration (Steinberg et al., 2000), and *M* is the mortality rate assumed as a constant of the migrating biomass of 4% (Andersen, 2004; Tutasi & Escribano, 2020).

# 3 Results

## 3.1 Hydrography

The oceanographic contours showed a narrow coastal band (<20 km) characterized by upwelling conditions, where lower near-surface temperatures and higher salinities revealed the ascent of the Equatorial Subsurface Water (ESSW). In contrast, warmer and less saline waters prevailed near the surface in the offshore region (Figs. 1B). The presence of the OMZ associated with ESSW waters was located within the upper 500 m, occupying almost the entire water column over the continental shelf (Fig. 1B). Chl-a increases were not evident in the coastal area, but they were most present in surface water at the offshore region, suggesting a potential cross-shelf advection from inshore to offshore (Fig. 1B).

Indeed, the highest values of up to 29.8 mg $m^{-3}$ were mostly found in the sunlit waters from offshore.

During the sampling period, NPP exhibited a marked cross-shelf gradient. The lowest values (<100 mg C $m^{-3}$ $d^{-1}$) shown the occurred in offshore region waters, while NPP progressively increased toward the coast, reaching values exceeding 175 mg C $m^{-3}$ $d^{-1}$. This distribution not only highlights the strong spatial heterogeneity of primary productivity in the study region, and indicates that, despite the higher although NPP is highest in the coastal zone, but the substantial fraction of this newly produced biomass was also exported offshore according to the distribution of Chl-a (Fig. 1A and 1B).

$M_x$ varied among coastal stations during the sampling period, being positive in all cases (i.e., towards the open ocean), increasing from inshore to offshore. At station St. 31 was $1.2x10^5$ $m^3$ $d^{-1}$ $km^{-1}$, followed by St. 26= $9.4x10^4$ $m^3$ $d^{-1}$ $km^{-1}$, and St. 18 exhibited the lowest transport= $3.9x10^4$ $m^3$ $d^{-1}$ $km^{-1}$.

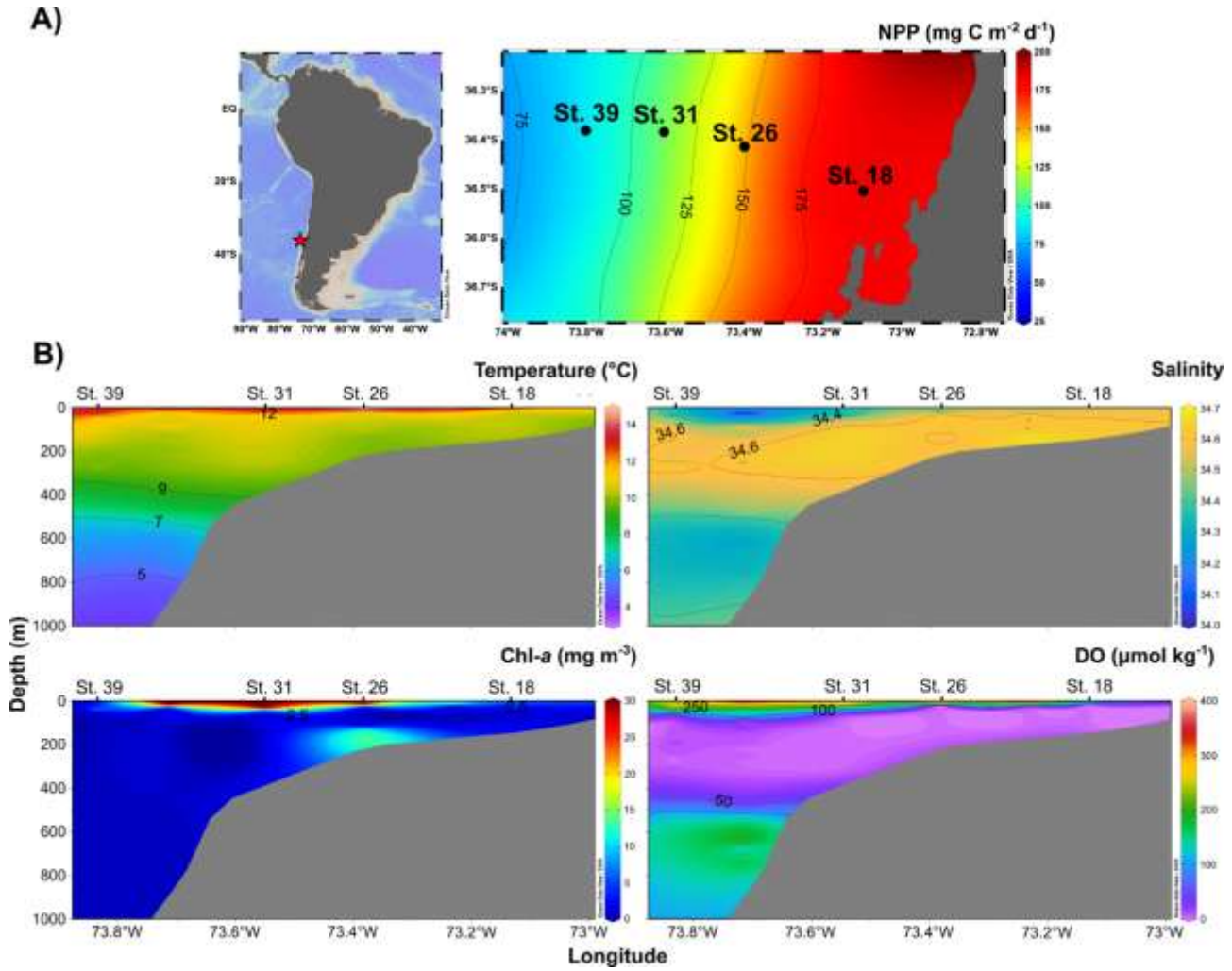


Figure 1. Sampling station off the coast of Concepción (Chile). (A) The net primary production (NPP) (mg C $m^{-2}$ $d^{-1}$) data from satellite products Global Ocean Color (Copernicus-GlobColour), Bio-Geo-Chemical, L4 (monthly and interpolated) from Satellite Observations (1997- ongoing) considered an averaged value for the So296/2-Leg 1 cruise, with a 4 km-resolution. (B) Cross-shore section of temperature (T °C), salinity, Chl-a (mg $m^{-3}$), and dissolved oxygen (DO, µmol $kg^{-1}$).

## 3.2 Zooplankton and micronekton community structure and vertical distribution

The composition and relative abundance of the zooplankton community structure were described by 19 groups as identified from the ZooScan (Fig. 2). The Upper-Oxy layer showed the highest abundance of all groups, with a progressive decline toward the deeper

layers (OMZ and lower-Oxy) (Fig. 2). The contribution of the other taxa in the Upper-Oxy layer shifted across stations: siphonophores, appendicularians, amphipods and bryozoans accounted for 53% of the total abundances at St. 18, it constituted 12% at St. 26, appendicularia and nauplii contributed with 23% at St. 31 and egg's fish (Sardine), pteropods, nauplius, appendicularians represented 38% of the abundances at St.39.

A Kruskal-Wallis test applied to the complete dataset revealed significant differences in zooplankton abundances across oxygen layers ($H= 94.14$, $df = 2$, $p < 0.001$) and between stations ($H= 37.64$, $df = 3$, $p <0.001$). In contrast, differences in abundances among size fractions were not significantly different ($H= 5.27$, $df = 3$, $p = 0.15$). The analysis for each station showed that the strongest vertical differences in zooplankton abundances (by oxygen layer) were found at St. 18 and St. 31 (St. 18: $H= 36.8$, $df = 1$, $p <0.001$; St. 31: $H= 26.9$, $df = 2$, $p<0.001$; St. 39 $H= 48.26$, $df = 4$, $p < 0.001$), while no significant vertical variation was detected at St. 26 ($p = 0.43$). Additionally, no significant differences in abundance were observed among size fractions within any station (all $p > 0.10$). At the oceanic station, abundances also did not differ significantly between day and night samples ($H = 0.80$, $df = 1$, $p = 0.37$).

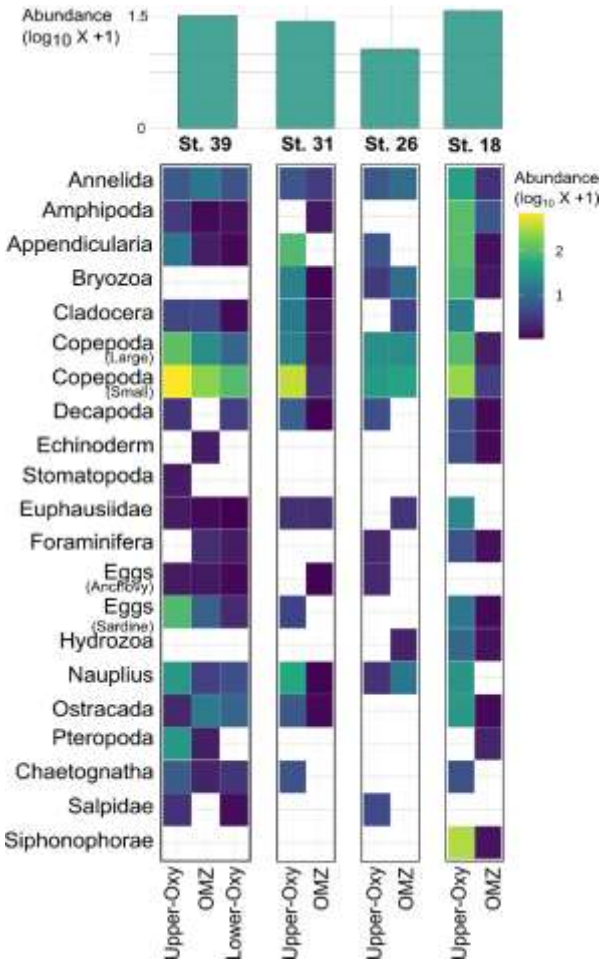


Figure 2. Zooplankton community structure at the upwelling area on the shelf off Concepcion, during the austral summer (January 2023). Each panel shows the average relative contribution of different taxa to the total zooplankton abundance in the water column. The color gradient represents the relative abundance (%).

The copepods were consistently among the top contributors, explaining up to 50-60% of the internal similarity within stations and accounting for over 35% of the dissimilarity between paired stations. The abundance and high relative contribution reflect their ecological dominance in the zooplankton assemblage. However, this strong influence may mask finer-scale compositional differences driven by less dominant but functionally diverse taxa. Therefore, a complementary analysis excluding copepods was performed to better understand the contribution of other groups to the observed spatial pattern in community structure.

The analysis of zooplankton assemblages, excluding copepods, showed a significant difference across stations (Global R = 0.3, $p = 0.002$) (Table 2). The largest differences were evident found when comparing the oceanic station (St. 39) and the neritic stations (St. 18, 26 and 31). In contrast, comparisons among the three more coastal stations that yielded lower showed low R values and non-significant differences (Table 2), suggesting a change in community composition from coastal to oceanic waters. ANOSIM also detected significant differences in zooplankton assemblages among the oxygen layers. The comparisons showed that upper-Oxy communities differed significantly from both OMZ ($R = 0.2$, $p = 0.002$) and lower-Oxy ($R = 0.3$, $p = 0.01$). However, the non-significant difference observed between OMZ and lower-Oxy ($R = 0.1$, $p = 0.3$) suggested similar taxonomic composition below the oxycline.

The analysis revealed distinct patterns in the zooplankton community composition across stations, along the coastal-oceanic transect. Between-station dissimilarities were high (>70%). The largest dissimilarity occurred between St. 39 and St. 18 (84.2%), driven mainly by changes in the relative abundance of annelids, ostracods, amphipods, and siphonophores. Comparisons between the other stations showed similar trends: dissimilarities between St. 26 and St. 31 against St. 18 were 83.7% and 82.3%, respectively, also reflecting strong compositional shifts from coastal to oceanic regions.

The nauplius stage and taxa such as appendicularians, and annelids were among the most influential in distinguishing station pairs across the entire transect, contributing consistently and significantly to Bray-Curtis's dissimilarity. Notably, bryozoans, ostracods, salps, and siphonophores were also discriminating against taxa depending on the pairwise comparison, reflecting shifts in functional groups and vertical niche distribution along the horizontal gradient.

Table 2. ANOSIM pairwise comparisons for zooplankton assemblages among stations and oxygen layers (excluding copepods).

| Variable | Comparison Group | R statistic | Significance level (%) |
|---|---|---|---|
| **Station** | **St. 39 vs. St. 18** | 0.4 | 0.1 |
| | **St. 39 vs. St. 26** | 0.3 | 0.6 |

| | | | |
|---|---|---|---|
| | **St. 39 vs. St. 31** | 0.2 | 4.7 |
| | **St. 26 vs. St. 18** | 0.1 | 15.3 |
| | **St. 31 vs. St. 26** | 0.1 | 21.0 |
| | **St. 31 vs. St. 18** | 0.1 | 26.4 |
| **Oxygen Layers** | **Upper-Oxy vs. OMZ** | 0.2 | 0.2 |
| | **Upper-Oxy vs. Lower-Oxy** | 0.3 | 0.9 |
| | **OMZ vs. Lower-Oxy** | 0.1 | 24.9 |

The micronekton community was dominated by fish and decapods (Fig. 3). Among fish, we identified individuals belonging to four different families: Myctophidae, Sternoptychidae, Melamphaidae, Stomiidae, as well as members of Alepocephaliformes. Decapods correspond to *Acanthephyra pelagica, Notostomus elegans* and members of *Gennadas* sp.

Myctophidae were the most abundant micronekton group, exhibiting high abundances throughout the water column. Other fish families and decapods (*A. pelagica* and *Gennadas* sp.) were distributed across the OMZ and Lower-Oxy layers. Notably, Melamphaidae, Alepocephaliformes and *N. elegans* were observed only in the Lower-Oxy layer. Kruskal-Walli's analysis did not show any significant differences in abundance between oxygen layers ($H = 3.9$, $df = 2$, $p = 0.14$) or sample times (day/night) ($H = 0.9$, $df = 1$, $p = 0.33$).

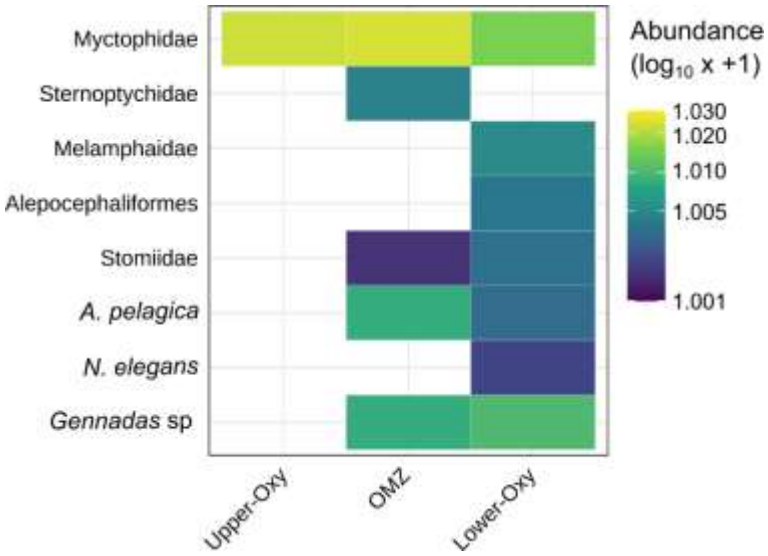


Figure 3. Distribution of micronekton abundance at station 39, located offshore of the upwelling zone off Concepción (January 2023). The color gradient represents the $\log_{10}$ transformed mean abundance (day and night) within each oxygen layer.

## 3.2 Trophic ecology of zooplankton and micronekton communities

The stable nitrogen isotopes of bulk material (Table S1) showed an increase in $\delta^{15}N$ with size, with micronekton exhibiting the highest values (15.8-18.5‰), followed by zooplankton (12.5-16.3‰). This difference likely results from the trophic enrichment across multiple trophic steps. The $\delta^{13}C$ values of both zooplankton and micronekton ranged between -15.3‰ and -19.0 ‰ (Fig. 4) throughout the water column, significant differences between samples ($F_{(1,73)}$=13.1 $p$<0.001), the difference were associated two the spatial and vertical distribution, suggesting a stronger influence of surface-derived carbon sources fueling the coastal component of the food web.

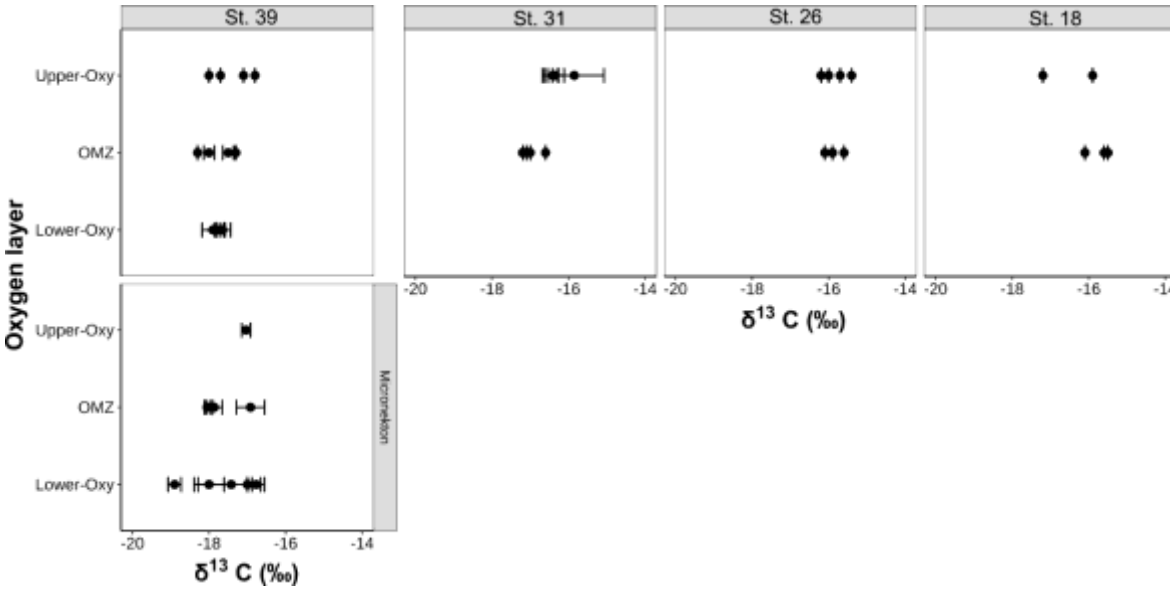


Figure 4. Vertical patterns of $\delta^{13}C$ (‰) in zooplankton (top panel) and micronekton (bottom panel) across the oxygen layers (Upper-Oxy, OMZ, Lower-Oxy) at each station from coast (St. 18) to offshore (St. 39). Points represent mean isotopic values, and horizontal error bars denote standard deviations.

The $\delta^{15}N$ PheC values for the size-fractionated zooplankton and micronekton ranged from 4.9‰ to 11.8‰ (Fig. 5). Still, differences in the $\delta^{15}N$ PheC between mesozooplankton and micronekton were significant ($F_{(1,76)}=20.9$, $p<0.001$). These differences, however, became non-significant between zooplankton size-classes or when comparing zooplankton from different oxygen layers ($F_{(3,42)}=0.7$, $p=0.6$; $F_{(2,43)}=1.3$, $p=0.3$) or stations (St. 18, 26, 31 and 39) ($F_{(1,44)}=1.1$ $p=0.3$). Micronekton $\delta^{15}N$ PheC values data from the were included. I, no significant differences were found at st. 39 differences when considering among oxygen layers, nor among the or taxa ($F_{(6,25)}=1.0$, $p=0.1$; $F_{(6,25)}=1.0$, $p=0.4$).

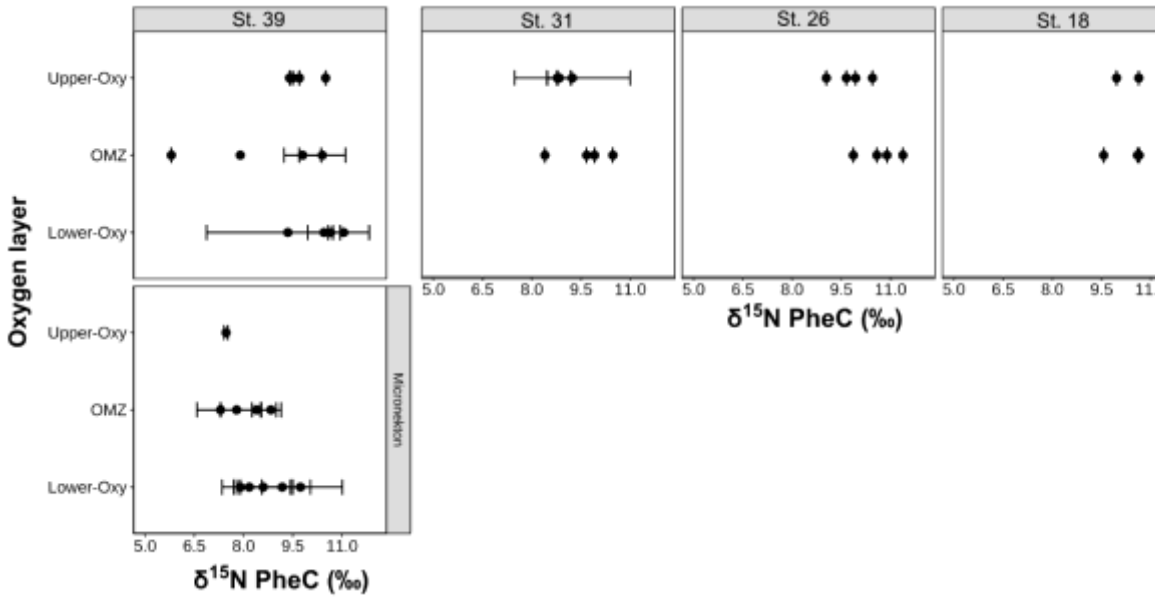


Figure 5. Vertical patterns of $\delta^{15}$N PheC (‰) in zooplankton (top panel) and micronekton (bottom panel) across the oxygen layers (Upper-Oxy, OMZ, Lower-Oxy) at each station from coast (St. 18) to offshore (St. 39). Points represent mean isotopic values, and horizontal error bars denote standard deviations.

However, the relationship between $\delta^{15}$N of Glx and Phe revealed a consistent increase in the TPs from zooplankton to micronekton (Fig. 6). The mesozooplankton exhibited omnivorous and carnivorous feeding habits with TPs ranging from 2.3 to 4. All micronekton taxa were strict carnivores, with TPs between 3.4 and 5.2.

A two-way ANOVA showed a significant interaction between oxygen layer and station in zooplankton TP ($F_{(1,41)}$=8.5, $p$<0.05), indicating that the effect of oxygen layer on TP varied across stations. For the zooplankton size fractions, the one-way ANOVA revealed no significant differences in trophic position ($F_{(3, 42)}$ = 0.8, p = 0.5). Similarly, the one-way ANOVA for micronekton taxa showed no significant differences ($F_{(6, 25)}$ = 1.6, p = 0.2).

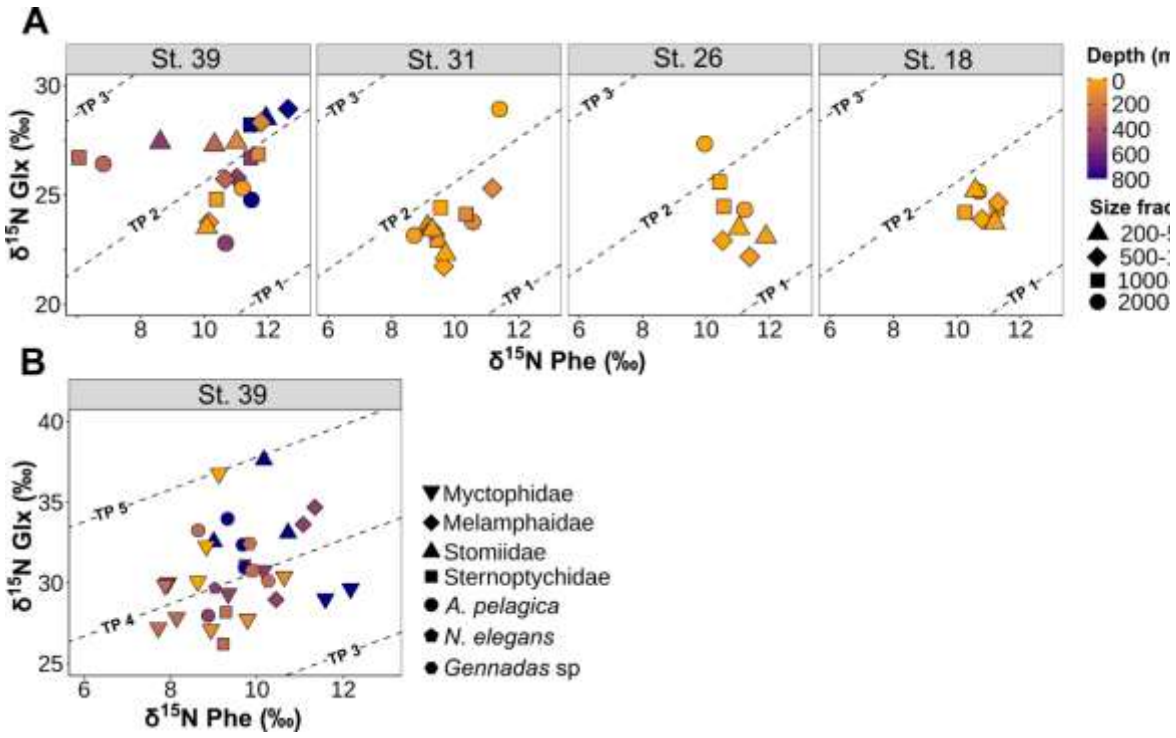


Figure 6**.** Biplot of δ15N-Glx values against δ15N-Phe values for (A) size-fractionated plankton and (B) micronekton samples. The color gradient represents the distribution within the water column, with lighter colors (yellow) indicating shallower depths and darker colors (dark blue), deeper depths. The trophic position of each sample was delineated by dashed trophoclines.

In this regard, we did not observe the significative difference between zooplankton and micronekton ($F_{(1,76)}$=0.2, $p$>0.05) (Fig. 7): while the microbial food web was between 5.0 to 38.25%, a mean value was 23.7% of the zooplankton diet, the contribution was between 8.0 to 35.4, and a mean value 24.6% as food resource for the micronekton.

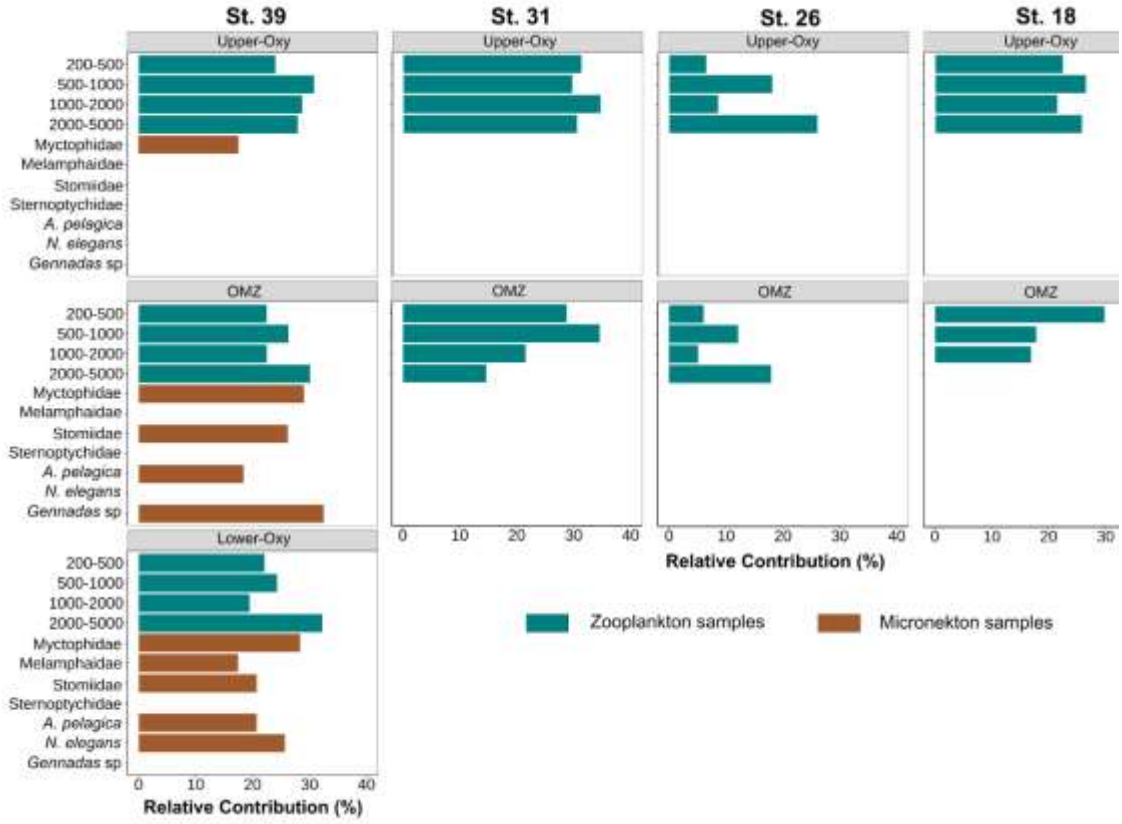


Figure 7. The relative microbial contribution (%) to zooplankton and micronekton diets.

## 3.3 Migrant Biomass and Carbon Flux

The analysis of the DVM in zooplankton revealed that euphausiids, appendicularians, annelids, decapod larvae, nauplii, large copepods, and amphipods were the main migrant taxa ($\Delta DVM \geq 100$ m) (Fig. 8A). Some of them exhibited reversed DVM, i.e. they migrated to deeper strata during the night. In the case of micronekton (Fig. 8B), WMD was located below 300 m, with Myctophidae, Melamphaidae, and Stomiidae identified as the main migratory taxa ($\Delta DVM \geq 100$ m). Migration patterns in these fish families occurred in both directions, night-day (Myctophidae and Melamphaidae) and day-night (Stomiidae), reflecting diverse vertical movement strategies (Fig. 8B). For subsequent analyses of active carbon flux, migrant zooplankton were represented by euphausiids, large copepods, and chaetognaths, whereas micronekton was represented by the three fish families mentioned above.

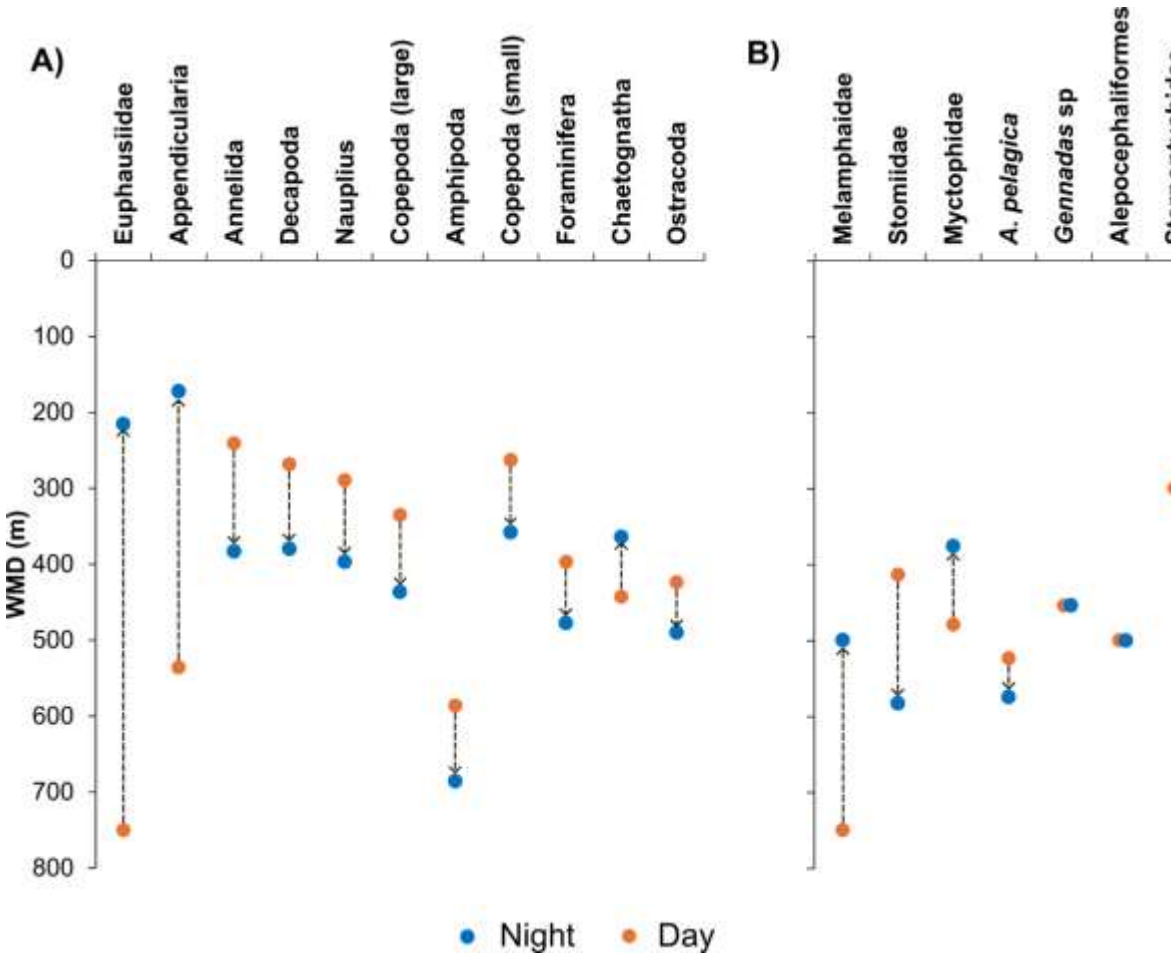


Figure 8. Amplitude of diel vertical migration in zooplankton (A) and micronekton (B). Dots represent the weighted mean depth (WMD) during the day (orange) and night (blue), with the difference in WMD defining the migration amplitude. The arrow showed the migration direction for each taxon.

Considering the biomass of migrants, our results revealed an increase in TP and biomass across depth layers (Fig. 9). Migrant zooplankton displayed a lower biomass than migrant micronekton across all oxygen strata, highlighting its numerical dominance in the system. Within the OMZ, migrant zooplankton were carnivorous taxa (TP 3.0-4.3), showing the highest TP values. By contrast, micronekton exhibited a broader distribution throughout the water column, with TP values consistently > 3.5.

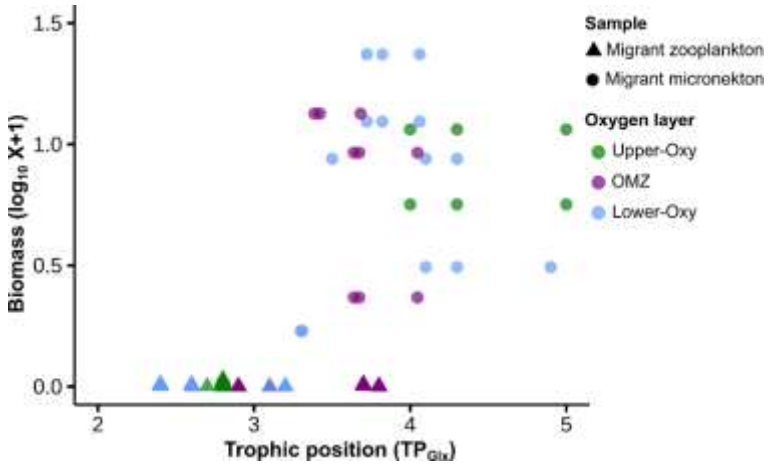


Figure 9. Relationship between trophic position ($TP_{Glx}$) and log-transformed biomass of migrant zooplankton (triangles) and migrant micronekton (circles). The colors indicate the three oxygen layers (Upper-Oxy, OMZ and Lower-Oxy).

Both migrant zooplankton and micronekton were primarily predators, and their migrant biomass (MB) showed maximum values in the surface layers and deeper strata (0-100 and 600-900 m) for the zooplankton and at 200-600 m for the micronekton (Table S3). In terms of biomass, micronekton outweighed zooplankton.

Table 3 summarizes the active carbon flux mediated by migrant organisms. Zooplankton contributed to the downward transport of carbon (Table 3), with fluxes ranging from 0.1 to 2.0 mg C $m^{-2}$ $d^{-1}$ (mean = 1.3 mg C $m^{-2}$ $d^{-1}$). In contrast, micronekton fluxes were several orders of magnitude higher, ranging from 15.1 to 70.8 mg C $m^{-2}$ $d^{-1}$ (mean = 37.0 mg C $m^{-2}$ $d^{-1}$).

Table 3. Carbon flux (C flux) of zooplankton and micronekton offshore of upwelling system of Concepción during the austral summer (January 2023). Migrant biomass (MB: mg C $m^{-2}$ $d^{-1}$); R was the respiration rate estimated for zooplankton following Ikeda (2014), and the micronecton following Belcher et al. (2020) to Myctophids and Ikeda (2016) for Melamphaidae, and Stomiidae. E is the excretion rate assumed as 30% of the respiration, and the M is the mortality rate assumed a 4% value (Andersen, 2004; Tutasi & Escribano, 2020) of the migrating biomass.

| Sample | Depth strata (m) | MB (mg C $m^{-2}$) | R | E | M | C flux (mg C $m^{-2}$ $d^{-1}$) |
|---|---|---|---|---|---|---|
| Zooplankton | 0-100 | 75.6 | 0.004 | 0.001 | 0.04 | 1.7 |

| | | | | | | |
|---|---|---|---|---|---|---|
| | 100-200 | 3.4 | 0.012 | 0.004 | 0.04 | 0.1 |
| | 200-400 | 66.1 | 0.005 | 0.002 | 0.04 | 1.5 |
| | 400-600 | 39.3 | 0.008 | 0.002 | 0.04 | 1 |
| | 600-900 | 73.7 | 0.01 | 0.003 | 0.04 | 2 |
| Micronekton | 0-100 | 586.8 | 0.009 | 0.003 | 0.04 | 15.1 |
| | 100-200 | 1,208.60 | 0.008 | 0.001 | 0.04 | 29.8 |
| | 200-400 | 2,821.70 | 0.008 | 0.002 | 0.04 | 70.8 |
| | 400-600 | 2,381.80 | 0.003 | 0.002 | 0.04 | 54.2 |
| | 600-1000 | 683.0 | 0.003 | 0.001 | 0.04 | 15.1 |
| Mean zooplankton | | | | | | 1.3 ± 0.7 |
| Mean micronekton | | | | | | 37.0 ± 24.8 |
| Total | | | | | | 37.0 ± 25.5 |

# 4 Discussion

## 4.1 Environmental conditions and zooplankton lateral transport

Active upwelling was occurring during the study while Ekman transport (Mx) favored lateral advection of zooplankton biomass. Since the average Mx during the week of study was about 85.2 m3 $d^{-1}$ $m^{-1}$ and the mean zooplankton biomass in the inshore region in the upper 100 m layer was 16.3 mg C m-3 (from Table S3), and assuming that this zooplankton biomass is distributed within the Ekman layer (ca. 20 m in this region), an approximate amount of 1.4 g C $m^{-3}$ $d^{-1}$ can be advected offshore. This lateral transport can also be enhanced by other advective processes, such as mesoscale eddies (Hormazabal et al., 2013; Keister et al., 2009; Morales et al., 2010; Muñoz et al., 2023), and geostrophic currents (González et al., 2023), potentially resulting in even greater advection of plankton biomass. On the other hand, the offshore propagation also contributes significantly to expanding the area of high Chl-a concentrations beyond the coastal upwelling area off Chile, supporting the relatively high abundances of zooplankton assemblages in the offshore ocean (Morales et al., 2010). As shown in other studies, Ekman transport seems a key process for the mesoscale circulation in coastal upwelling zones, transporting huge volumes of coastal water offshore, and as seen in other regions a single upwelling filament may advect large amounts of water offshore as far as 1000 km from the coastline in the Oregon and California coast each summer (Keister et al. (2009). The offshore transport of such filaments in coastal upwelling systems is clearly reflected in the dominance of neritic taxa offshore which can occur over a meander of the upwelling jet as ~0.5 Sv, and a biomass flux of >900 tons of carbon per day in zooplankton alone (Keister et al. (2009).

We also find that wind-driven transport intensifies progressively from the coast toward the ocean. while the abundance of zooplankton showed the highest concentrations at the coastal station (St. 18) and the lowest values at the offshore station (St. 39), although having a similar community composition. The higher zooplankton abundance or biomass at the inshore in this upwelling zone results from a high secondary production, as previously reported (Fernández-Urruzola et al., 2023; González et al., 2023; González et al., 2019). The possibility that carbon fixed in the productive coastal upwelling zone is transported and utilized offshore is a key issue in this study. In upwelling systems, the primary source of organic C and N is derived from new production supported by nitrate enriched in $^{15}N$, with $\delta^{15}N$ values of particulate organic matter (POM) typically ranging between 6 and 12‰ in the Chilean upwelling system (Pantoja, 2006). Thus, our approach enabled us to evaluate whether $\delta^{15}N$-Phe C values remain consistent between coastal and offshore stations (Fig. 5), serving as an indicator of lateral transport processes. $\delta^{15}N$ PheC values ranged between 4.9 and1.8‰), without significant differences between inshore and offshore stations, indicating that the nitrogen source fueling primary production was consistent from the coastal upwelling sites to the offshore area. The variation in the baseline $\delta^{15}N$-Phe values in oligotrophic and highly productive upwelling zone were reported by Fernández-Urruzola et al. (2023) and mentioned that a positive discrimination of primary producers in favor of the lighter isotope ($^{14}N$) might have progressively enriched the residual $NO^{-3}$ pool as it is horizontally advected and between 85.9 % and 99.0 % of the biological production at the upwelling zone relied on upwelled $NO^{-3}$. The $\delta^{13}C$ on the other hand showed a narrow range across stations (-15% and -19%) reflecting values observed in rapidly growing phytoplankton (Rau et al., 1989). It is important to note that the variation in $\delta^{15}N$-Phe and $\delta^{13}C$ when comparing the biomasses of zooplankton and micronekton was significant, but both markers varied within a narrow and similar range between components. This variability most likely obeys the utilization of additional food sources in the offshore region, especially in deeper strata.

The spatial patterns of both $\delta^{15}N$-Phe and $\delta^{13}C$ strongly support the hypothesis that lateral transport acts as a key mechanism linking nutrient-rich coastal production with offshore ecosystems. In particular, the observed homogeneity in baseline isotopic values across the cross-shelf gradient suggests that shelf-derived production is advected toward the

open ocean. A previous study, González et al. (2023), provided additional evidence suggesting that most of the organic matter present over the Atacama Trench ultimately originates in the coastal upwelling zone, where new production predominates. Their analysis of isotopic niches showed an overlap, and zooplankton community structure further supports the hypothesis that both organic matter and plankton are laterally advected from the productive coastal system to the near-surface layers above the trench. The large overlap of isotopic niches is consistent with the utilization of a common food resource; most likely particulate organic matter derived from high primary productivity in the euphotic zone.

## 4.2 Biomass of migrating zooplankton and micronekton

Once advected offshore, the zooplankton biomass can be subsequently transferred to deeper layers, where it will sustain the metabolic demands of the deep-sea resident biota. In this context, vertically migrating zooplankton plays a crucial role in actively transporting substantial amounts of carbon to the mesopelagic and bathypelagic zones, a process that is particularly important in highly productive ecosystems such as this upwelling system. Zooplankton's DVM has long been recognized as one of the most important biological mechanisms driving vertical carbon flux in the ocean. In the upwelling system off northern Chile, Tutasi and Escribano (2020) showed that migrating zooplankton, particularly copepods and euphausiids, contribute actively to the downward transport of organic matter through respiration, excretion, and mortality at depth, representing up to ~4% of daily primary production being exported below the euphotic zone. Similar processes have been documented in other oxygen minimum zones, where physiological strategies, such as metabolic suppression allow zooplankton to survive and migrate across hypoxic waters, although this adaptation also reduces respiration rates and therefore modifies the efficiency of active flux (Kiko & Hauss, 2019).

The DVM estimates revealed that the zooplankton and micronekton migrated during daytime and nighttime are main forces driven biomass redistribution across depth strata. These patterns are consistent with the behavior of large zooplankton, such as copepods (e.g. *Calanus finmarchicus*, *C. pacificus*, *Euchaeta elongata*) and euphausiids (e.g. *Euphausia mucronata*, *E. pacifica*, *E. eximia*), which are known to perform extensive diel vertical migrations across several hundred meters (ca. 800 m) from near surface to depth (Bode &

Hernández-León, 2018; Riquelme-Bugueño et al., 2020). However, our data also showed that not all taxa follow the ascension during the night, and in other cases, the biomass persisted within intermediate and deeper strata during nighttime implying the presence of species that either do not migrate or exhibit reverse migrations. Such behaviors have been shown for copepods like *Pleuromamma abdominalis* and decapods, such as *Sergia splendens*, which can remain within or migrate into the OMZ core (Ariza et al., 2015; Wishner et al., 2018).

The migrant community in central-southern Chile is composed not only of strong vertical migrants, but also of taxa adopting partial or reversed migration. Such strategies, including residence within or excursions into hypoxic layers, may still contribute to carbon transport by fueling deep resident communities and facilitating organic matter cycling below the euphotic zone (Escribano and Riquelme-Bugueño, 2015). These findings stress that the magnitude of zooplankton and micronekton-mediated transport does not only depend on the amount of migrating biomass, but also on the behavioral migration and environmental constraints, particularly oxygen concentration, which could affect the width of the depth strata and the amplitude of vertical migration.

Migrating zooplankton are predominantly omnivorous and carnivorous (TP= 2.5 to 4), with organisms >500 μm contributing significantly to the downward transfer of organic matter. The maximal migrating biomass was concentrated on the near surface layers during the night (Table S2). Micronektonic organisms on the other hand, notably mesopelagic fishes and decapods, emerged as pivotal drivers of active carbon transport across the ocean's midwater layers due to their DVM (Hernández-León et al., 2019; Kwong et al., 2020). Other studies have demonstrated that vertically migrating micronekton displays elevated trophic positions compared to non-migrants, suggesting enhanced carbon processing and export (Bode et al., 2021). Moreover, research from various other marine regions has shown that in tropical and subtropical Atlantic waters, zooplankton and micronekton together underpin a substantial portion often exceeding 25% of total carbon flux via active transport mechanisms, with micronekton increasingly dominant in more productive zones (Hernández-León et al., 2019). Collectively, these studies highlight that micronekton DVM is a crucial vector of carbon transfer to the deep ocean. Accurate

assessments, including taxonomic resolution, are required to properly assess their contribution to vertical flux estimation of C.

Regarding the qualitative aspects of micronekton contribution to downward C flux, our findings revealed that Myctophidae fish were the most abundant group, compared to other groups, such as Stomiidae and, Melamphaidae which also migrated through the OMZ layers and contributed to vertical carbon transport. This finding contrasts with reports from other regions where active flux is typically attributed to a narrower set of dominant migrant taxa (e.g. only myctophids). Moreover, the strong carnivorous signal (TP > 3) found in our samples (Fig. 6) indicated that active transport in this system is not only biomass-driven, but also functionally shaped by the trophic structure of the migrants. Thus, in contrast to the general assumption that biomass is the best predictor of active flux, our findings highlight the importance of considering trophic behavior and prey-predators as key modulators of vertical transport efficiency in productive upwelling ecosystems.

## 4.2 Zooplankton and Micronekton

In our study area off Concepción, active carbon flux mediated by zooplankton ranged between 0.1 and 2.0 mg C $m^{-2}$ $d^{-1}$, depending on the depth layer, while the depth integrated value was 1.3 ± 0.7 mg C $m^{-2}$ $d^{-1}$. These numbers fall within the lower spectrum reported for other upwelling or productive systems (Table 4). For instance, in the South China Sea, Ge et al. (2021) estimated active carbon fluxes of 4.64 mg C $m^{-2}$ $d^{-1}$ - more than twice our mean value- compared to 1.80 mg C $m^{-2}$ $d^{-1}$ in the adjacent Western Philippine Sea. In the Benguela Upwelling System, actively transported POC by zooplankton comprised approximately 62-73% of the total POC flux, underscoring a relatively stronger role for DVM in that region (Meiritz et al., 2024). Meanwhile, in the coastal upwelling region off northern Chile, Tutasi and Escribano (2020) reported zooplankton DVM provide ~71 mg C $m^{-2}$ $d^{-1}$ into the OMZ via a migrant biomass of nearly 960 mg C $m^{-2}$ $d^{-1}$ equivalent to about 4% of local net primary production.

Our data suggest that the micronekton showed high values of C fluxes compared to other estimates (Table 4), revealing an enhanced contribution to the active transport of C to the deep ocean in this region. Similar findings have been reported in other productive ecosystems where myctophids and other mesopelagic fishes dominated the migrating biomass and played a major role in carbon export to depth (Ariza et al., 2015; Hidaka et al.,

2001; Kwong et al., 2020). The magnitude of fluxes determined in this study suggests that micronekton not only supplements, but it largely exceeds the role of zooplankton in fueling deeper layers, particularly under OMZ conditions where predator-prey interactions upon prevalence of carnivory may enhance the downward transport of C. Overall, our results indicate that the contribution of zooplankton and micronekton to the active carbon export in this upwelling system represented approximately 2.7% of the local NPP in the offshore zone and 2.1% of NPP in the inshore area.

Table 4. Comparison of active transport of carbon rates from published studies with our estimates.

| **Sample** | **Carbon flux (mg C $m^{-2}$ $d^{-1}$)** | **Location** | **Source** |
|---|---|---|---|
| Zooplankton | 2.8-8.8 | Sargasso Sea | Longhurst et al. (1990) |
| | 2.0-9.9 | Bermuda | Steinberg et al. (2000) |
| | 1.92-4.29 | Canary Islands | Hernández-León et al. (2001) |
| | 7.3-19.05 | W. Eq. Pacific | Hidaka et al. (2001) |
| | 14.1 | E. S. Pac. N. Chile | Hidalgo et al. (2005) |
| | 7200 | E. S. Pac. N. Chile | Escribano et al. (2009) |
| | 3.2-13.6 | N. Hawaii ALOHA | Steinberg et al. (2008) |
| | 3.4 ± 1.9 | Canary Islands | Ariza et al. (2015) |
| | 0.9-83.3 | Atlantic Ocean | Hernández-León et al. (2019) |
| | 71±64 | E. S. Pac. N. Chile | Tutasi and Escribano (2020) |
| | 5.4-88 | Eastern coast of Australia | Kwong et al. (2020) |
| | 4.64 | South China Sea | Ge et al. (2021) |
| | 0.1-2.0 | Concepción upwelling | This study |
| Micronekton | 15.2-29.9 | W. Eq. Pacific | Hidaka et al. (2001) |
| | 8.0-30.8 | N. E. Pacific | Davison et al. (2013) |
| | 2.92 ± 0.95 | Canary Islands | Ariza et al. (2015) |
| | 0.4-6.7 | Eastern coast of Australia | Kwong et al. (2020) |
| | 0.25-0.91 | Scotia Sea | Belcher et al. (2020) |
| | 0.04-21.69 | Southwest Coast of Oahu | Kwong et al. (2022) |
| | 0.001-0.045 | Kerguelen Islands | Cotté et al. (2022) |
| | 0.13-6.3 | Northeast Atlantic Ocean | McMonagle et al. (2024) |
| | 15.1-70.8 | Concepción upwelling | This study |

The idea that prey-predator interactions occurring in the offshore zone can enhance the active transport of C provide evidence for the existence of a “trophic ladder” (Vinogradov,

1962) in the upwelling system of central-southern Chile, where different zooplankton groups and micronekton taxa contribute sequentially to the transfer of carbon from surface production to deep layers. Large copepods, chaetognaths and euphausiids acted as primary mediators of vertical flux, either through direct migration or by exploiting sinking detritus, while micronekton further integrated this carbon and sustained deeper trophic levels. Kelly et al. (2019) in the California Current found that migrating mesozooplankton and fish supply a substantial portion of carbon export, acting as consumers (diurnal predator levels) on migrating zooplankton and in turn becoming prey for higher trophic levels, which builds a ladder of trophic transfers. In the other case, Anderson et al. (2019) mentioned that the principal support for the mesopelagic fish biomass is by vertical migrators that link surface primary production into the mesopelagic zone, complemented by detritivores and surface-resident copepods. Our study shows that migrant zooplankton and micronekton in our system differentially contribute to carbon export, with micronekton being the principal contributors to this ladder by coupling surface-derived production (via zooplankton migrants) to deeper OMZ layers. Our results, together with previous work, support the 'trophic ladder' hypothesis, wherein carbon is transferred from phytoplankton to migrant and non-migrant zooplankton (omnivorous and carnivorous) and ultimately to carnivorous micronekton, which couples surface production to deep OMZ communities. Furthermore, they reveal that this vertical mechanism is coupled with horizontal transport from the coastal upwelling to the deep ocean.

## 5 Conclusions

Our findings indicate that biological-physical processes are coupled to redistribute the plankton biomass produced in the upwelling zone along the central-southern Chilean margin. The CSIA-AA analyses revealed a low variability in $\delta^{15}$N-Phe baseline across coastal and offshore stations, pointing to lateral transport of coastal-derived nitrogen. In parallel, isotopic and community composition confirmed that both zooplankton and micronekton depend on resources advected from the upwelling zone, reinforcing the strong connectivity between coastal production and offshore ecosystems. Thereafter, the vertical transport mediated by migrant zooplankton contributed to rather a low flux of carbon, while micronekton dominated the contribution to the vertical export of C. This contrast highlights

the complementary roles of prey-predator interactions and DVM as drivers for active flux of C. Together, these mechanisms strengthen the link between surface productivity and deep-ocean layers, underscoring the ecological pathways that couple upwelling-driven production with offshore carbon sequestration. Combined physical processes including Ekman transport and mesoscale eddies and DVM and trophic interaction within and between zooplankton and micronekton promoting the downward flux of C produced in the upwelling zone are illustrated in Fig. 10. Such conceptual model highlights the existence of a highly efficient mechanism not only to fuel organic C the deep ocean ecosystem, but also to sequester large amounts of C produced in highly productive upwelling regions.

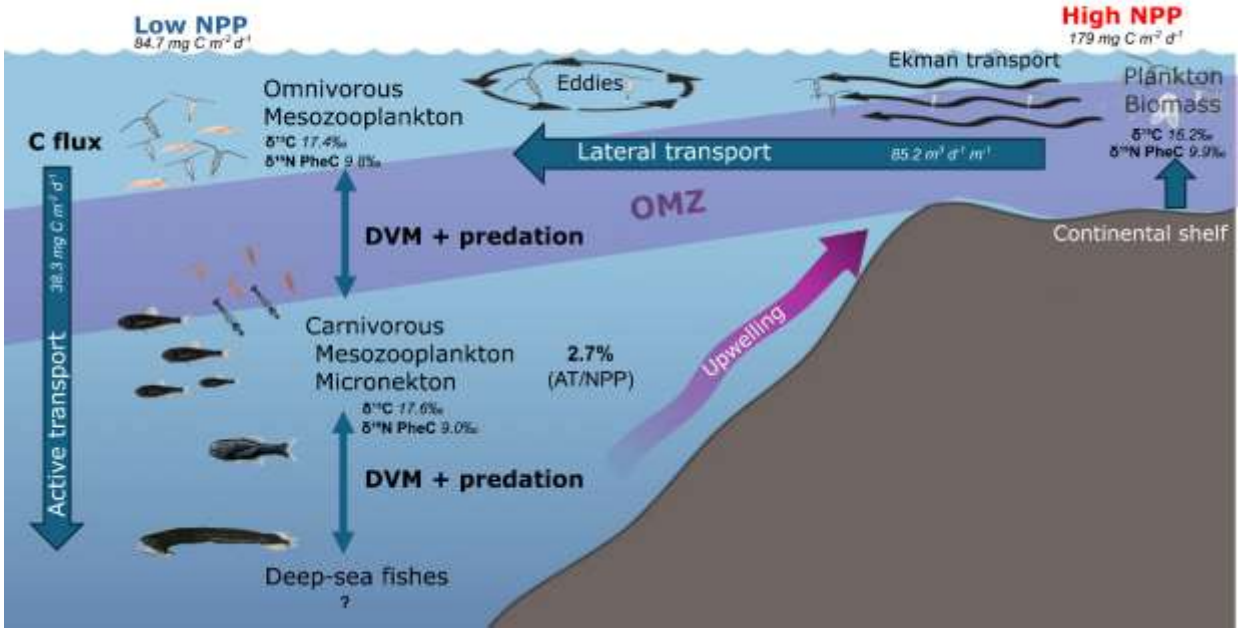


Figure 10. Conceptual model illustrating the physical processes (Ekman transport and mesoscales eddies) promoting lateral transport of plankton from the inshore to the offshore regions in a coastal upwelling zone which, in combination with trophic interactions and diel vertical migration of zooplankton and micronekton, may promote the downward flux of C produced in the upwelling zone to the deep ocean ecosystem. AT= Active transport; NPP= net primary production. The scheme also provides estimates of the physical and biological processes involved on a daily basis, except for the unknown C flux mediated by other deep-sea fishes.

**As Applicable – Inclusion in Global Research Statement**

**Acknowledgments**

This research was supported by the Chilean National Agency of Research and Development (ANID) through grants AIM23-0003, FONDECYT 11221079, and Scholarship 21211977. Additional support was provided by the IN607A 2022/05 grant to IEO from Xunta de Galicia (Spain). SO296/2 cruise Leg 1 on the R/V Sonne was supported by the German Federal Ministry of Research, Technology and Space (BMFTR) grant No. 03G0296A. The authors declare that they have no conflicts of interest. We thank Daniel Toledo for assistance in obtaining and processing zooplankton and micronekton samples for isotope analyses, and for scanning and processing zooplankton samples. We also thank Luis Ñacari and Guillermo Guzmán for support with micronekton taxonomic identification.

**Data Availability Statement**

The Net Primary production (NPP) as a product of the Global Ocean Color (Copernicus-GlobColour), Bio-Geo-Chemical data (L4 monthly and interpolated) from Satellite Observations (1997- ongoing) provided by the Copernicus Marine Environment Monitoring Service (CMEMS, 2023). The Ekman transport, which was calculated using a hourly sea surface wind data obtained from the Global Ocean Level-4 product (CMEMS, 2024). further details can be found in the methods section. The zooplankton and micronekton data, as abundance, biomasa and isotopic signatures of the bulk and CSIA-AA for all samples in this study, can be accessed through the following publication: Cabrera-Núñez & Fernández-Urruzola (2025)

**References**

Andersen, V. (2004). Vertical distributions of zooplankton across the Almeria-Oran frontal zone (Mediterranean Sea). *Journal of Plankton Research*, *26*(3), 275-293. https://doi.org/10.1093/plankt/fbh036

Anderson, T. R., Martin, A. P., Lampitt, R. S., Trueman, C. N., Henson, S. A., Mayor, D. J., & Link, J. (2019). Quantifying carbon fluxes from primary production to mesopelagic fish using a simple food web model. *ICES Journal of Marine Science*, *76*(3), 690-701. https://doi.org/10.1093/icesjms/fsx234

Garijo, J. C., Landeira, J. M., Bordes, F., & Hernández-León, S. (2015). Migrant biomass and respiratory carbon flux by zooplankton and micronekton in the subtropical northeast Atlantic Ocean (Canary Islands). *Progress in Oceanography*, *134*, 330-342. https://doi.org/10.1016/j.pocean.2015.03.003

Belcher, A., Cook, K., Bondyale-Juez, D., Stowasser, G., Fielding, S., Saunders, R. A., Mayor, D. J., Tarling, G. A., & Proud, R. (2020). Respiration of mesopelagic fish: a comparison of respiratory electron transport system (ETS) measurements and allometrically calculated rates in the Southern Ocean and Benguela Current. *ICES Journal of Marine Science*, *77*(5), 1672-1684. https://doi.org/10.1093/icesjms/fsaa031

Bode, A., & Hernández-León, S. (2018). Trophic Diversity of Plankton in the Epipelagic and Mesopelagic Layers of the Tropical and Equatorial Atlantic Determined with Stable Isotopes. *Diversity*, *10*(2). https://doi.org/10.3390/d10020048

Bode, A., Olivar, M. P., & Hernandez-Leon, S. (2021). Trophic indices for micronektonic fishes reveal their dependence on the microbial system in the North Atlantic. *Sci Rep*, *11*(1), 8488. https://doi.org/10.1038/s41598-021-87767-x

Cabrera-Nuñez, S., & Fernández-Urruzola, I. (2025). Zooplankton and Micronekton Data from the Upwelling System off Central-Southern Chile [Data set]. Zenodo. https://doi.org/10.5281/zenodo.17567850

Chikaraishi, Y., Ogawa, N. O., Kashiyama, Y., Takano, Y., Suga, H., Tomitani, A., Miyashita, H., Kitazato, H., & Ohkouchi, N. (2009). Determination of aquatic food-web structure based on compound-specific nitrogen isotopic composition of amino acids. *Limnology and Oceanography*, *7*, 740-750.

CMEMS. (2023). *20230101-20230131_cmems_obs-oc_glo_bgc-pp_my_l4-multi-4km_P1M* Global Ocean Colour (Copernicus-GlobColour), Bio-Geo-Chemical, L4 (monthly and interpolated) from Satellite Observations (1997-ongoing). https://doi.org/https://doi.org/10.48670/moi-00281

CMEMS. (2024). *WIND_GLO_PHY_L4_MY_012_006* https://doi.org/https://doi.org/10.48670/moi-00185

Cook, K. B., Belcher, A., Juez, D. B., Stowasser, G., Fielding, S., Saunders, R. A., Elsafi, M. A., Wolff, G. A., Blackbird, S. J., Tarling, G. A., & Mayor, D. J. (2023). Carbon budgets of Scotia Sea mesopelagic zooplankton and micronekton communities during austral spring. *Deep Sea Research Part II: Topical Studies in Oceanography*, *210*. https://doi.org/10.1016/j.dsr2.2023.105296

Cotté, C., Ariza, A., Berne, A., Habasque, J., Lebourges-Dhaussy, A., Roudaut, G., Espinasse, B., Hunt, B. P. V., Pakhomov, E. A., Henschke, N., Péron, C., Conchon, A., Koedooder, C., Izard, L., & Cherel, Y. (2022). Macrozooplankton and micronekton diversity and associated carbon vertical patterns and fluxes under distinct productive conditions around the Kerguelen Islands. *Journal of Marine Systems*, *226*. https://doi.org/10.1016/j.jmarsys.2021.103650

Davison, P. C., Checkley, D. M., Koslow, J. A., & Barlow, J. (2013). Carbon export mediated by mesopelagic fishes in the northeast Pacific Ocean. *Progress in Oceanography*, *116*, 14-30. https://doi.org/10.1016/j.pocean.2013.05.013

Escribano, R., Hidalgo, P., & Krautz, C. (2009). Zooplankton associated with the oxygen minimum zone system in the northern upwelling region of Chile during March 2000. *Deep Sea Research Part II: Topical Studies in Oceanography*, *56*(16), 1083-1094. https://doi.org/10.1016/j.dsr2.2008.09.009

Escribano, R., & Schneider, W. (2007). The structure and functioning of the coastal upwelling system off central/southern Chile. *Progress in Oceanography*, *75*(3), 343-347. https://doi.org/10.1016/j.pocean.2007.08.020

Fernández-Urruzola, I., Bode, A., Loick-Wilde, N., Schneider, W., Lindsay, D., & Escribano, R. (2023). Trophic ecology of midwater zooplankton along a productivity gradient in the Southeast Pacific. *Frontiers in Marine Science*, *10*. https://doi.org/10.3389/fmars.2023.1057502

Flores, E., Fernández-Urruzola, I., Cantarero, S. I., Pizarro-Koch, M., Zabel, M., Sepúlveda, J., & Ulloa, O. (2023). Particulate Organic Matter in the Atacama Trench: Tracing Sources and Possible Transport Mechanisms to the Hadal Seafloor. *Journal of Geophysical Research: Biogeosciences*, *128*(8). https://doi.org/10.1029/2023jg007401

García-Seoane, R., Viana, I. G., & Bode, A. (2023). Seasonal upwelling influence on trophic indices of mesozooplankton in a coastal food web estimated from δ15N in amino acids. *Progress in Oceanography*, *219*. https://doi.org/10.1016/j.pocean.2023.103149

Ge, R., Chen, H., Zhuang, Y., & Liu, G. (2021). Active Carbon Flux of Mesozooplankton in South China Sea and Western Philippine Sea. *Frontiers in Marine Science*, *8*. https://doi.org/10.3389/fmars.2021.697743

Gloeckler, K., Choy, C. A., Hannides, C. C. S., Close, H. G., Goetze, E., Popp, B. N., & Drazen, J. C. (2017). Stable isotope analysis of micronekton around Hawaii reveals suspended particles are an important nutritional source in the lower mesopelagic and upper bathypelagic zones. *Limnology and Oceanography*, *63*(3), 1168-1180. https://doi.org/10.1002/lno.10762

González, C. E., Bode, A., Fernández-Urruzola, I., Hidalgo, P., Oerder, V., & Escribano, R. (2023). The lateral transport of zooplankton explains trophic and taxonomic similarities over the zonal gradient of central Chile. *Journal of Marine Systems*, *238*. https://doi.org/10.1016/j.jmarsys.2022.103840

González, C. E., Escribano, R., Bode, A., & Schneider, W. (2019). Zooplankton Taxonomic and Trophic Community Structure Across Biogeochemical Regions in the Eastern South Pacific. *Frontiers in Marine Science*, *5*. https://doi.org/10.3389/fmars.2018.00498

Hannides, C. C. S., Popp, B. N., Choy, C. A., & Drazen, J. C. (2013). Midwater zooplankton and suspended particle dynamics in the North Pacific Subtropical Gyre: A stable isotope perspective. *Limnology and Oceanography*, *58*(6), 1931-1946. https://doi.org/10.4319/lo.2013.58.6.1931

Hernández-León, S., Gómez, M., Pagazaurtundua, M. a., Portillo-Hahnefeld, A. n., Montero, I., & Almeida, C. (2001). Vertical distribution of zooplankton in Canary Island waters: implications for export flux. *Deep Sea Research Part I: Oceanographic*

*Research Papers*, *48*(4), 1071-1092. https://doi.org/https://doi.org/10.1016/S0967-0637(00)00074-1

Hernandez-Leon, S., Koppelmann, R., Fraile-Nuez, E., Bode, A., Mompean, C., Irigoien, X., Olivar, M. P., Echevarria, F., Fernandez de Puelles, M. L., Gonzalez-Gordillo, J. I., Cozar, A., Acuna, J. L., Agusti, S., & Duarte, C. M. (2020). Large deep-sea zooplankton biomass mirrors primary production in the global ocean. *Nat Commun*, *11*(1), 6048. https://doi.org/10.1038/s41467-020-19875-7

Hernández-León, S., Olivar, M. P., Fernández de Puelles, M. L., Bode, A., Castellón, A., López-Pérez, C., Tuset, V. M., & González-Gordillo, J. I. (2019). Zooplankton and Micronekton Active Flux Across the Tropical and Subtropical Atlantic Ocean. *Frontiers in Marine Science*, *6*. https://doi.org/10.3389/fmars.2019.00535

Hidaka, K., Kawaguchi, K., Murakami, M., & Takahashi, M. (2001). Downward transport of organic carbon by diel migratory micronekton in the western equatorial Paci"c: its quantitative and qualitative importance. *Deep-Sea Research I*, *48*, 1923-1939.

Hidalgo, P., Escribano, R., & Morales, C. E. (2005). Ontogenetic vertical distribution and diel migration of the copepod Eucalanus inermis in the oxygen minimum zone off northern Chile (20–21° S). *Journal of Plankton Research*, *27*(6), 519-529. https://doi.org/10.1093/plankt/fbi025

Hormazabal, S., Combes, V., Morales, C. E., Correa-Ramirez, M. A., Di Lorenzo, E., & Nuñez, S. (2013). Intrathermocline eddies in the coastal transition zone off central Chile (31-41°S). *Journal of Geophysical Research: Oceans*, *118*(10), 4811-4821. https://doi.org/10.1002/jgrc.20337

Keister, J. E., Peterson, W. T., & Pierce, S. D. (2009). Zooplankton distribution and cross-shelf transfer of carbon in an area of complex mesoscale circulation in the northern California Current. *Deep Sea Research Part I: Oceanographic Research Papers*, *56*(2), 212-231. https://doi.org/10.1016/j.dsr.2008.09.004

Kelly, T. B., Davison, P. C., Goericke, R., Landry, M. R., Ohman, M. D., & Stukel, M. R. (2019). The Importance of Mesozooplankton Diel Vertical Migration for Sustaining a Mesopelagic Food Web. *Frontiers in Marine Science*, *6*. https://doi.org/10.3389/fmars.2019.00508

Kiko, R., & Hauss, H. (2019). On the Estimation of Zooplankton-Mediated Active Fluxes in Oxygen Minimum Zone Regions. *Frontiers in Marine Science*, *6*. https://doi.org/10.3389/fmars.2019.00741

Koppelmann, R., Weikert, H., & Lahajnar, N. (2003). Vertical distribution of mesozooplankton and its δ15N signature at a deep-sea site in the Levantine Sea (eastern Mediterranean) in April 1999. *Journal of Geophysical Research: Oceans*, *108*(C9). https://doi.org/10.1029/2002jc001351

Kwong, L. E., Bahl, A. A., & Pakhomov, E. A. (2022). Variability in micronekton active carbon transport estimates on the Southwest Coast of Oahu using three different sampling gears. *Frontiers in Marine Science*, *9*. https://doi.org/10.3389/fmars.2022.948485

Kwong, L. E., Henschke, N., Pakhomov, E. A., Everett, J. D., & Suthers, I. M. (2020). Mesozooplankton and Micronekton Active Carbon Transport in Contrasting Eddies. *Frontiers in Marine Science*, *6*. https://doi.org/10.3389/fmars.2019.00825

Longhurst, A. R., Bedo, A. W., Harrison, W. G., Head, E. J. H., & Sameoto, D. D. (1990). Vertical flux of respiratory carbon by oceanic diel migrant biota. *Deep Sea Research Part A. Oceanographic Research Papers*, *37*(4), 685-694. https://doi.org/https://doi.org/10.1016/0198-0149(90)90098-G

Massing, J. C., Schukat, A., Auel, H., Auch, D., Kittu, L., Pinedo Arteaga, E. L., J., C. A., & W., H. (2022). Toward a Solution of the "Peruvian Puzzle": Pelagic Food-Web Structure and Trophic Interactions in the Northern Humboldt Current Upwelling System Off Peru. *Frontiers in Marine Science*, *8*, 759603. https://doi.org/10.3389/fmars.2021.759603

McCarthy, M. D., Benner, R., Lee, C., & Fogel, M. L. (2007). Amino acid nitrogen isotopic fractionation patterns as indicators of heterotrophy in plankton, particulate, and dissolved organic matter. *Geochimica et Cosmochimica Acta*, *71*(19), 4727-4744. https://doi.org/https://doi.org/10.1016/j.gca.2007.06.061

McClelland, J. W., & Montoya, J. P. (2002). Trophic Relationships and the nitrogen isotopic composition of amino acids in plankton. *Ecology*, *83*(8), 2173-2180.

McMonagle, H., Llopiz, J. K., Maas, A. E., Steinberg, D. K., Govindarajan, A. F., Essington, T. E., & Gerringer, M. (2024). Quantifying uncertainty in the contribution of

mesopelagic fishes to the biological carbon pump in the Northeast Atlantic Ocean. *ICES Journal of Marine Science*, *81*(10), 2037-2051. https://doi.org/10.1093/icesjms/fsae149

Medellín-Mora, J., Atkinson, A., Escribano, R., & Ji, R. (2020). Community structured production of zooplankton in the eastern boundary upwelling system off central/southern Chile (2003–2012). *ICES Journal of Marine Science*. https://doi.org/10.1093/icesjms/fsz193

Meiritz, L. C., Rixen, T., van der Plas, A. K., Lamont, T., & Lahajnar, N. (2024). The influence of zooplankton and oxygen on the particulate organic carbon flux in the Benguela Upwelling System. *Biogeosciences*, *21*(22), 5261-5276. https://doi.org/10.5194/bg-21-5261-2024

Morales, C. E., Loreto Torreblanca, M., Hormazabal, S., Correa-Ramírez, M., Nuñez, S., & Hidalgo, P. (2010). Mesoscale structure of copepod assemblages in the coastal transition zone and oceanic waters off central-southern Chile. *Progress in Oceanography*, *84*(3-4), 158-173. https://doi.org/10.1016/j.pocean.2009.12.001

Muñoz, R., Vergara, O. A., Figueroa, P. A., Mardones, P., Sobarzo, M., & Saldías, G. S. (2023). On the phenology of coastal upwelling off central-southern Chile. *Dynamics of Atmospheres and Oceans*, *104*, 101405. https://doi.org/https://doi.org/10.1016/j.dynatmoce.2023.101405

Omori, M., & Ikeda, T. (1984). *Methods in Zooplankton Ecology*. Wiley. https://books.google.cl/books?id=OB0VAQAAIAAJ

Pantoja, S. (2006). Biogeochemistry of the OMZ of Chile. *Gayana*, *70*, 62-67. https://doi.org/10.4067/S0717-65382006000300013

Rau, G. H., Takahashi, T., & Marais, D. J. D. (1989). Latitudinal variations in plankton δ13C: implications for CO2 and productivity in past oceans. *Nature*, *341*(6242), 516-518. https://doi.org/10.1038/341516a0

Ringelberg, P. (2010). *Diel Vertical Migration of Zooplankton in Lakes and Oceans*. Springer. https://doi.org/10.1007/978-90-481-3093-1

Siegel, D. A., DeVries, T., Cetinić, I., & Bisson, K. M. (2023). Quantifying the Ocean's Biological Pump and Its Carbon Cycle Impacts on Global Scales. *Annual Review of*

*Marine Science*, *15*(Volume 15, 2023), 329-356. https://doi.org/https://doi.org/10.1146/annurev-marine-040722-115226

Steinberg, D. K., Carlson, C. A., Bates, N. R., Goldthwait, S. A., Madin, L. P., & Michaels, A. F. (2000). Zooplankton vertical migration and the active transport of dissolved organic and inorganic carbon in the Sargasso Sea. *Deep Sea Research Part I: Oceanographic Research Papers*, *47*(1), 137-158. https://doi.org/https://doi.org/10.1016/S0967-0637(99)00052-7

Steinberg, D. K., Cope, J. S., Wilson, S. E., & Kobari, T. (2008). A comparison of mesopelagic mesozooplankton community structure in the subtropical and subarctic North Pacific Ocean. *Deep Sea Research Part II: Topical Studies in Oceanography*, *55*(14), 1615-1635. https://doi.org/https://doi.org/10.1016/j.dsr2.2008.04.025

Steinberg, D. K., & Landry, M. R. (2017). Zooplankton and the Ocean Carbon Cycle. *Ann Rev Mar Sci*, *9*, 413-444. https://doi.org/10.1146/annurev-marine-010814-015924

Team, R. C. (2025). R language definition. *Vienna, Austria: R foundation for statistical computing*.

Tutasi, P., & Escribano, R. (2020). Zooplankton diel vertical migration and downward C flux into the oxygen minimum zone in the highly productive upwelling region off northern Chile. *Biogeosciences*, *17*(2), 455-473. https://doi.org/10.5194/bg-17-455-2020

Wang, W.-L., Fu, W., Le Moigne, F. A. C., Letscher, R. T., Liu, Y., Tang, J.-M., & Primeau, F. W. (2023). Biological carbon pump estimate based on multidecadal hydrographic data. *Nature*, *624*(7992), 579-585. https://doi.org/10.1038/s41586-023-06772-4

Wishner, K. F., Seibel, B. A., Roman, C., Deutsch, C., Outram, D., Shaw, C. T., Birk, M. A., Mislan, K. A. S., Adams, T. J., Moore, D., & Riley, S. (2018). Ocean deoxygenation and zooplankton: Very small oxygen differences matter. *Science Advances*, *4*(12), eaau5180. https://doi.org/doi:10.1126/sciadv.aau5180

# 5. DISCUSIÓN

Las interacciones presa-depredador y la migración vertical de los organismos pelágicos son procesos clave que contribuyen al transporte activo de carbono hacia el océano profundo. Considerando la hipótesis de que el efecto combinado entre ambos mecanismos promueve significativamente este transporte, es importante destacar que la conceptualización de una "escalera trófica" puede verse modulada por las condiciones oceanográficas locales, que determinan la estructura de las comunidades de zooplancton y micronecton. En este contexto, la propuesta del *Trophic Behavior Index* (TBI) aporta un indicador ecológico y un descriptor comunitario, el cual considera e integra tres factores biológicos importantes: 1) el tamaño del organismo, que es reconocido como una de las propiedades esenciales de las comunidades biológicas en lo que respecta a la ecología trófica y al flujo de energía en cualquier ecosistema (Peters, 1983; Décima, 2022). 2) La migración vertical diaria, por su parte, está estrechamente vinculada con las interacciones presa-depredador (Kelly et al., 2019; Tutasi y Escribano, 2020), mientras que 3) la posición trófica a partir del isótopo $\delta^{15}N$ se ha utilizado ampliamente para evaluar la ecología trófica de los distintos componentes dentro de las tramas tróficas (Post, 2002; Massing et al., 2022).

Este índice es una herramienta que permite distinguir grupos funcionales, más allá del nivel de especie, otorgando información en términos de intensidad de depredación, desde zooplancton clasificado como depredadores débiles hasta depredadores fuertes en diferentes comunidades planctónicas conformadas por una amplia variedad de consumidores. Determinar estas interacciones tróficas en la columna de agua no solo permite entender la dinámica de la comunidad

pelágica, sino también su efecto directo en el transporte activo de carbono hacia el océano profundo.

En el sistema de surgencia del centro-sur de Chile, la combinación de procesos físicos, como el transporte lateral a partir del transporte de Ekman, remolinos de mesoescala u otros, y el transporte vertical activo, considerado como la amplitud de migración vertical diaria, influyen en la transferencia de carbono entre la superficie y el océano profundo, considerando que las interacciones tróficas modulan un porcentaje de este transporte. Nuestros resultados muestran que tanto el zooplancton como el micronecton contribuyen de manera complementaria a este transporte activo: los primeros mediante una rápida asimilación y transformación de la materia orgánica derivada de la alta productividad superficial, y los segundos a través de su capacidad de migrar entre la capa epipelágica y mesopelágica, facilitando el flujo de carbono hacia profundidades mayores (Hidaka et al., 2001; Davison et al., 2013; Bianchi et al., 2014). El análisis isotópico de aminoácidos respalda esta conexión trófica al evidenciar una gradiente clara en la posición trófica entre grupos funcionales, consistente con una "escalera trófica" que refleja acoplamiento entre niveles tróficos intermedios (TP 2.5-3) y consumidores superiores (TP >3) (Chikaraishi et al., 2009; Décima et al., 2017). Estas observaciones sugieren que la estructura trófica integrada entre zooplancton y micronecton en la región de Concepción no solo refleja una alta conectividad entre estratos, sino también un mecanismo eficiente de transporte vertical y lateral de carbono orgánico.

### 5.1. Condiciones ambientales y estructura de la comunidad de zooplancton

Las condiciones oceanográficas observadas reflejan la marcada variabilidad ambiental que caracteriza al sistema de surgencia costera del Pacífico suroriental, tanto en dirección costa-océano como entre las regiones

norte y sur. En las estaciones del norte, la marcada zonación entre las capas oxigenadas superficiales y los límites superiores de la ZMO estuvo asociada a una estratificación vertical de la abundancia de zooplancton, con una disminución progresiva hacia las capas más profundas, probablemente condicionada por la hipoxia, que limita la presencia o migración de ciertas especies sensibles (Escribano et al., 2009; Tutasi y Escribano, 2020). Por el contrario, en la zona centro-sur, la columna de agua fue más homogénea y la depleción de oxígeno ocurrió a mayor profundidad, la distribución vertical de taxones fue más uniforme, sugiriendo una mayor mezcla y una menor restricción ambiental para los migradores verticales.

El análisis de la estructura de tamaño de la comunidad evidenció un cambio sistemático con la profundidad, donde las clases de mayor tamaño dominaron las capas superficiales y los organismos más pequeños predominaron en profundidad, tal como lo mostró la pendiente más pronunciada de los espectros de biomasa. Este resultado es consistente entre estaciones, sugiere una composición selectiva a lo largo de la columna de agua de acuerdo con el tamaño, reflejando la organización trófica y la dinámica que se establece entre las capas superficiales productivas y las zonas subsuperficiales más pobres en oxígeno. Las diferencias significativas en las pendientes de los espectros de biomasa entre estaciones, especialmente entre T5 y T39, refuerzan la influencia de las condiciones locales sobre la composición y la estructura de la comunidad del zooplancton.

En paralelo, en la zona centro-sur, la comparación de las condiciones físico-biogeoquímicas entre estaciones costeras (St. 18, St.26 y St. 31) y oceánica (St. 39) evidenció la fuerte influencia del transporte lateral asociado a la surgencia costera, lo que resalta la interacción entre procesos físicos y biológicos en la configuración de la comunidad. La surgencia costera,

impulsada por el transporte de Ekman y la circulación a mesoescala (p. ej., remolinos y filamentos), genera un gradiente transversal de productividad y nutrientes que se refleja directamente en la estructura trófica y en la distribución del zooplancton (Hormazabal et al., 2013; Keister et al., 2009; Morales et al., 2010; Muñoz et al., 2023). Durante el periodo de muestreo (verano 2023), se observó un gradiente claro de transporte Ekman desde la costa hacia el océano, lo que sugiere una intensificación progresiva del transporte inducido por el viento. Este proceso, facilita la advección de materia orgánica y nutrientes desde las zonas de surgencia hacia el talud y áreas oceánicas, contribuyendo a la mantención o distribución de comunidades zooplanctónica en regiones más oceánicas (Morales et al., 2010).

La homogeneidad isotópica observada en los valores de $\delta^{15}$N-Phe entre estaciones costeras y oceánicas (4.9-11.8‰) indica una fuente común de nitrógeno inorgánico que alimenta la productividad primaria a lo largo del transecto. Dado que la fenilalanina presenta un fraccionamiento trófico mínimo, sus valores reflejan fielmente el origen del nitrógeno en el sistema (McCarthy et al., 2007; McMahon & McCarthy, 2016). Este patrón isotópico, junto con la alta productividad costera y la evidencia de transporte lateral, respalda la hipótesis de que gran parte del material orgánico presente en el océano abierto proviene de la zona de surgencia costera (Fernández-Urruzola et al., 2023; González et al., 2023). La baja variabilidad en la línea base entre estaciones refuerza la idea de un acoplamiento trófico en un gradiente costa-océano, donde la producción nueva costera sostiene comunidades pelágicas distantes mediante el transporte de partículas y organismos.

En conjunto, estos resultados demuestran que la estructura trófica y la distribución del zooplancton están moduladas no solo por los gradientes verticales de oxígeno, temperatura y tamaño, sino también por los procesos

físicos de surgencia y transporte lateral que vinculan la alta productividad costera con el ecosistema oceánico. Las estaciones costeras constituyen, por tanto, zonas fuente de producción biológica y materia orgánica, mientras que las estaciones de talud y oceánicas actúan como zonas de transferencia, donde la interacción entre migración vertical y transporte horizontal regula la exportación activa de carbono hacia el océano profundo. Este acoplamiento físico-biológico es esencial para comprender el papel del plancton en el ciclo del carbono y en la dinámica trófica del ecosistema pelágico del Pacífico suroriental.

## 5.2 Interacciones tróficas y migración vertical

Los resultados del TBI demostraron que la comunidad de mesozooplancton presenta una distribución vertical, donde ciertos grupos taxonómicos actúan como depredadores activos asociado a su mayor amplitud de migración, alta posición trófica y su tamaño. La comparación diurna nocturna en la abundancia reveló que grupos como copépodos ( *Corycaeus* sp. y *Oncaea* sp. ), ostrácodos, anélidos y quetognatos presentaron migraciones verticales diarias más amplias (>200 m), en tanto que otros organismos presentan una amplitud de migración menor o nula, permaneciendo así en los primeros 100 m de la columna de agua. Esto sugiere que el acceso a recursos para alimentación y la distribución de la materia orgánica a lo largo de la columna presentaría efectos que a su vez modulan la contribución de cada grupo del zooplancton en la exportación activa de carbono.

Estos resultados concuerdan con estudios previos que destacan la migración vertical diaria como uno de los principales mecanismos de transporte activo de carbono (Steinberg et al., 2000; Davison et al., 2013). Sin embargo, el uso del TBI permitió demostrar que no todos los grupos zooplanctónicos

contribuyen de igual forma, y que la estructura trófica, así como la diferenciación en comportamientos migratorios son factores determinantes. Este hallazgo añade una perspectiva novedosa al conocimiento existente, al mostrar que la eficiencia del transporte activo de carbono depende de la interacción entre la migración vertical y la posición trófica.

Por su parte, la integración de los análisis de isótopos estables de carbono y nitrógeno evidenciaron un incremento progresivo de la posición trófica desde los estratos superficiales dominados por herbívoros hacia organismos carnívoros y omnívoros de la zona mesopelágica. Este gradiente isotópico confirma que la migración vertical conecta niveles tróficos, reforzando la idea de que la escalera trófica emerge como resultado de la interacción entre depredación y migración vertical.

Particularmente, el micronecton representó un porcentaje mayor en flujo de carbono vertical. Representantes de familias como Myctophidae, Stomiidae y Sternoptychidae, presentaron posiciones tróficas altas (>3) y una marcada capacidad migratoria, lo que los convierte en intermediarios clave en la transferencia de carbono. Estos resultados son consistentes con lo observado en otros sistemas de surgencia y en el océano abierto, donde los peces mesopelágicos se han identificado como actores fundamentales en el transporte activo de carbono (Irigoien et al., 2014; Hernández-León et al., 2020).

La comparación con trabajos previos revela que, si bien la magnitud del flujo de carbono puede variar entre regiones y estaciones, el patrón general se mantiene: la combinación de zooplancton migrador y depredadores mesopelágicos genera una vía eficiente para transportar carbono desde la zona eufótica hacia profundidades intermedias y profundas (Bianchi et al., 2013). Nuestra investigación contribuye al conocimiento existente al demostrar que, en sistemas costeros altamente productivos, como la zona de surgencia del

Pacífico suroriental, este mecanismo no solo está presente, sino que adquiere una importancia particular debido a la alta biomasa disponible y a la presencia de una comunidad tróficamente estructurada.

### 5.3 Flujo de carbono del zooplancton y micronecton

La integración de biomasa, migración diurna vertical y posición trófica permitió estimar la contribución de la escalera trófica al transporte activo de carbono. Los resultados muestran que el flujo vertical no puede explicarse únicamente por la migración de organismos individuales, sino por la interacción entre diferentes niveles tróficos que redistribuyen carbono a lo largo de la columna de agua.

Estudios previos han estimado que la migración vertical de organismos pelágicos puede contribuir entre un 10-30% del flujo total de carbono exportado hacia la zona mesopelágica (Davison et al., 2013; Steinberg & Landry, 2017). Nuestros resultados se encuentran alrededor del 2.7% de la PPN, sin embargo, en el caso de sistemas de surgencia, la eficiencia del transporte puede verse incrementada por la presencia de una escalera trófica bien definida, donde depredadores de niveles superiores continúan el transporte vertical iniciado por migradores de menor tamaño.

Este hallazgo tiene implicancias relevantes para la comprensión de la bomba biológica de carbono, ya que demuestra que la exportación activa no depende únicamente de procesos pasivos como la sedimentación de partículas, sino que es fuertemente modulada por la estructura y el comportamiento de la comunidad pelágica.

La evidencia presentada en este estudio respalda la existencia de una "escalera trófica" (Vinogradov, 1962) en el sistema de surgencia del centro-sur de Chile, donde las interacciones presa-depredador que ocurren tanto en la zona

costera como en el talud favorecen la transferencia secuencial de carbono orgánico desde la producción superficial hacia las capas más profundas. Observamos que diferentes grupos de mesozooplancton (copépodos, eufáusidos y quetognatos) actúan como mediadores primarios del transporte activo de carbono, ya sea mediante migración vertical o mediante el aprovechamiento de POC. Estos flujos son posteriormente integrados por el micronecton, el cual incorpora el carbono procedente del zooplancton migrador y sostiene niveles tróficos más profundos dentro de la ZMO. Resultados similares han sido reportados en otros sistemas de surgencia, como en la Corriente de California, donde organismos migradores y peces mesopelágicos aportan una fracción significativa al transporte vertical de carbono, funcionando como consumidores de zooplancton migrador y, a su vez, como recurso para depredadores mayores, configurando una estructura trófica escalonada (Kelly et al., 2019). Asimismo, Anderson et al. (2019) señalan que la biomasa de peces mesopelágicos depende en gran medida del flujo de carbono proporcionado por migradores verticales y detritívoros que vinculan la producción superficial con la zona mesopelágica. Nuestros resultados son consistentes con estos hallazgos y sugieren que el micronecton cumple un rol clave en la articulación de esta escalera trófica, acoplando la producción superficial, que es transportada activamente por el zooplancton migrador, con las comunidades que habitan las capas profundas y pobres en oxígeno. Además, esta dinámica vertical se encuentra acoplada a un transporte lateral desde la zona costera hacia el océano abierto, lo que refuerza el papel del sistema de surgencia como un motor biogeoquímico que conecta la superficie con el océano profundo.

# 6. CONCLUSIÓN

La variabilidad de las condiciones oceanográficas en la zona de surgencia influye en la composición de la comunidad de zooplancton a través de respuestas a los cambios a la temperatura, las concentraciones de oxígeno disuelto y la estratificación de la columna de agua. Sin embargo, nuestros resultados sugieren que la estructura trófica del zooplancton está determinada principalmente por atributos ecológicos, tales como el tamaño, la migración vertical diaria y la posición trófica. Estas características pueden integrarse eficazmente mediante el TBI, el cual se ha demostrado como un indicador ecológico del zooplancton en sistemas de surgencia. El TBI proporciona así una clasificación que permite comparaciones significativas entre diferentes condiciones ambientales, al considerar no solo la presencia de determinados grupos funcionales, sino también su contribución relativa a en la estructura comunitaria.

Por otra parte, el análisis isotópico compuesto de aminoácidos reveló una baja variabilidad en los valores de referencia de $\delta^{15}$N-Phe entre estaciones costeras y oceánicas, indicando un transporte lateral materia orgánica desde la zona de surgencia hacia el océano. Considerando la relación entre la producción costera y la oceánica está conectada mediante el transporte por advección y también por las comunidades del zooplancton en conjunto con el micronecton. En este contexto, la migración vertical diaria contribuyó al transporte activo de carbono hacia capas profundas, aunque con diferencias en magnitud entre grupos: el zooplancton aportó un flujo relativamente bajo, mientras que el micronecton dominó el flujo vertical de exportación de carbono debido a su mayor biomasa y amplitud de migración.

En conjunto, estos resultados sugieren que el efecto combinado de las interacciones tróficas y la migración vertical constituye un mecanismo para la transferencia de carbono orgánico desde la zona fótica hacia el océano profundo. Además, demuestran que la organización funcional de la comunidad pelágica a través del TBI, es clave para comprender la dinámica ecológica que vincula la alta productividad de la surgencia con la exportación y secuestración de carbono en regiones oceánicas profundas. Este mecanismo integrado (transporte lateral, migración vertical, interacción trófica) resalta la importancia de los organismos migradores como agentes esenciales en la bomba biológica y en la conexión biogeoquímica entre la costa y el océano profundo.

El aporte de las comunidades de zooplancton y micronecton destaca los roles complementarios de las interacciones presa-depredador y la migración vertical diaria como impulsores del flujo activo de carbono. Ya que estos mecanismos fortalecen el vínculo entre la productividad superficial y las capas profundas del océano, demostrando que conectan la producción impulsada por la surgencia con el secuestro de carbono en el océano profundo.

The magnitude of fluxes determined in this study suggests that micronekton not only supplements, but it largely exceeds the role of zooplankton in fueling deeper layers, particularly under OMZ

La presente tesis provee apoyo a la hipótesis sobre la existencia de una escalera trófica que promueve y acelera el flujo vertical de carbono orgánico hacia el océano profundo. Sin embargo, se requieren estudios adicionales que permitan establecer con mayor certeza las conexiones entre depredadores y sus presas y sus correspondientes amplitudes de migración. Estudios futuros podrían incluir análisis complementarios sobre otros indicadores o marcadores de depredador-presa, tales como análisis de contenido estomacal sobre la base

de marcadores moleculares, en conjunto a estimaciones de amplitud de migración.

## 7. REFERENCIAS


Andersen, V. (2004). Vertical distributions of zooplankton across the Almeria-Oran frontal zone (Mediterranean Sea). Journal of Plankton Research, 26(3), 275-293. https://doi.org/10.1093/plankt/fbh036

Anderson, T. R., Martin, A. P., Lampitt, R. S., Trueman, C. N., Henson, S. A., Mayor, D. J., & Link, J. (2019). Quantifying carbon fluxes from primary production to mesopelagic fish using a simple food web model. ICES Journal of Marine Science, 76(3), 690-701. https://doi.org/10.1093/icesjms/fsx234

Archibald, K. M., Siegel, D. A., & Doney, S. C. (2019). Modeling the Impact of Zooplankton Diel Vertical Migration on the Carbon Export Flux of the Biological Pump. Global Biogeochemical Cycles, 33(2), 181-199. https://doi.org/10.1029/2018gb005983

Ariza, A., Garijo, J. C., Landeira, J. M., Bordes, F., & Hernández-León, S. (2015). Migrant biomass and respiratory carbon flux by zooplankton and micronekton in the subtropical northeast Atlantic Ocean (Canary Islands). Progress in Oceanography, 134, 330-342. https://doi.org/10.1016/j.pocean.2015.03.003

Bates, N. R. (2019). Ocean Carbon Cycle. In Encyclopedia of Ocean Sciences (pp. 418-428). https://doi.org/10.1016/b978-0-12-409548-9.11598-2

Belcher, A., Cook, K., Bondyale-Juez, D., Stowasser, G., Fielding, S., Saunders, R. A., Mayor, D. J., Tarling, G. A., & Proud, R. (2020). Respiration of mesopelagic fish: a comparison of respiratory electron transport system (ETS) measurements and allometrically calculated rates in the Southern Ocean and Benguela Current. ICES Journal of Marine Science, 77(5), 1672-1684. https://doi.org/10.1093/icesjms/fsaa031

Bianchi, D., Stock, C., Galbraith, E. D., & Sarmiento, J. L. (2013). Diel vertical migration: Ecological controls and impacts on the biological pump in a one-dimensional ocean model. Global Biogeochemical Cycles, 27(2), 478-491. https://doi.org/https://doi.org/10.1002/gbc.20031

Bode, A., & Hernández-León, S. (2018). Trophic Diversity of Plankton in the Epipelagic and Mesopelagic Layers of the Tropical and Equatorial Atlantic Determined with Stable Isotopes. Diversity, 10(2). https://doi.org/10.3390/d10020048

Bode, A., Olivar, M. P., & Hernández-León, S. (2021). Trophic indices for micronektonic fishes reveal their dependence on the microbial system in the North Atlantic. Sci Rep, 11(1), 8488. https://doi.org/10.1038/s41598-021-87767-x

Boyd, P. W., Claustre, H., Levy, M., Siegel, D. A., & Weber, T. (2019). Multi-faceted particle pumps drive carbon sequestration in the ocean. Nature, 568(7752), 327-335. https://doi.org/10.1038/s41586-019-1098-2

Buesseler, K. O., & Boyd, P. W. (2009). Shedding light on processes that control particle export and flux attenuation in the twilight zone of the open ocean. Limnology and Oceanography, 54(4), 1210-1232.

Cahuin, S. M., Cubillos, L. A., Escribano, R., Luis Blanco, J., Ñiquen, M., & Serra, R. (2013). Sensitivity of recruitment rates anchovy (*Engraulis ringens*) to environmental changes in Southern Peru—Northern Chile. Environmental Development, 7, 88-101. https://doi.org/https://doi.org/10.1016/j.envdev.2013.03.004

Chikaraishi, Y., Ogawa, N. O., Kashiyama, Y., Takano, Y., Suga, H., Tomitani, A., Miyashita, H., Kitazato, H., & Ohkouchi, N. (2009). Determination of aquatic food-web structure based on compound-specific nitrogen isotopic composition of amino acids. Limnology and Oceanography, 7, 740-750.

Cotté, C., Ariza, A., Berne, A., Habasque, J., Lebourges-Dhaussy, A., Roudaut, G., Espinasse, B., Hunt, B. P. V., Pakhomov, E. A., Henschke, N., Péron, C., Conchon, A., Koedooder, C., Izard, L., & Cherel, Y. (2022). Macrozooplankton and micronekton diversity and associated carbon vertical patterns and fluxes under distinct productive conditions around the Kerguelen Islands. Journal of Marine Systems, 226. https://doi.org/10.1016/j.jmarsys.2021.103650

Daneri, G., Dellarossa, V., Quiñones, R., Jacob, B., Montero, P., & Ulloa, O. (2000). Primary production and community respiration in the Humboldt Current System off Chile and associated oceanic areas. Marine Ecology Progress Series, 197, 41-49. https://doi.org/10.3354/meps197041

Davison, P. C., Checkley, D. M., Koslow, J. A., & Barlow, J. (2013). Carbon export mediated by mesopelagic fishes in the northeast Pacific Ocean. Progress in Oceanography, 116, 14-30. https://doi.org/10.1016/j.pocean.2013.05.013

De La Rocha, C. L., & Passow, U. (2007). Factors influencing the sinking of POC and the efficiency of the biological carbon pump. Deep Sea Research Part II: Topical Studies in Oceanography, 54(5), 639-658. https://doi.org/https://doi.org/10.1016/j.dsr2.2007.01.004

Décima, M. (2022). Zooplankton trophic structure and ecosystem productivity. Marine Ecology Progress Series, 692, 23-42. https://doi.org/10.3354/meps14077

Escribano, R., Daneri, G., Farías, L., Gallardo, V. A., González, H. E., Gutiérrez, D., Lange, C. B., Morales, C. E., Pizarro, O., Ulloa, O., & Braun, M. (2004). Biological and chemical consequences of the 1997–1998 El Niño in the Chilean coastal upwelling system: a synthesis. Deep Sea Research Part II: Topical Studies in Oceanography, 51(20), 2389-2411. https://doi.org/https://doi.org/10.1016/j.dsr2.2004.08.011

Escribano, R., Hidalgo, P., González, H., Giesecke, R., Riquelme-Bugueño, R., & Manríquez, K. (2007). Seasonal and inter-annual variation of mesozooplankton in the coastal upwelling zone off central-southern Chile. Progress in Oceanography, 75(3), 470-485. https://doi.org/10.1016/j.pocean.2007.08.027

Escribano, R., & McLaren, I. (1999). Production of *Calanus chilensis* in the upwelling area of Antofagasta, northern Chile. Marine Ecology Progress Series, 177, 147-156. https://doi.org/10.3354/meps177147

Escribano, R., & Morales, C. E. (2004). Sistemas de surgencia costera. In I. C. Werlinger (Ed.), Biología Marina y oceanografía: conceptos y procesos. Consejo Nacional del Libro y Lectura-UdeC.

Escribano, R., & Morales, C. E. (2012). Spatial and temporal scales of variability in the coastal upwelling and coastal transition zones off central-southern Chile (35–40°S). Progress in Oceanography, 92-95, 1-7. https://doi.org/https://doi.org/10.1016/j.pocean.2011.07.019

Escribano, R., & Schneider, W. (2007). The structure and functioning of the coastal upwelling system off central/southern Chile. Progress in Oceanography, 75(3), 343-347. https://doi.org/10.1016/j.pocean.2007.08.020

Fernández-Urruzola, I., Bode, A., Loick-Wilde, N., Schneider, W., Lindsay, D., & Escribano, R. (2023). Trophic ecology of midwater zooplankton along a productivity gradient in the Southeast Pacific. Frontiers in Marine Science, 10. https://doi.org/10.3389/fmars.2023.1057502

Fernandez-Urruzola, I., Ulloa, O., Glud, R. N., Pinkerton, M. H., Schneider, W., Wenzhofer, F., & Escribano, R. (2021). Plankton respiration in the Atacama Trench region: Implications for particulate organic carbon flux into the hadal realm. Limnol Oceanogr, 66(8), 3134-3148. https://doi.org/10.1002/lno.11866

Gorsky, G., Ohman, M. D., Picheral, M., Gasparini, S., Stemmann, L., Romagnan, J.-B., Cawood, A., Pesant, S., García-Comas, C., & Prejger, F. (2010). Digital zooplankton image analysis using the ZooScan integrated system. Journal of Plankton Research, 32(3), 285-303. https://doi.org/10.1093/plankt/fbp124

Hansen, A. N., & Visser, A. W. (2016). Carbon export by vertically migrating zooplankton: an optimal behavior model. Limnology and Oceanography, 61(2), 701-710. https://doi.org/10.1002/lno.10249

Hernandez-Leon, S., Koppelmann, R., Fraile-Nuez, E., Bode, A., Mompean, C., Irigoien, X., Olivar, M. P., Echevarria, F., Fernandez de Puelles, M. L., Gonzalez-Gordillo, J. I., Cozar, A., Acuna, J. L., Agusti, S., & Duarte, C. M. (2020). Large deep-sea zooplankton biomass mirrors primary production in the global ocean. Nat Commun, 11(1), 6048. https://doi.org/10.1038/s41467-020-19875-7

Hernández-León, S., Olivar, M. P., Fernández de Puelles, M. L., Bode, A., Castellón, A., López-Pérez, C., Tuset, V. M., & González-Gordillo, J. I. (2019). Zooplankton and Micronekton Active Flux Across the Tropical and Subtropical Atlantic Ocean. Frontiers in Marine Science, 6. https://doi.org/10.3389/fmars.2019.00535

Honjo, S., Manganini, S. J., Krishfield, R. A., & Francois, R. (2008). Particulate organic carbon fluxes to the ocean interior and factors controlling the biological pump: A synthesis of global sediment trap programs since 1983. Progress in Oceanography, 76(3), 217-285. https://doi.org/10.1016/j.pocean.2007.11.003

Hyslo, E. J. (1980). Stomach contents analysis-a review of methods and their application. Journal of Fish Biology, 17, 411-429.

Ikeda, T. (2014). Respiration and ammonia excretion by marine metazooplankton taxa: synthesis toward a global-bathymetric model. Marine Biology, 161(12), 2753-2766. https://doi.org/10.1007/s00227-014-2540-5

Ikeda, T. (2016). Routine metabolic rates of pelagic marine fishes and cephalopods as a function of body mass, habitat temperature and habitat depth. Journal of Experimental Marine Biology and Ecology, 480, 74-86. https://doi.org/10.1016/j.jembe.2016.03.012

Irigoien, X., Klevjer, T. A., Røstad, A., Martinez, U., Boyra, G., Acuña, J. L., Bode, A., Echevarria, F., Gonzalez-Gordillo, J. I., Hernandez-Leon, S., Agusti, S., Aksnes, D. L., Duarte, C. M., & Kaartvedt, S. (2014). Large mesopelagic fishes biomass and trophic efficiency in the open ocean. Nat Commun, 5, 3271. https://doi.org/10.1038/ncomms4271

Iverson, S. J., Field, C., Don Bowen, W., & Blanchard, W. (2004). Quantitative fatty acid signatue analysis: a new method of estimating predator diets. Ecological Monographs, 74(2), 211-235.

Kelly, T. B., Davison, P. C., Goericke, R., Landry, M. R., Ohman, M. D., & Stukel, M. R. (2019). The Importance of Mesozooplankton Diel Vertical Migration for Sustaining a Mesopelagic Food Web. Frontiers in Marine Science, 6. https://doi.org/10.3389/fmars.2019.00508

Le Moigne, F. A. C. (2019). Pathways of Organic Carbon Downward Transport by the Oceanic Biological Carbon Pump. Frontiers in Marine Science, 6. https://doi.org/10.3389/fmars.2019.00634

Longhurst, A. R., & Glen Harrison, W. (1989). The biological pump: Profiles of plankton production and consumption in the upper ocean. Progress in Oceanography, 22(1), 47-123. https://doi.org/https://doi.org/10.1016/0079-6611(89)90010-4

Lorrain, A., Graham, B., Ménard, F., Popp, B., Bouillon, S., van Breugel, P., & Cherel, Y. (2009). Nitrogen and carbon isotope values of individual amino acids: a tool to study foraging ecology of penguins in the Southern Ocean. Marine Ecology Progress Series, 391, 293-306. https://doi.org/10.3354/meps08215

Massing, J. C., Schukat, A., Auel, H., Auch, D., Kittu, L., Pinedo Arteaga, E. L., J., C. A., & W., H. (2022). Toward a Solution of the "Peruvian Puzzle": Pelagic Food-Web Structure and Trophic Interactions in the Northern Humboldt Current Upwelling System Off Peru. Frontiers in Marine Science, 8, 759603. https://doi.org/10.3389/fmars.2021.759603

McCarthy, M. D., Benner, R., Lee, C., & Fogel, M. L. (2007). Amino acid nitrogen isotopic fractionation patterns as indicators of heterotrophy in plankton, particulate, and dissolved organic matter. Geochimica et Cosmochimica Acta, 71(19), 4727-4744. https://doi.org/https://doi.org/10.1016/j.gca.2007.06.061

McClelland, J. W., & Montoya, J. P. (2002). Trophic Relationships and the nitrogen isotopic composition of amino acids in plankton. Ecology, 83(8), 2173-2180.

Medellín-Mora, J., Atkinson, A., Escribano, R., & Ji, R. (2020). Community structured production of zooplankton in the eastern boundary upwelling system off central/southern Chile (2003–2012). ICES Journal of Marine Science. https://doi.org/10.1093/icesjms/fsz193

Peters, R. H. (1983). The ecological implications of body size. Cambridge Univ, Press, Cambridge, UK.

Post, D. M. (2002). Using Stable Isotopes to Estimate Trophic Position: Models, Methods, and Assumptions. Ecology, 83(3). https://doi.org/10.1890/0012-9658(2002)083[0703:Usitet]2.0.Co;2

Ringelberg, P. (2010). Diel Vertical Migration of Zooplankton in Lakes and Oceans. Springer. https://doi.org/10.1007/978-90-481-3093-1

Riquelme-Bugueño, R., Perez-Santos, I., Alegria, N., Vargas, C. A., Urbina, M. A., & Escribano, R. (2020). Diel vertical migration into anoxic and high-pCO(2) waters: acoustic and net-based krill observations in the Humboldt Current. Sci Rep, 10(1), 17181. https://doi.org/10.1038/s41598-020-73702-z

Riquelme-Bugueño, R., Núñez, S., Jorquera, E., Valenzuela, L., Escribano, R., & Hormazábal, S. (2012). The influence of upwelling variation on the spatially-structured euphausiid community off central-southern Chile in 2007–2008. Progress in Oceanography, 92-95, 146-165. https://doi.org/10.1016/j.pocean.2011.07.003

Schneider, W., Fuenzalida, R., & Garcés, J. (2004). Corrientes marinas y masas de agua. In I. C. Werlinger (Ed.), Biología Marina y oceanografía: conceptos y procesos. Consejo Nacional del Libro y Lectura-UdeC.

Sobarzo, M., Shearman, R. K., & Lentz, S. (2007). Near-inertial motions over the continental shelf off Concepción, central Chile. Progress in Oceanography, 75(3), 348-362. https://doi.org/https://doi.org/10.1016/j.pocean.2007.08.021

Steinberg, D. K., Carlson, C. A., Bates, N. R., Goldthwait, S. A., Madin, L. P., & Michaels, A. F. (2000). Zooplankton vertical migration and the active transport of dissolved organic and inorganic carbon in the Sargasso Sea. Deep Sea Research Part I: Oceanographic Research Papers, 47(1), 137-158. https://doi.org/https://doi.org/10.1016/S0967-0637(99)00052-7

Steinberg, D. K., Cope, J. S., Wilson, S. E., & Kobari, T. (2008). A comparison of mesopelagic mesozooplankton community structure in the subtropical and subarctic North Pacific Ocean. Deep Sea Research Part II: Topical Studies in Oceanography, 55(14), 1615-1635. https://doi.org/https://doi.org/10.1016/j.dsr2.2008.04.025

Steinberg, D. K., & Landry, M. R. (2017). Zooplankton and the Ocean Carbon Cycle. Ann Rev Mar Sci, 9, 413-444. https://doi.org/10.1146/annurev-marine-010814-015924

Strub, P., Mesias, J., Montecino, V., Rutllant, J., & Salinas, S. (1998). Coastal ocean circulation off western South America. In A. Robinson & K. Brink (Eds.), The Sea (Vol. 11). Wiley, Hoboken.

Turner, J. T. (2015). Zooplankton fecal pellets, marine snow, phytodetritus and the ocean's biological pump. Progress in Oceanography, 130, 205-248. https://doi.org/https://doi.org/10.1016/j.pocean.2014.08.005

Tutasi, P., & Escribano, R. (2020). Zooplankton diel vertical migration and downward C flux into the oxygen minimum zone in the highly productive upwelling region off northern Chile. Biogeosciences, 17(2), 455-473. https://doi.org/10.5194/bg-17-455-2020

Ulloa, O., & Pantoja, S. (2009). The oxygen minimum zone of the eastern South Pacific. Deep Sea Research Part II: Topical Studies in Oceanography, 56(16), 987-991. https://doi.org/https://doi.org/10.1016/j.dsr2.2008.12.004

Vinogradov M.E. (1962). Feeding of the deep-sea zooplankton. Rapp. P.-v Réun. Cons. perm. int. Explor. Mer, 153: 114-120.

Wang, F., Wu, Y., Chen, Z., Zhang, G., Zhang, J., Zheng, S., & Kattner, G. (2019). Trophic Interactions of Mesopelagic Fishes in the South China Sea Illustrated by Stable Isotopes and Fatty Acids. Frontiers in Marine Science, 5. https://doi.org/10.3389/fmars.2018.00522

Wang, F., Wu, Y., Chen, Z., Zhang, G., Zhang, J., Zheng, S., & Kattner, G. (2019). Trophic Interactions of Mesopelagic Fishes in the South China Sea Illustrated by Stable Isotopes and Fatty Acids. Frontiers in Marine Science, 5. https://doi.org/10.3389/fmars.2018.00522

Weber, S. C., Loick-Wilde, N., Montoya, J. P., Bach, M., Doan-Nhu, H., Subramaniam, A., Liskow, I., Nguyen-Ngoc, L., Wodarg, D., & Voss, M. (2021). Environmental Regulation of the Nitrogen Supply, Mean Trophic Position, and Trophic Enrichment of Mesozooplankton in the Mekong River Plume and Southern South China Sea. Journal of Geophysical Research, 126, e2020JC017110. https://doi.org/10.1029/2020JC017110

Wishner, K. F., Seibel, B. A., Roman, C., Deutsch, C., Outram, D., Shaw, C. T., Birk, M. A., Mislan, K. A. S., Adams, T. J., Moore, D., & Riley, S. (2018). Ocean deoxygenation and zooplankton: Very small oxygen differences matter. Science Advances, 4(12), eaau5180. https://doi.org/doi:10.1126/sciadv.aau5180

Xing, D., Choi, B., Takizawa, Y., Fan, R., Sugaya, S., Tsuchiya, M., Ohkouchi, N., & Chikaraishi, Y. (2020). Trophic hierarchy of coastal marine fish communities viewed via compound-specific isotope analysis of amino acids. Marine Ecology Progress Series, 652, 137-144. https://doi.org/10.3354/meps13475

# 8. ANEXOS

Supplementary Material of:

**Assessing the food web structure of the mesozooplankton community in the highly variable coastal upwelling system of the southeast Pacific.**

Susana Cabrera-Núñez, Fernández-Urruzola, I. Bode A., Hernández-Trujillo, S., Hidalgo, P., and Escribano R.

S1. Metada Multinet deployed during LowpHox II (Summer 2018) and So296/2-Leg 1 cruise (Summer 2023). VF: Filtred Volumen

| Station | Lat (°S) | Long (°W) | Date | Time (h) | Depth strata (m) | VF ($m^{-3}$) |
|---|---|---|---|---|---|---|
| T5 | -20.1 | -70.5 | 04/02/2018 | 09:30 | 30-0 | 10 |
| | | | | | 90-30 | 17 |
| | | | | | 150-90 | 18 |
| | | | | | 400-150 | 73 |
| | | | | | 800-400 | 117 |
| | | | | 02:59 | 30-0 | 8 |
| | | | | | 90-30 | 15 |
| | | | | | 150-90 | 15 |
| | | | | | 400-150 | 69 |
| | | | | | 800-400 | 112 |
| | | | | 17:11 | 30-0 | 12 |
| | | | | | 90-30 | 21 |
| | | | | | 150-90 | 18 |
| | | | | | 400-150 | 78 |
| | | | | | 800-400 | 125 |
| T3 | -20.1 | -70.3 | 05/02/2018 | 12:00 | 30-0 | 10 |
| | | | | | 90-30 | 23 |
| | | | | | 150-90 | 19 |
| | | | | | 400-150 | 78 |
| | | | | | 800-400 | 118 |
| | | | | 02:45 | 30-0 | 8 |
| | | | | | 90-30 | 23 |
| | | | | | 150-90 | 19 |
| | | | | | 400-150 | 69 |
| | | | | | 800-400 | 113 |
| | | | | 15:00 | 30-0 | 8 |
| | | | | | 90-30 | 18 |
| | | | | | 150-90 | 21 |
| | | | | | 400-150 | 73 |
| | | | | | 800-400 | 118 |
| | | | | 20:30 | 30-0 | 9 |
| | | | | | 90-30 | 18 |
| | | | | | 150-90 | 17 |
| | | | | | 400-150 | 74 |
| | | | | | 800-400 | 131 |
| T39 | -36.4 | -73.8 | 22/01/2023 | 06:04 | 100-0 | 28 |
| | | | | | 200-100 | 27 |
| | | | | | 400-200 | 55 |
| | | | | | 600-400 | 58 |
| | | | | | 1000-600 | 86 |
| | | | | 07:28 | 100-0 | 32 |
| | | | | | 200-100 | 27 |
| | | | | | 400-200 | 55 |
| | | | | | 600-400 | 56 |
| | | | | | 1000-600 | 85 |
| | | | | 18:49 | 100-0 | 27 |
| | | | | | 200-100 | 28 |
| | | | | | 400-200 | 54 |
| | | | | | 600-400 | 57 |
| | | | | | 1000-600 | 83 |
| | | | | 20:07 | 100-0 | 28 |
| | | | | | 200-100 | 27 |

| | | |
|---|---|---|
| | 400-200 | 55 |
| | 600-400 | 58 |
| | 1000-600 | 86 |

S2. Zooplankton identified by Zooscan analysis. COD: Abbreviation of identified taxa. A: Abundance absolute (ind. $m^{-3}$). A%: Relative abundance. ESD: Equivalent Spherical Diameter. The shaded section represents ~85% of zooplankton abundance.

| T5 | | | | | T3 | | | | | T39 | | | | |
|---|---|---|---|---|---|---|---|---|---|---|---|---|---|---|
| **Taxa** | **COD.** | **A (ind. $m^{-3}$)** | **A%** | **ESD (mm)** | **Taxa** | **COD.** | **A (ind. $m^{-3}$)** | **A%** | **ESD (mm)** | **Taxa** | **COD.** | **A (ind. $m^{-3}$)** | **A%** | **ESD (mm)** |
| Smaller copepods | COP_S | 1039 | 43.9 | 0.6 | Smaller copepods | COP_S | 13868 | 39.4 | 0.6 | Smaller copepods | COP_S | 419.0 | 22.2 | 0.5 |
| *Calanus* | *Cal* | 297 | 12.5 | 0.6 | Large copepods | COP_L | 6833 | 19.4 | 1.3 | *Oithona* | Oit | 406.0 | 21.5 | 0.5 |
| Appendicularia | APN | 180 | 7.6 | 0.8 | *Calanus* | *Cal* | 5953 | 16.9 | 0.6 | *Calanus* | Cal | 312 | 16.5 | 0.8 |
| *Oncaea* | *Onc* | 137 | 5.8 | 0.5 | *Acartia* | *Aca* | 2612 | 7.4 | 0.8 | *Acartia* | Aca | 191 | 10.1 | 0.7 |
| Large copepods | COP_L | 125 | 5.3 | 1.5 | *Oncaea* | *Onc* | 1809 | 5.1 | 0.5 | *Oncaea* | Onc | 108 | 5.7 | 0.6 |
| *Oithona* | *Oit* | 111 | 4.7 | 0.5 | *Corycaeus* | *Cor* | 1542 | 4.4 | 0.6 | Ichthyoplankton (egss) | HUE | 106 | 5.6 | 1 |
| Salpidae | SAL | 93 | 3.9 | 2.8 | *Oithona* | *Oit* | 1034 | 2.9 | 0.5 | Large copepods | COP_L | 99 | 5.3 | 1.6 |
| Siphonophora | SIF | 77 | 3.2 | 1.8 | Appendicularia | APN | 557 | 1.6 | 0.9 | Ostracoda | OST | 47 | 2.5 | 0.8 |
| Hydrozoa | HYD | 57 | 2.4 | 2.4 | Briozoa | BRI | 299 | >1 | 0.5 | Nauplius | NAU | 46 | 2.4 | 0.5 |
| Ichthyoplankton (egss) | HUE | 51 | 2 | 1 | Annelida | ANE | 211 | >1 | 1.1 | Annelida | ANE | 41 | 2.2 | 1.2 |
| *Corycaeus* | *Cor* | 46 | 1.9 | 0.5 | Euphausiacea | EUF | 89 | >1 | 2.7 | Pteropoda | PTE | 35 | 1.9 | 0.5 |
| Annelida | ANE | 28 | 1.2 | 0.8 | Ichthyoplankton (egss) | HUE | 79 | >1 | 0.54 | *Rincalanus* | Rin | 22 | 1.1 | 2.4 |
| Chaetognath | QUE | 28 | 1.2 | 1.6 | Chaetognath | QUE | 65 | >1 | 1.7 | Appendicularia | APN | 14 | >1 | 0.9 |
| *Acartia* | *Aca* | 18 | >1 | 0.7 | Ostracoda | OST | 56 | >1 | 0.5 | Chaetognath | QUE | 11 | >1 | 2.4 |
| Nauplius | NAU | 18 | >1 | 0.5 | Decapod larva (zoea) | DEC | 47 | >1 | 0.9 | Cladocera | CLA | 10 | >1 | 0.5 |
| Cladocera | CLA | 15 | >1 | 0.6 | Hydrozoa | HYD | 43 | >1 | 1.9 | Decapod larva (zoea) | DEC | 4 | >1 | 1 |
| Ostracoda | OST | 13 | >1 | 0.7 | Siphonophora | SIF | 23 | >1 | 1.8 | Foraminifera | FOR | 4 | >1 | 0.4 |
| Pteropoda | PTE | 11 | >1 | 1 | Nauplius | NAU | 12 | >1 | 0.7 | Anfipoda | ANF | 3 | >1 | 1.8 |
| Briozoa | BRI | 11 | >1 | 0.6 | Pteropoda | PTE | 12 | >1 | 0.4 | Euphausiacea | EUF | 2 | >1 | 4.6 |
| Anfipoda | ANF | 4 | >1 | 2.6 | Salpidae | SAL | 8 | >1 | 1.5 | Salpidae | SAL | 2 | >1 | 1.8 |
| Euphausiacea | EUF | 4 | >1 | 3.1 | *Rincalanus* | *Rin* | 7 | >1 | 1.6 | *Corycaeus* | Cor | 1 | >1 | 0.6 |
| Decapod larva (zoea) | DEC | 3 | >1 | 0.8 | Foraminifera | FOR | 6 | >1 | 0.4 | Echinoidea larva | ECH | 1 | >1 | 0.5 |
| Foraminifera | FOR | 2 | >1 | 0.5 | Anfipoda | ANF | 1 | >1 | 3.4 | Stomatopod | EST | 1 | >1 | 0.6 |
| Ctenofora | CTE | 1 | >1 | 2.4 | | | | | | | | | | |
| Paralarvae | CEF | 1 | >1 | 4.3 | | | | | | | | | | |

S3. T-test comparing different sample pairs across stations, diel periods (Day/Night), and depth strata for T3, T5, and T39. The table presents the t-value and corresponding p-value for each comparison. Significant p-values ($p < 0.05$) are highlighted in red.

| T-test variable | Pair-sample | t-value | p-value |
|---|---|---|---|
| **Station** | T3 vs T5 | -1.15 | 0.13 |
| | T3 vs T39 | 1.38 | 0.09 |
| | T5 vs T39 | 2.49 | 0.01 |
| **Day/Nigth** | d_T3 vs n_T3 | 0.38 | 0.36 |
| | d_T5 vs n_T5 | -0.74 | 0.24 |
| | d_T39 vs n_T39 | -0.35 | 0.37 |
| **Depth strata T3** | 30-0 vs 90-30 | 1.85 | 0.16 |
| | 30-0 vs 150-90 | 13.64 | 0.00 |
| | 30-0 vs 400-150 | 4.23 | 0.07 |
| | 30-0 vs 800-400 | 3.34 | 0.09 |
| | 90-30 vs 150-90 | 2.12 | 0.14 |
| | 90-30 vs 400-150 | 0.82 | 0.25 |
| | 90-30 vs 800-400 | 2.06 | 0.09 |
| | 150-90 vs 400-150 | -1.74 | 0.17 |
| | 150-90 vs 800-400 | 1.16 | 0.23 |
| | 400-150 vs 800-400 | 1.71 | 0.17 |
| **Depth strata T5** | 30-0 vs 90-30 | 5.04 | 0.02 |
| | 30-0 vs 150-90 | 1.11 | 0.23 |
| | 30-0 vs 400-150 | 1.77 | 0.16 |
| | 30-0 vs 800-400 | 2.48 | 0.12 |
| | 90-30 vs 150-90 | 0.29 | 0.41 |
| | 90-30 vs 400-150 | 0.66 | 0.31 |
| | 90-30 vs 800-400 | 0.82 | 0.28 |
| | 150-90 vs 400-150 | 0.16 | 0.44 |
| | 150-90 vs 800-400 | 0.10 | 0.47 |
| | 400-150 vs 800-400 | -0.10 | 0.46 |
| **Depth strata T39** | 100-0 vs 200-100 | 11.01 | 0.03 |
| | 100-0 vs 400-200 | 3.10 | 0.10 |
| | 100-0 vs 600-400 | 1.00 | 0.25 |
| | 100-0 vs 900-600 | 1.41 | 0.20 |
| | 200-100 vs 400-200 | -5.21 | 0.02 |
| | 200-100 vs 600-400 | -5.44 | 0.02 |
| | 200-100 vs 900-600 | -2.01 | 0.15 |
| | 400-200 vs 600-400 | -1.05 | 0.20 |
| | 400-200 vs 900-600 | 0.32 | 0.40 |
| | 600-400 vs 900-600 | 0.86 | 0.27 |

S4. Analysis of variance (ANOVA) results testing the effects of station, depth strata, and size fraction on bulk $\delta^{15}N$ and $\delta^{13}C$ values. Significant results ($p < 0.05$) are marked with an asterisk (*). Depth strata and size fraction analyses were conducted separately for stations T3/T5 ([1]) and T39 ([2]).

| Source of variation | Variable | Df (Factor) | Df (Residual) | F value | p-value |
|---|---|---|---|---|---|
| **Station** | **$\delta^{15}N$** | 2 | 58 | 5.8 | <0.001* |
| | **$\delta^{13}C$** | 2 | 58 | 34.3 | <0.001* |
| **Depth strata** | **$\delta^{15}N^{1}$** | 4 | 37 | 5.3 | 0.002* |
| | **$\delta^{13}C^{1}$** | 4 | 37 | 2.1 | 0.1 |
| | **$\delta^{15}N^{2}$** | 4 | 14 | 12.5 | <0.001* |
| | **$\delta^{13}C^{2}$** | 4 | 14 | 1.1 | 0.4 |

**S5. Summary of the stepwise linear regression model explaining the variability of the Trophic Behavior Index (TBI) as a function of temperature (T), dissolved oxygen (DO), and chlorophyll-a (Chl-*a*). The table shows the source of variation, degrees of freedom (Df), sum of squares (SS), F-statistics, partial $R^2$, and p-values. Only variables retained in the final model (T and DO) are shown with statistical values. Chlorophyll-*a* was excluded during the model selection process.**

| Source of Variation | Df | Sum Sq (SS) | F value | $R^2$ | p-value |
|---|---|---|---|---|---|
| **T (°C)** | 1 | 1.5854 | 15.98 | 0.0615 | 8.57e-05 |
| **DO (µmol $Kg^{-1}$)** | 1 | 0.2442 | 2.22 | 0.0047 | 0.138 |
| **Chl-*a* (mg $m^{-3}$)** | – | – | – | – | – |
| **Residuals** | 235 | 25.843 | – | 0.9338 | – |

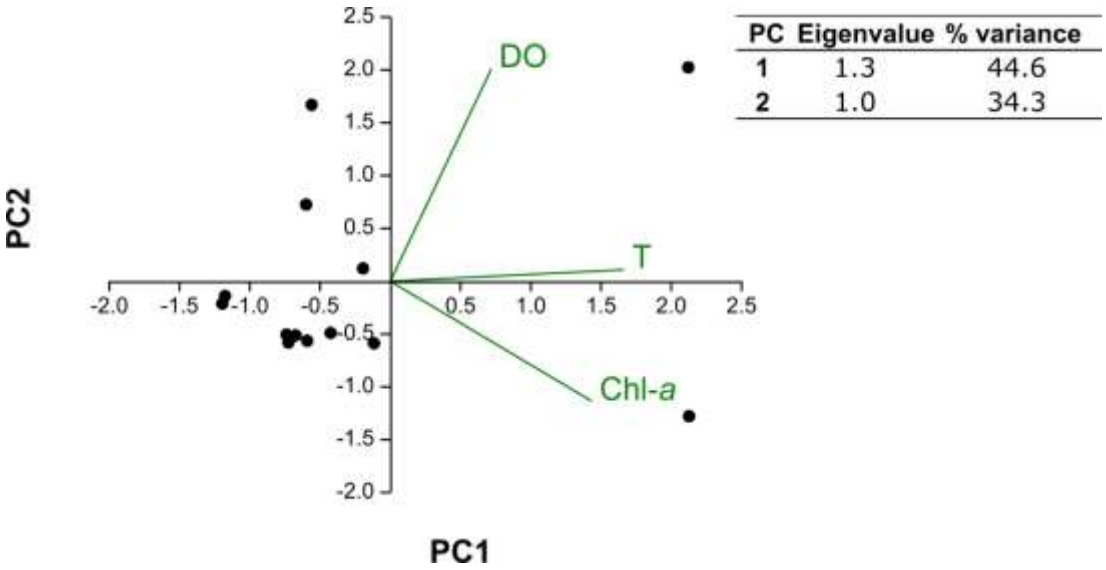


S6. Principal Component Analysis (PCA) biplot showing the ordination of samples based on environmental variables: Temperature (T °C), dissolved oxygen (DO µmol $Kg^{-1}$), and Chlorophyll-a concentration (Chl-*a* mg $m^{-3}$). Arrows represent the direction and strength of each variable's contribution to the principal components. PC1 and PC2 explain 44.6% and 34.3% of the total variance, respectively.

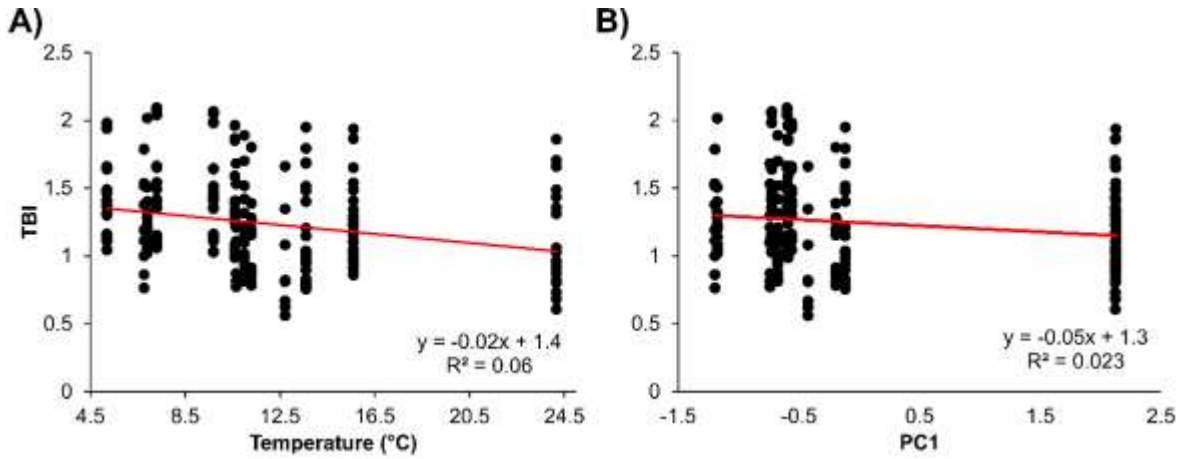


Fig. S7. The relationship between the Trophic Behavior Index (TBI) and temperature (A), and between TBI and the First Principal Component (PC1) (B) after a PCA analysis including the independent factors temperature, dissolved oxygen and Chl-*a* of the zooplankton community sampled at 3 stations in the northern and southern upwelling region of Chile.

*JGR:biogeosciences*

Supporting Information for

# Biological and Physical Drivers of the Downward Carbon Flux Mediated by Zooplankton and Micronekton in the Upwelling System Off Central-Southern Chile

S. Cabrera-Núñez[1, 2], I. Fernández-Urruzola[2,3], A. Bode[4], N. Osma[2,3], V. Mohrholz[5], and R. Escribano[2,6]

[1]Programa de Postgrado en Oceanografía, Departamento de Oceanografía, Facultad de Ciencias Naturales y Oceanográficas, Universidad de Concepción, Casilla 160-C, Concepción, Chile.

[2]Millennium Institute of Oceanography, Universidad de Concepción, Concepción, Chile.

[3]Instituto de Ciencias Naturales Alexander von Humboldt, Universidad de Antofagasta, Antofagasta, Chile.

[4]Centro Oceanográfico de A Coruña, Instituto Español de Oceanografía, CSIC, A Coruña, España.

[5] Leibniz-Institute for Baltic Sea Research Warnemünde, Seestraße 15, 18119 Rostock, Germany

[6]Departamento de Oceanografía, Universidad de Concepción, Concepción, Chile.

## Contents of this file



## Additional Supporting Information (Files uploaded separately)



## Introduction

This Supporting Information provides detailed isotopic and amino acid data (Table S1), mesozooplankton biomass by depth and station (Table S2), and migrant biomass estimates (Table S3). These data complement the analyses presented in the main text. Non-determined (n.d.) values indicate samples that could not be analyzed due to insufficient material or low ion signal (< 100 mV).

Table S1. Isotopic and amino acid composition of zooplankton, and micronekton samples collected across depth strata (m). The table includes bulk $\delta^{15}N$ (‰), $\delta^{13}C$ (‰), and C:N values, $\delta^{15}N$ of trophic, source and the metabolic amino acid . Additionally, baseline-corrected $\delta^{15}N$ values of Phe (PheC) are presented across different sizes (µm). n.d. indicates non-determined values due to insufficient sample material for derivatization or values below the reliable detection threshold for ion signals in the mass spectrometer (>100 mV).

| Sample | St | Depth strata (m) | Size (µm) | Bulk | | | Trp AA $\delta^{15}N$ | | | | | | | Source AA $\delta^{15}N$ | | Metabolic AA | $\delta^{15}N$ PheC |
|---|---|---|---|---|---|---|---|---|---|---|---|---|---|---|---|---|---|
| | | | | $\delta^{15}N$ (‰) | $\delta^{13}C$ (‰) | C:N | Ala | Asx | Glx | Ile | Leu | Pro | Val | Phe | Lys | Thr | |
| **Zoopl.** | **St. 18** | 60-20 | 200-500 | 14.7 | -16.7 | 4.4 | 25.9 | 18.3 | 23.7 | n.d | 19.6 | 18.3 | n.d | 11.2 | 11.9 | n.d | 10.6 |
| | | 60-20 | 500-1000 | 14.2 | -17.5 | 4.7 | 24.4 | 18.9 | 24.7 | n.d | 17.9 | 19.5 | n.d | 11.3 | 9.9 | n.d | 10.6 |
| | | 60-20 | 1000-2000 | 13.8 | -17.7 | 5.6 | 23.7 | 18.4 | 24.2 | n.d | 15.9 | 20.3 | n.d | 10.3 | 10.8 | 5.5 | 9.6 |
| | | 20-0 | 200-500 | 14.0 | -6.7 | 4.2 | 25.8 | 18.0 | 25.2 | n.d | 16.3 | 19.2 | n.d | 10.6 | 10.9 | 1.8 | 9.8 |
| | | 20-0 | 500-1000 | 13.9 | -8.6 | 4.7 | 25.3 | 18.7 | 23.9 | n.d | 16.9 | 16.8 | 19 | 10.8 | 4.0 | 5.7 | 10.2 |
| | | 20-0 | 2000-5000 | 13.6 | -17.2 | 5.2 | 26.4 | 19.7 | 25.2 | n.d | 17.8 | 16.8 | 23.7 | 10.7 | 3.5 | 3.4 | 10.0 |
| | | 20-0 | 1000-2000 | 13.7 | -17.7 | 3.7 | 24.8 | 17.1 | 24.4 | n.d | 16.5 | 19.3 | n.d | 11.3 | 9.2 | 3.9 | 10.6 |
| | **St. 26** | 80-20 | 200-500 | 13.6 | -17.1 | 4.5 | 21.5 | 18.2 | 23.1 | n.d | 17.2 | 19.8 | n.d | 11.9 | 7.7 | n.d | 11.4 |
| | | 80-20 | 500-1000 | 12.8 | -17.0 | 4.7 | 21.4 | 17.0 | 22.2 | n.d | 16.4 | 15.2 | n.d | 11.4 | 4.4 | n.d | 10.9 |
| | | 80-20 | 2000-5000 | 13.3 | -16.9 | 4.2 | 24.1 | 18.9 | 24.3 | n.d | 16.4 | 16.4 | n.d | 11.2 | 5.4 | n.d | 10.6 |
| | | 80-20 | 1000-2000 | 13.3 | -16.8 | 4.2 | 22.2 | 18.4 | 24.5 | n.d | 15.9 | 18.7 | n.d | 10.6 | 8.8 | n.d | 9.9 |
| | | 20-0 | 200-500 | 13.1 | -18.0 | 5.4 | 21.7 | 18.4 | 23.5 | n.d | 15.7 | 20.0 | n.d | 11.0 | 9.1 | n.d | 10.4 |
| | | 20-0 | 500-1000 | 12.5 | -19.0 | 7.0 | 22.8 | 18.1 | 22.9 | n.d | 16.4 | 15.8 | n.d | 10.5 | 2.9 | n.d | 9.9 |
| | | 20-0 | 2000-5000 | 13.8 | -17.9 | 5.9 | 28.7 | 19.3 | 27.3 | n.d | 17.8 | 21.1 | n.d | 10.0 | 8.4 | n.d | 9.0 |
| | | 20-0 | 1000-2000 | 12.9 | -18.2 | 5.0 | 23.5 | 20.0 | 25.6 | n.d | 18.2 | 21.3 | n.d | 10.4 | 9.3 | n.d | 9.7 |
| | **St. 31** | 200-80 | 200-500 | 13.5 | -17.6 | 4.3 | 25.6 | 18.4 | 23.6 | n.d | 20.1 | 19.2 | n.d | 9.1 | 10.8 | n.d | 8.4 |
| | | 200-80 | 500-1000 | 14.1 | -18.2 | 4.3 | 28.8 | 19.0 | 25.3 | n.d | 20.0 | 20.7 | n.d | 11.2 | 9.8 | n.d | 10.5 |
| | | 200-80 | 2000-5000 | 13.4 | -17.1 | 3.9 | 23.0 | 19.7 | 23.8 | n.d | 17.7 | 19.6 | n.d | 10.6 | 10.9 | n.d | 9.9 |
| | | 200-80 | 1000-2000 | 14.0 | -17.0 | 3.9 | 24.5 | 18.6 | 24.1 | n.d | 17.8 | 19.7 | n.d | 10.3 | 12.1 | n.d | 9.7 |
| | | 80-25 | 200-500 | 13.2 | -16.4 | 4.5 | 26.9 | 19.0 | 23.4 | n.d | 13.6 | 19.5 | n.d | 9.3 | 8.5 | n.d | 8.6 |
| | | 80-25 | 500-1000 | 13.4 | -18.0 | 5.0 | 26.4 | 19.1 | 23.4 | n.d | 15.7 | 20.1 | 20.5 | 9.3 | 11.3 | 5.8 | 8.6 |
| | | 80-25 | 2000-5000 | 14.0 | -17.3 | 4.1 | 27.8 | 18.5 | 23.2 | n.d | 16.5 | 19.4 | 20.6 | 8.7 | 10.4 | -2.6 | 8.0 |
| | | 80-25 | 1000-2000 | 14.5 | -17.2 | 4.4 | 27.5 | 18.2 | 22.9 | n.d | 15.8 | 18.4 | n.d | 9.4 | 11.1 | n.d | 8.8 |
| | | 25-0 | 200-500 | 13.4 | -17.7 | 4.6 | 24.1 | 16.5 | 22.3 | n.d | 15.7 | 18.8 | 21.3 | 9.7 | 11.2 | 8.2 | 9.1 |
| | | 25-0 | 500-1000 | 13.7 | -17.6 | 4.5 | 23.2 | 17.0 | 21.7 | n.d | 17.3 | 13.0 | n.d | 9.6 | 1.8 | n.d | 9.1 |
| | | 25-0 | 2000-5000 | 13.7 | -17.4 | 5.0 | 29.4 | 21.6 | 28.9 | n.d | 20.2 | 15.3 | n.d | 11.4 | 3.1 | n.d | 10.5 |

| | | | | | | | | | | | | | | | | | |
|---|---|---|---|---|---|---|---|---|---|---|---|---|---|---|---|---|---|
| | 25-0 | 1000-2000 | 13.5 | -17.9 | 4.2 | 27.0 | 20.7 | 24.4 | n.d | 17.3 | 19.7 | 19.4 | 9.5 | 7.3 | 3.4 | 8.8 |

Table S1. Be continued

| Sample | St | Depth strata (m) | Size (µm) | Bulk | | | Trp AA $\delta^{15}N$ | | | | | | | Source AA $\delta^{15}N$ | | Metabolic AA | $\delta^{15}N$ PheC |
|---|---|---|---|---|---|---|---|---|---|---|---|---|---|---|---|---|---|
| | | | | $\delta^{15}N$ (‰) | $\delta^{13}C$ (‰) | C:N | Ala | Asx | Glx | Ile | Leu | Pro | Val | Phe | Lys | Thr | |
| | **St. 39** | 1000-600 | 200-500 | 15.6 | -17.7 | 5.0 | 28.2 | 23.1 | 28.5 | n.d | 24.0 | 25.7 | 26.1 | 11.9 | 12.9 | 0.2 | 11.3 |
| | | 1000-600 | 500-1000 | 16.1 | -17.5 | 4.6 | 28.8 | 23.0 | 28.9 | n.d | 23.6 | 17.5 | 25.1 | 12.6 | 4.6 | 1.9 | 12.0 |
| | | 1000-600 | 1000-2000 | 15.2 | -17.8 | 4.5 | 27.9 | 23.2 | 28.2 | n.d | 21.4 | 20.4 | 22.7 | 11.5 | 4.5 | -1.4 | 10.8 |
| | | 1000-600 | 2000-5000 | 14.1 | -18.2 | 4.1 | 27.2 | 20.3 | 24.8 | n.d | 18.8 | 14.1 | 20.3 | 11.5 | 3.3 | -0.3 | 11.0 |
| | | 600-400 | 200-500 | 16.3 | -17.6 | 4.6 | 28.6 | 22.0 | 27.4 | n.d | 24.0 | 24.9 | 23.9 | 8.6 | 13.2 | -0.9 | 7.8 |
| | | 600-400 | 500-1000 | 15.8 | -17.8 | 4.2 | 27.8 | 22.2 | 25.8 | n.d | 22.4 | 12.8 | n.d | 11.0 | 4.0 | -1.9 | 10.4 |
| | | 600-400 | 1000-2000 | 15.1 | -17.9 | 4.9 | 26.7 | 22.9 | 26.7 | n.d | 23.1 | 13.3 | 27.1 | 11.5 | 4.2 | -2.6 | 10.8 |
| | | 600-400 | 2000-5000 | 15.7 | -17.7 | 4.1 | 25.9 | 18.7 | 22.8 | n.d | 17.1 | 19.2 | 20.4 | 10.7 | 8.7 | -0.1 | 10.2 |
| | | 400-200 | 200-500 | 15.7 | -17.3 | 4.4 | 27.6 | 22.2 | 27.3 | n.d | 22.4 | 24.0 | n.d | 10.3 | 12.6 | 3.0 | 9.6 |
| | | 400-200 | 500-1000 | 16.1 | -17.4 | 4.3 | 28.3 | 21.5 | 25.7 | n.d | 22.5 | 14.3 | n.d | 10.7 | 2.1 | -0.9 | 10.0 |
| | | 400-200 | 1000-2000 | 15.0 | -18.1 | 4.5 | 27.3 | 21.4 | 26.7 | n.d | 20.8 | 23.5 | 21.8 | 6.1 | 12.0 | -0.2 | 5.1 |
| | | 400-200 | 2000-5000 | 15.6 | -18.3 | 4.4 | 29.0 | 21.0 | 26.4 | n.d | 18.8 | 21.6 | n.d | 6.8 | 6.1 | -4.0 | 6.0 |
| | | 200-100 | 200-500 | 15.5 | -17.3 | 4.4 | 28.0 | 21.9 | 27.4 | n.d | 20.9 | 23.8 | 23.5 | 11.0 | 13.9 | 3.1 | 10.3 |
| | | 200-100 | 500-1000 | 15.0 | -17.7 | 4.3 | 28.6 | 22.8 | 28.3 | n.d | 22.2 | 24.0 | 23.4 | 11.8 | 14.0 | 8.4 | 11.1 |
| | | 200-100 | 1000-2000 | 14.7 | -17.9 | 4.5 | 27.1 | 21.1 | 26.9 | n.d | 18.7 | 22.1 | n.d | 11.7 | 13.0 | n.d | 11.1 |
| | | 100-0 | 200-500 | 13.2 | -17.1 | 4.1 | 24.5 | 18.9 | 23.5 | n.d | 15.9 | 20.7 | 19.8 | 10.1 | 12.0 | 5.5 | 9.6 |
| | | 100-0 | 500-1000 | 13.6 | -16.8 | 4.1 | 26.2 | 20.7 | 23.8 | 18.1 | 18.1 | 11.2 | 19.3 | 10.1 | 2.5 | 9.7 | 9.6 |
| | | 100-0 | 1000-2000 | 13.5 | -18.0 | 4.5 | 26.8 | 21.9 | 24.8 | 17.5 | 18.1 | 21.1 | 19.3 | 10.4 | 13.4 | 4.7 | 9.8 |
| | | 100-0 | 2000-5000 | 13.3 | -17.4 | 3.6 | 27.1 | 22.0 | 25.3 | 16.5 | 19.2 | 20.9 | 20.1 | 11.2 | 8.6 | 3.0 | 10.6 |
| **Micron.** | **St. 39** | 1000-600 | $2.0x10^5$ | 15.8 | -18.1 | 3.5 | 31.2 | 24.2 | 32.4 | 23.6 | 26.4 | 28.0 | 27.2 | 9.7 | 12.1 | -10.6 | 8.5 |
| | | 1000-600 | $1.7x10^5$ | 16.1 | -18.5 | 3.5 | 30.6 | 23.8 | 30.9 | 25.3 | 26.4 | 27.7 | 25.4 | 9.7 | 12.3 | -12.6 | 9.4 |
| | | 1000-600 | $1.4x10^5$ | 16.7 | -17.6 | 3.4 | 32.4 | 25.8 | 34.0 | n.d. | 29.3 | 29.7 | 25.8 | 9.3 | 13.0 | -11.0 | 7.6 |
| | | 1000-600 | $2.5x10^4$ | 17.7 | -19.0 | 3.2 | 34.6 | 24.7 | 32.6 | 28.0 | 28.8 | 27.3 | 28.5 | 9.0 | 12.7 | -12.4 | 8.5 |
| | | 1000-600 | $2.0x10^4$ | 18.2 | -18.7 | 3.5 | 34.9 | 25.8 | 37.6 | 30.2 | 31.3 | 27.4 | 31.8 | 10.2 | 6.5 | -13.0 | 8.3 |
| | | 1000-600 | $4.3x10^4$ | 18.5 | -18.2 | 3.3 | 30.9 | 24.4 | 29.6 | n.d | 27.8 | 29.2 | 22.9 | 9.0 | 11.5 | -10.7 | 7.9 |
| | | 1000-600 | $5.3x10^4$ | 17.9 | -18.5 | 3.4 | 29.4 | 25.0 | 29.6 | n.d | 27.8 | 27.1 | 27.2 | 12.2 | 13 | -6.2 | 11.2 |
| | | 1000-600 | $6.0x10^4$ | 17.8 | -19.0 | 3.5 | 32.5 | 23.4 | 33.1 | 27.6 | 27.5 | 31.7 | 28.2 | 10.7 | 11.5 | -15.7 | 7.8 |

| | | | | | | | | | | | | | | | | |
|---|---|---|---|---|---|---|---|---|---|---|---|---|---|---|---|---|
| | 600-400 | $4.9x10^4$ | 17.0 | -19.2 | 5.6 | 30.6 | 25.2 | 33.6 | 24.8 | 27.7 | 31.9 | 26.9 | 11.1 | 14.2 | -10.2 | 9.7 |
| | 600-400 | $5.2x10^4$ | 17.1 | -19.0 | 5.7 | 31.7 | 25.9 | 34.7 | 27.6 | 28.5 | 32.8 | 25.9 | 11.3 | 14.3 | -10.4 | 10.0 |
| | 600-400 | $6.0x10^4$ | 17.1 | -19.4 | 6.1 | 31.6 | 25.6 | 29.0 | 26.9 | 28.5 | 31.9 | 27.4 | 10.4 | 13.4 | -9.8 | 9.4 |

Table S1. Be continued

| Sample | St | Depth strata (m) | Size (µm) | Bulk | | | Trp AA $\delta^{15}N$ | | | | | | | Source AA $\delta^{15}N$ | | Metabolic AA | $\delta^{15}N$ PheC |
|---|---|---|---|---|---|---|---|---|---|---|---|---|---|---|---|---|---|
| | | | | $\delta^{15}N$ (‰) | $\delta^{13}C$ (‰) | C:N | Ala | Asx | Glx | Ile | Leu | Pro | Val | Phe | Lys | Thr | |
| | | 600-400 | $5.3x10^4$ | 15.9 | -17.8 | 3.2 | 29.6 | 24.9 | 28.0 | n.d | 27.3 | 29.4 | 25.1 | 8.9 | 8.1 | -8.8 | 7.8 |
| | | 600-400 | $8.8x10^4$ | 17.4 | -20.6 | 7.1 | 31.8 | 24.1 | 29.0 | n.d | 28.0 | 20.9 | 26.8 | 11.6 | 3.3 | -6.1 | 10.7 |
| | | 600-400 | $9.4x10^4$ | 18.2 | -20 | 6.8 | 31.8 | 24.1 | 29.3 | n.d | 28.4 | 28.9 | 29.0 | 9.3 | 12.8 | -7.8 | 8.2 |
| | | 600-400 | $9.7x10^4$ | 18.3 | -19.4 | 5.9 | 33.8 | 23.8 | 30.0 | n.d | 28.5 | 30.6 | 29.5 | 7.9 | 12.2 | -6.7 | 6.7 |
| | | 400-200 | $6.1x10^4$ | n.d | n.d | n.d | 29.1 | 23.4 | 28.2 | 26.2 | 26.6 | 30.8 | 24.7 | 9.3 | 12.2 | -10.2 | 8.3 |
| | | 400-200 | $4.4x10^4$ | 17.3 | -18.0 | 3.1 | 30.2 | 23.5 | 31.1 | 24.9 | 27.1 | 29.9 | 27.2 | 9.7 | 11.9 | -9.4 | 8.5 |
| | | 400-200 | $3.2x10^4$ | 17.4 | -18.1 | 3.1 | 30.4 | 24.2 | 26.2 | n.d | 27.0 | 30.3 | 28.6 | 9.2 | 13.6 | -7.2 | 8.2 |
| | | 400-200 | $6.2x10^4$ | 16.5 | -19.8 | 6.2 | 33.0 | 25.7 | 30.8 | 27.4 | 29.3 | 31.5 | 27.7 | 10.2 | 7.9 | -10.1 | 9.00 |
| | | 400-200 | $6.7x10^4$ | 17.1 | -19.5 | 6.1 | 29.9 | 21.6 | 27.2 | n.d | 26.2 | 28.5 | 28.7 | 7.7 | 11.2 | -6.5 | 6.7 |
| | | 400-200 | $7.9x10^4$ | 17.6 | -19.0 | 5.7 | 31.0 | 22.5 | 27.8 | n.d | 26.6 | 28.6 | 26.7 | 8.1 | 12.1 | -7.7 | 7.1 |
| | | 400-200 | $3.5x10^4$ | 16.4 | -17.8 | 3.1 | 31.2 | 24.2 | 29.9 | n.d | 28.2 | 28.9 | 26.7 | 7.9 | 12 | n.d | 6.7 |
| | | 400-200 | $3.6x10^4$ | 16.3 | -17.7 | 3.1 | 34.2 | 26.2 | 30.8 | n.d | 25 | 24.4 | 27.1 | 9.9 | 11.5 | -8.3 | 8.7 |
| | | 400-200 | $3.8x10^4$ | 16.9 | -18.1 | 3.1 | 33.8 | 25.9 | 30.1 | 24.1 | 25.2 | 25.4 | 27.0 | 10.3 | 11.3 | -8.6 | 9.2 |
| | | 400-200 | $4.7x10^4$ | 16.1 | -17.9 | 3.1 | 32.0 | 24.9 | 33.3 | 25.1 | 27.7 | 24.9 | 27.8 | 8.6 | 6.0 | -10.1 | 7.2 |
| | | 200-100 | $6.1x10^4$ | 16.6 | -19.7 | 5.4 | 36.2 | 28.1 | 32.5 | 22.6 | 26.5 | 24.6 | 27.7 | 9.8 | 11.4 | -10.7 | 8.6 |
| | | 200-100 | $6.7x10^4$ | 17.0 | -19.1 | 5.8 | 29.3 | 22.1 | 27.1 | n.d | 25.1 | 27.3 | 27 | 8.9 | 11.7 | -12.0 | 8.0 |
| | | 200-100 | $8.9x10^4$ | 17.8 | -19.8 | 6.3 | 30.3 | 22.6 | 27.7 | n.d | 27.1 | 27.4 | n.d | 9.8 | 10.7 | -9.2 | 8.8 |
| | | 100-0 | $8.0x10^4$ | 16.9 | -19.1 | 5.4 | 32.2 | 25.6 | 36.8 | 28.1 | 29.3 | 33.1 | 27.2 | 9.1 | 13.7 | -10.5 | 7.4 |
| | | 100-0 | $7.5x10^4$ | 16.7 | -19.9 | 6.2 | 33.8 | 28.1 | 32.3 | 26.3 | 27.2 | 27.0 | 27.6 | 8.8 | 13.6 | -12.6 | 7.4 |
| | | 100-0 | $7.2x10^4$ | 17.5 | -19.3 | 5.7 | 29.1 | 23.9 | 30.1 | 21.1 | 25.4 | 30.6 | 22.8 | 8.6 | 10.9 | -7.5 | 7.4 |

Table S2. Mesozooplankton biomass (µg C $m^{-3}$) by station (St) and depth stratum (Depth) during the study period. Values correspond to the biomass estimated from samples collected at each station, with day and night conditions distinguished at Station 39.

| St | Depth (m) | Biomass (µg C $m^{-3}$) |
|---|---|---|
| St. 18 | 20-0 | 39,369.3 |
| | 80-20 | 6,69.8 |
| St. 26 | 20-0 | 3,646.5 |
| | 80-20 | 2,666.0 |
| St. 31 | 25-0 | 5,465.0 |
| | 80-25 | 16,078.6 |
| | 200-80 | 964.0 |
| St. 39 (day) | 100-0 | 1,554.8 |
| | 200-100 | 373.0 |
| | 400-200 | 1,121.8 |
| | 600-400 | 650.0 |
| | 900-600 | 256.5 |
| St. 39 (night) | 100-0 | 2,602.6 |
| | 200-100 | 298.4 |
| | 400-200 | 710.3 |
| | 600-400 | 992.2 |
| | 900-600 | 617.5 |

Table S3. Migrant biomass (MB) calculated as nighttime minus daytime zooplankton and micronekton biomass (mg C $m^{-2}$) across depth strata at St. 39.

| Sample | Depth strata (m) | Biomass (mg C $m^{-2}$) | | MB (mg C $m^{-2}$) |
|---|---|---|---|---|
| | | Day | Night | |
| Zooplankton | 100-0 | 104.8 | 180.4 | 75.6 |
| | 200-100 | 10.7 | 14.1 | 3.4 |
| | 400-200 | 145.8 | 79.6 | 66.1 |
| | 600-400 | 74.9 | 114.2 | 39.3 |
| | 900-600 | 39.2 | 113 | 73.7 |
| Micronekton | 100-0 | 464.5 | 1,051.2 | 586.8 |
| | 200-100 | 1,238.6 | 30.0 | 1,208.6 |
| | 400-200 | 3,108.5 | 286.8 | 2,821.7 |
| | 600-400 | 7,132.6 | 4,750.8 | 2,381.8 |
| | 1000-600 | 1,953.4 | 1,270.4 | 683.0 |